

DEVELOPMENT OF A PORTABLE, MODULAR UNIT FOR THE  
OPTIMIZATION OF ULTRASOUND-ASSISTED OXIDATIVE  
DESULFURIZATION OF DIESEL

by

Meng-Wei Wan

---

A Dissertation Presented to the  
FACULTY OF THE GRADUATE SCHOOL  
UNIVERSITY OF SOUTHERN CALIFORNIA  
In Partial Fulfillment of the  
Requirements for the Degree  
DOCTOR OF PHILOSOPHY  
(ENVIRONMENTAL ENGINEERING)

May 2006

Copyright 2006

Meng-Wei Wan

UMI Number: 3233795

Copyright 2006 by  
Wan, Meng-Wei

All rights reserved.

#### INFORMATION TO USERS

The quality of this reproduction is dependent upon the quality of the copy submitted. Broken or indistinct print, colored or poor quality illustrations and photographs, print bleed-through, substandard margins, and improper alignment can adversely affect reproduction.

In the unlikely event that the author did not send a complete manuscript and there are missing pages, these will be noted. Also, if unauthorized copyright material had to be removed, a note will indicate the deletion.

**UMI<sup>®</sup>**

---

UMI Microform 3233795

Copyright 2006 by ProQuest Information and Learning Company.

All rights reserved. This microform edition is protected against  
unauthorized copying under Title 17, United States Code.

ProQuest Information and Learning Company  
300 North Zeeb Road  
P.O. Box 1346  
Ann Arbor, MI 48106-1346

## DEDICATION

*To the memory of my father*

*Kuo-Yang Wan*

*His love for family,*

*thirst for knowledge,*

*and brave for challenge*

*continue to inspire me today.*

## ACKNOWLEDGMENTS

I am extremely grateful to my advisor, Professor Teh Fu Yen, for his guidance, financial support, and encouragement during my graduate study at USC. I also would like to thank Professor Massoud M. Pirbazari and Professor Katherine S. Shing for being my committee members, and for their valuable comments and suggestions.

I wish to express thanks to all of my colleagues and friends in the Environmental Engineering Program for their friendly assistance and discussion throughout my research period, especially Dr. Jesse Tu, Dr. Christine Lai, Omid Etemadi, Victor Chen, and Ngo-Yeung Chan. Special thanks are extended to Erick Hernandez, Lance Hill, and Ken Lee for their technical supports.

I sincerely express my appreciation to Professor Shung at Department of Biomedical Engineering, USC for his valuable suggestions and guidance. I am grateful for Dr. Geng at Blatek Tech. Inc. for his remarkable support in producing this sonoreactor. A special thank goes to Mr. Larry Darwin for being such an invaluable consultant. I also thank the financial support and instrument grant from Office of Naval Research and Army Research Laboratory to make this research possible.

Finally, but most significantly, I sincerely express my deepest gratitude to my mother Jung-Li Chen, my sister Meng-Lin Wan, and my cousin Ya-Wen Hsu for giving me unlimited love and support throughout my Ph.D. study. I could not complete this research without their love and encouragements.

# TABLE OF CONTENTS

<b>DEDICATION</b>	ii
<b>ACKNOWLEDGMENTS</b>	iii
<b>LIST OF TABLES</b>	ix
<b>LIST OF FIGURES</b>	x
<b>ABBREVIATIONS</b>	xiv
<b>ABSTRACT</b>	xvi
<b>1. INTRODUCTION</b>	1
1.1 DIESEL FUEL	1
1.2 REGULATIONS ON DIESEL FUEL SULFUR	2
1.2.1 Environmental Concern	2
1.2.2 U.S. EPA Diesel Fuel Standards	3
1.2.2.1 On-Road Diesel Fuel	3
1.2.2.2 Nonroad Diesel Fuel	3
1.2.3 California Diesel Fuel Standards	4
1.2.4 Recent European Union Action	5
1.3 DISULFURIZATION TECHNIQUES	6
1.3.1 Hydrodesulfurization (HDS) and Its Limitation	6
1.3.2 Biodesulfurization	8
1.3.3 Sulfur Adsorption	11
1.3.3.1 Reactive Adsorption for Sulfur Capture from Diesel Stream	11
1.3.3.2 Selective Adsorption for Deep Desulfurization.	12
1.3.4 Oxidative Desulfurization	15
<b>2. THEORETICAL BACKGROUND</b>	17
2.1 INTRODUCTION	17

2.2 SONOCHEMISTRY	18
2.2.1 Fundamental of ultrasound	18
2.2.2.1 Cavitation Mechanism	19
2.2.2.2 Cavitation Chemistry	21
2.2.2 Factors Affecting Sonochemistry	22
2.2.2.1 Temperature.	23
2.2.2.2 External Pressure	24
2.2.2.3 Ultrasonic Frequency	24
2.2.2.4 Ultrasonic Intensity	25
2.2.2.5 Choice of Solvent	25
2.2.3 Ultrasound and Phase Transfer Catalysis	26
2.3 HYDROGEN PEROXIDE AS OXIDANT	27
2.4 POLYOXOMETALATE CATALYSIS	29
2.4.1 Polyoxometalates	29
2.4.2 Heteropoly Acids – Keggin Heteropolyanions	30
2.4.3 Ishii-Venturello Expoxidation	33
2.5 PHASE TRANSFER CATALYSIS	36
2.5.1 Quaternary Ammonium Salts	36
2.5.2 Starks' Extraction Mechanism	37
2.5.3 Solid-Liquid Anion Exchange	38
2.5.4 The Design of Catalytic System	39
2.5.5 Phase Transfer Agent	41
<b>3. ULTRASOUND IN INDUSTRIAL APPLICATION</b>	42
3.1 INTRODUCTION	42
3.2 ULTRASONIC TRANSDUCER	44
3.2.1 Transducer	44
3.2.2 Mechanical Transducer	44
3.2.2.1 Whistle	44
3.2.2.2 Jet-edge Devices	46
3.2.3 Electromechanic Transducers	47
3.2.3.1 Piezoelectric Transducer	48
3.2.3.2 Magnetostrictive Transducers	50
3.3 ULTRASONIC SYSTEM TYPES	52
3.3.1 Ultrasonic Bath	52
3.3.2 Probe (Horn) Systems	53

3.4 MODULE DESIGN OF CONTINUOUS ULTRASONIC DESULFURIZATION	56
3.4.1 Module Design	56
3.4.2 The Portable Continuous UAOD Unit	57
3.4.2.1 The Design of Sonoreactor	58
3.4.2.2 RF Amplifier	60
3.4.2.3 Funtion Generator	62
3.4.2.4 Portable Continuous Desulfurization Unit	62
<b>4. UAOD ON MODEL SULFUR COMPOUND</b>	64
4.1 INTRODUCTION	64
4.2 MATERIALS AND EXPERIMENT METHODS	65
4.2.1 Materials	65
4.2.2 Experimental Method	66
4.3 QUANTIFICATION OF ORGANIC SULFUR COMPOUND ANALYSIS	67
4.3.1 Total Sulfur Content	67
4.3.2 Low Sulfur Content Determination	68
4.4 RESULTS AND DISCUSSION	70
4.4.1 Process Optimization	70
4.4.1.1 Effect of the Structure of QASs as Phase Transfer Agent	70
4.4.1.2 Effect of the amount of QASs as Phase Transfer Agent	73
4.4.1.3 Solid-Liquid Anion Exchange on Phase Transfer Agent	76
4.4.1.4 High Yield of Benzothiophene sulfone from Fluoride containing Phase Transfer Agent	80
4.4.1.5 Effects of the Transition Metal Catalyst	87
4.4.2 UAOD on Other Model Sulfur Compounds and Kinetic Study	89
4.5 SUMMARY	95
<b>5. UAOD ON COMMERCIAL DIESEL FUELS</b>	98
5.1 INTRODUCTION	98
5.2 MATERIALS AND EXPERIMENT METHODS	100
5.2.1 Materials	100
5.2.2 Experimental Method	100
5.2.3 Selective Ion Monitoring (SIM) Technique	101
5.2.4 Tungsten Analysis	101

5.3 ANALYTICAL METHODS	102
5.3.1 Total Sulfur Content	102
5.3.2 Identification of Organic Sulfur Compounds in Diesel	103
5.4 RESULT AND DISCUSSION	103
5.4.1 Characterization of Diesel Fuels	103
5.4.2 The UAOD on F76 Marine Logistical Diesel	106
5.4.3 The UAOD on MGO Marine Logistical Diesel	108
5.4.4 The UAOD on JP5 Marine Logistical Diesel	110
5.4.5 The UAOD on JP8 Jet Fuel Diesel	112
5.4.6 The UAOD on Transportation Diesel	113
5.4.7 Effects of UAOD on Main Hydrocarbons in Diesel Fuels	116
5.4.8 Catalyst Recovery	120
5.4.9 Different Concentration of Hydrogen Peroxide in UAOD	122
5.5 SUMMARY	126
<b>6. A PORTABLE, MODULAR DESIGN UNIT – SONOREACTOR APPLIED TO SULFUR REMOVER ON DIESEL FUEL</b>	129
6.1 INTRODUCTION	129
6.2 MATERIALS AND EXPERIMENT METHOD	131
6.2.1 Materials	131
6.2.2 Probe Type Ultrasound Reactor in Recirculation Loop Continuous Flow	131
6.2.3 Tubular Reactors	133
6.2.3.1 Branson 8500 Serious – Pentagonal Processor	133
6.2.3.2 Sonoreactor	135
6.2.4 Experiment Method	135
6.3 RESULT AND DISCUSSION	136
6.3.1 Sulfur Removal at Different Ultrasonic Frequency	136
6.3.2 Sulfur Removal on Continuous UAOD Process	138
6.3.3 Large Scale Applications on Continuous UAOD Process	141
6.3.4 Different Concentrations of Hydrogen Peroxide in Continuous Unit	147
6.3.5 Idea Reactor Model Applied to Continuous UAOD Process	149
6.3.6 Economic Analysis of Continuous Desulfurization Unit	152
6.3.7 Capacity for Power Generation of Continuous UAOD Process	153
6.4 SUMMARY	156



<b>7. CONCEPTUAL MODEL OF UAOD PROCESS</b>	159
7.1 INTRODUCTION	159
7.2 MECHANISM OF UAOD PROCESS	159
7.3 CONCEPTUAL MODEL APPLIED TO EXPERIMENTAL RESULTS	163
7.4 SUMMARY	168
<b>8. SUMMARY AND RECOMMENDATION</b>	169
8.1 SUMMARY	169
8.1.1 The Optimization of UAOD Process	170
8.1.2 Development of a Portable, Continuous Desulfurization Unit	174
8.2 RECOMMENDATION	177
<b>REFERENCES</b>	186

## LIST OF TABLES

1.1	U.S. EPA diesel fuel standards	4
1.2	California diesel fuel standards	5
2.1	Single oxygen atoms donors	28
2.2	The order of different properties for the most common HPAs	32
4.1	Peak area of low sulfur contained compounds	69
4.2	Effect of different types of surfactants on UAOD process	71
4.3	Oxidation efficiency of different amount of phase transfer agent	74
4.4	Oxidation efficiency on different amount of sodium chloride	77
4.5	Oxidation efficiency on different phase transfer agents	82
4.6	Electron density on sulfur atom and rate constants	91
5.1	Tungsten recovery after UAOD process	121
5.2	Spent catalyst reused in UAOD process	122
5.3	Different H <sub>2</sub> O <sub>2</sub> concentrations applied to different diesels in UAOD process	124
5.4	Desulfurization efficiency of UAOD process on diesel fuels	126
6.1	Desulfurization efficiency of MGO at deferent ultrasonic frequency	138
6.2	Operating Conditions in the study of continuous UAOD on MGO	139
6.3	Desulfurization efficiency of MGO by deferent continuous flow reactors	140
6.4	Operating conditions of continuous UAOD on MGO at 5 lb/hour	141
6.5	Desulfurization efficiency of continuous UAOD on MGO by deferent sonication time at 5 lb/hour	142
6.6	Operating conditions of continuous UAOD on MGO at 12.5 lb/hour	145
6.7	Sulfur reduction of MGO by different sonication times at 12.5 lb/hour	145
6.8	Sulfur reduction of portable desulfurization unit by using different hydrogen peroxide concentrations on MGO	147

## LIST OF FIGURES

1.1	4S pathway of biological desulfurization for model compound dibenzothiophene	9
1.2	Basic principle of S-Zorb process developed by Phillips Petroleum for sulfur removal from liquid fuel under low H <sub>2</sub> pressure	11
1.3	Faujasite supercage with copper ions occupying 6-ring windows sites (A); $\sigma$ - Here donation of $\pi$ -electrons of thiophene to the 4s orbital of copper-(I) (B); $d-\delta^*$ back-donation of electrons from 3d orbitals of copper (I) to $\pi^*$ orbitals of thiophene 3d represents $d_{xy}$ , $d_{yz}$ , or $d_{xz}$ , or 3 of the 5 3d orbitals	14
2.1	The Keggin structure of the $[XM_{12}O_{40}]^{x-8}$ anion ( $\alpha$ -isomer); terminal (O <sup>1</sup> ), edge-bridging (O <sup>2</sup> ), and corner-bridging (O <sup>3</sup> ) oxygen atoms	31
2.2	Molecular structure of $\{PO_4[WO(O_2)_2]_4\}^{3-}$	34
2.3	Dominant processes in Ishii-Venturello exoxidation	35
2.4	General structure of quaternary ammonium salts	37
2.5	Starks' extraction mechanism	37
3.1	Cross-section through Galton's whistle	45
3.2	Cross-section through Hartmann's whistle	46
3.3	Cross-section through a jet-edge system	47
3.4	Schematic diagram of piezoelectric transducer	49
3.5	Piezoelectric transducers in commercial application	50
3.6	Basic equivalent circuit for a magnetostrictive transducers and its commercial application	51
3.7	Ultrasonic bath systems with (a) mounted transducers and (b) submersed Transducers	52
3.8	Schematic flow diagram of the continuous ultrasound assisted oxidative desulfurization process	56
3.9	Flow diagram of sonoreactor (a) in series or (b) in parallel	58

3.10 Schematic design diagram of the sonoreactors	59
3.11 Picture of sonoreactor	60
3.12 Portable unit of continuous flow system	63
4.1 Calibration curve for quantification of sulfur concentration	69
4.2 Effect of different structure of QASs on oxidation of BT to BTO	72
4.3 Effect of amount of PTA on conversion of BT to BTO	74
4.4 GC-PFPD chromatograms of BT after UAOD process under 0.1 g PTA	75
4.5 GC-PFPD chromatograms of BT after UAOD process under 0.2 g PTA	76
4.6 Effect of amount of NaCl on conversion of BT to BTO	78
4.7 GC-PFPD chromatograms of BT after UAOD process with 0.5 g NaCl	79
4.8 GC-MS chromatograms of BT after UAOD with different conditions	80
4.9 Comparison of yields of different quaternary salts	82
4.10 GC-PFPD chromatograms of BT using TOAF as PTA in different sonication time	83
4.11 GC-PFPD chromatograms of comparison of 2MBT after UAOD process by using different PTA	84
4.12 GC-PFPD chromatograms of comparison of DBT after UAOD process by using different PTA	85
4.13 Comparison of yields of model sulfur compounds using different PTA	86
4.14 Comparison of yields of BT and BTO by using different TMC	88
4.15 Conversion of BT, 2MBT, DBT, 4MDBT and 46DMDBT at different sonication time	92
4.16 Plot of $\ln(C_0/C_i)$ versus time for oxidation of BT, 2MBT, DBT, 4MDBT and 46DMDBT under pseudo first order condition	93
4.17 Comparison of the rate constants ( $k$ ) with the electron densities for different model compounds	94
5.1 Composition and distribution of organic sulfur compounds in diesel fuels in GC-PFPD chromatogram	104

5.2	Composition and distribution of organic sulfur compounds in F76, MGO, JP5 and transportation diesel	105
5.3	GC-PFPD chromatograms of F76 marine diesel in UAOD process	106
5.4	Organic sulfur compounds remain in the desulfurized F76 after UAOD process	107
5.5	GC-PFPD chromatograms of MGO Marine diesel under UAOD process	108
5.6	Organic sulfur compounds remain in the desulfurized MGO after UAOD process	109
5.7	GC-PFPD chromatograms of JP5 marine diesel under UAOD process	110
5.8	Organic sulfur compounds remain in the desulfurized JP5 after UAOD process	111
5.9	GC-PFPD chromatograms of JP8 Jet fuel diesel in UAOD process	112
5.10	Organic sulfur compounds remain in the desulfurized JP8 after UAOD process	113
5.11	GC-PFPD chromatograms of transportation diesel under UAOD process	114
5.12	Organic sulfur compounds remain in the desulfurized transportation diesel after UAOD process	115
5.13	Effects of UAOD on saturated hydrocarbons in marine logistic fuel. (a) <i>n</i> - paraffins, (b) <i>n</i> -alkyl cyclohexanes	118
5.14	Effects of UAOD on saturated hydrocarbons in marine logistic fuel (a) <i>n</i> -alkyl benzenes, (b) alkyl naphthalenes	119
5.15	Desulfurization efficiency of different hydrogen peroxide concentrations on MGO under UAOD conditions	125
6.1	Schematic diagram of a probe type ultrasound reactor in recirculation loop continuous flow application	132
6.2	Schematic diagram of pentagonal processor.	134
6.3	Schematic diagram of a continuous flow sonoreactor	135
6.4	Plot of $\ln (C_0/C_i)$ versus time for MGO desulfurization under pseudo first order condition	144
6.5	Sulfur reduction of continuous UAOD in different H <sub>2</sub> O <sub>2</sub> Concentration	148
6.6	Continuous-flow stirred tank reactor (CSTR)	149
7.1	Conceptual model of catalytic oxidation in UAOD process	162

7.2	Comparison of yields of BT and BTO by using different TMC	164
7.3	IR spectra of catalyst isolated from UAOD system	167
8.1	Block diagram of continuous UAOD process	177
8.2	Schematic flow diagram of the solid adsorption tower after continuous UAOD process	180
8.3	Ultrasonic reactor configurations for sonications at 513 kHz	182
8.4	Formation of different zeolites by cage structure	183

## ABBREVIATIONS

2MBT	: 2-Methylbenzothiophene
4MDBT	: 4-Methyldibenzothiophene
46DMDBT	: 4,6-Dimethyldibenzothiophene
BDS	: Biodesulfurization
BT	: Benzothiophene
BTO	: Benzothiophene Sulfone
DBT	: Dibenzothiophene
DBTO	: Dibenzothiophene Sulfone
CSTR	: Continuous-flow Stirred Tank Reactor
GC	: Gas Chromatograph
GC/MS	: Gas Chromatograph / Mass Spectrometer
HDS	: Hydrodesulfurization
ICP	: Inductively-Coupled Plasma
HPAs	: Heteropoly Acids
HPW	: Phosphotungstic Acid
HPMo	: Phosphomolybdic Acid
MBAC	: Methyltributylammonium Chloride
MBAH	: Methyltributylammonium Hydroxide
NaPW	: Sodium Phosphotungstic Acid
NaPMo	: Sodium Phosphomolybdic Acid
NDXRF	: Non-Dispersive X-Ray Fluorescence
ODS	: Oxidative Desulfurization
OSC	: Organic Sulfur Compounds
PFPD	: Pulsed Flame Photometric Detector
POM	: Polyoxometalates
PPM	: Polyperoxometalate
PTA	: Phase Transfer Agent
PTC	: Phase Transfer Catalysis
QAS	: Quaternary Ammonium Salts
SARS	: Selective Adsorption for Removing Sulfur
SIM	: Selective Ion Monitoring
TBAB	: Tetrabutylammonium Bromide
TMAF	: Tetramethylammonium Fluoride
TMC	: Transition Metal Catalyst
TOAB	: Tetraoctylammonium Bromide
TOAF	: Tetraoctylammonium Fluoride
TODAB	: Tttraoctadecylammonium Bromide

TS-1 : Titanium Silicalite-1  
Ti-B : Titanium Beta  
UAOD : Ultrasound-Assisted Oxidative Desulfurization  
ULSD : Ultra-Low-Sulfur Diesel



## ABSTRACT

Due to the stringent rules requiring ultra-low sulfur content in diesel fuels, it is necessary to develop alternative methods of desulfurization of fossil fuel derived oil, such as diesel. Current technology is not sufficient to solve this problem. Based on previous researches, ultrasound applied to oxidative desulfurization which combined three complementary techniques: ultrasonication, phase transfer catalysis (PTC) and transition metal catalyzed oxidation, has accomplished high sulfur removal in a short contact time at ambient temperature and atmospheric pressure. However, the problems of bromo-byproducts and low oxidation efficiency of BT and its families can be a drawback to enhance the deep desulfurization.

This study has successfully demonstrated that the higher oxidation efficiency of BT to BTO and free of any by-products by using tetraoctylammonium fluoride as phase transfer agent. The oxidation rate of BT to BTO increased with increasing the carbon chain length of QAS cations. Under the same length of carbon chain, the oxidation rate of BT to BTO increased with decreasing the molecular size of QAS anions. Moreover, through the reaction of solid-liquid anion exchange, adding solid salts to the system has performed a significant effect on quaternary ammonium salts to transfer the oxidized metal anion into organic phase.

For diesel fuels containing various levels of sulfur content, UAOD process followed by solvent extraction has demonstrated that the sulfur reduction can reach above 95 % removal efficiency or final sulfur content below 15 ppm in mild

condition. Moreover, this study has also demonstrated that spent TMCs can be fully recovered in aqueous phase, and still exhibit high efficiency and high selectivity, and thus restore the catalytic cycle. In addition, this study has indicated that hydrogen peroxide diluted to 3 % can perform the same sulfur removal efficiency as 30 % hydrogen peroxide.

This study has already accomplished high sulfur removal with a probe type unit. However, the probe type unit is merely at a batch scale. This is sufficient for research purposes but inadequate for large-scale commercial production. A continuous flow system can fulfill the needs of practical application. Among all manufactories, only Branson Inc. could provide us with a commercial unit that met our requirements. However, because of the inappropriate frequency and large capacity, this unit couldn't achieve the best results. Therefore, a tailor-made module reactor was successfully assembled by Blatek Tech.

This continuous desulfurization unit, which consists of a sonoreactor, an RF amplifier, a function generator, a pretreatment tank, and a pipeline system, was operated at mild conditions for a given time. A single unit only needs 2' x 4' x 1' space. The results indicated that the remarkable 92% removal efficiency for the sulfur in marine logistic diesel, even at a treatment rate as high as 25 lb/hour which is approximately 2 barrels per day. Therefore, this sonoreactor has demonstrated the feasibility of large-scale operation even in a relatively small installation with low capital investment and maintenance cost. It also ensures the safety considerations by operating with diluted hydrogen peroxide under ambient temperature and pressure.

# **CHAPTER 1**

## **INTRODUCTION**

### **1.1 DIESEL FUEL**

Diesel fuels are complex mixtures of alkanes, cycloalkanes and aromatic hydrocarbons with carbon numbers in the range of C<sub>9</sub>-C<sub>28</sub> and with a boiling-range of 150-390 °C. Diesel fuel is one of the three most important transportation fuels, including gasoline, diesel and jet fuels, which are widely used in transportation of the world. Because diesel engines are inherently more thermally efficient than gasoline engines, it is expected that diesel demand and utilization will increase more in the next few decades in the 21st century (Song, et al. 2000). Recently, California Energy Commission has reported the annual diesel fuel consumption in state of California. From 1990 to 2003, annual consumption of diesel fuel has increased by nearly 60%. In 2003, consumption was 2.7 billion gallons. Statewide, diesel fuel consumption is expected to increase 2.4% annually.

Diesel engines have historically been more versatile and cheaper to run than gasoline engines or other sources of power. However, diesel engines are a major source of fine-particle pollution, which contains substances that can pose a risk to human health. Therefore, increasing demand for diesel fuels, developing analysis for fuel characterizations and rising standards for reducing sulfur content have resulted in high interest worldwide on chemistry of diesel fuels.

## **1.2 REGULATIONS ON DIESEL FUEL SULFUR**

### **1.2.1 Environmental Concern**

Because of different sulfur-containing compounds in diesel, sulfur content is usually expressed as the weight percentage of sulfur in the fuel. Sulfur content in diesel fuel is an environmental concern, upon combustion, sulfur leads directly to emission of SO<sub>2</sub> and sulfate particulate matter (PM), which endangers public health and welfare.

For fuel cells, liquid hydrocarbons (gasoline, kerosene, jet fuel, or diesel) are ideal fuels due to the high energy density, ready availability, ease of transport, and storage. However, sulfur in petroleum often poisons catalytic converters, corrodes parts of internal combustion engines, and leads to air pollution. Because the sulfur compounds are poisonous to the shift catalyst in hydrocarbon conversion process and the electrode catalyst in fuel cell process, the sulfur content of these petroleum fuels has to be decreased to less than 0.1 ppm.

Those exhaust gases of diesel engines contain sulfur compounds, which can significantly impair the emission control technology designed to meet NO<sub>x</sub> and PM emission standards. Therefore, less sulfur will not only reduce the emission of SO<sub>2</sub>, it will also improve the performance of pollution control equipment on vehicles designed to reduce the release of NO<sub>x</sub> and PM emission. Recently, EPA has set standards for low sulfur diesel, which will help to ensure the effectiveness of low emission-control technologies and reduce harmful air pollution.

## **1.2.2 U.S. EPA Diesel Fuel Standards**

### **1.2.2.1 On-Road Diesel Fuel**

EPA has established separate diesel fuel specifications for on-road diesel fuel and nonroad diesel fuel. The current EPA on-road diesel fuel standards have been applicable since October 1993. The regulation prohibits the sale or supply of diesel fuel for use in on-road motor vehicles, unless the diesel fuel has sulfur content no greater than 500 ppmw. On January 18, 2001, EPA published a final rule which specifies that, starting from June 1, 2006, refiners must begin producing highway diesel fuel that meets a maximum sulfur standard of 15 ppmw. All 2007 and later model year diesel-fueled vehicles must be fueled with this new low sulfur diesel. Both the current and future on-road diesel fuel standards are shown in Table 1.1 (U.S. EPA, 2000).

### **1.2.2.2 Nonroad Diesel Fuel**

On June 29, 2004, EPA published a final rule for the control of emissions from nonroad diesel engines and fuel. starting from June 1, 2007, refiners would be required to produce nonroad, locomotive, and marine diesel fuel that meet a maximum sulfur level of 500 ppmw. In 2010, nonroad diesel fuel will be required to meet the 15 ppmw standard except for locomotives and marine vessels. In 2012, nonroad diesel fuel used in locomotives and marine applications must meet the 15 ppmw standard. The nonroad diesel fuel standards are shown in Table 1.1 (U.S. EPA, 2000).

**Table 1.1 U.S. EPA diesel fuel standards (U.S. EPA, 2000)**

Applicability	Implementation Date	Maximum Sulfur Level (ppmw)	Aromatics Maximum (% by volume)	Cetane Index (Minimum)
On-road	1993	500	35	40
On-Road	2006	15	35	40
Nonroad	1993	5,000	35	40
Nonroad	2007	500	35	40
Nonroad, <i>excluding loco/marine</i>	2010	15	35	40
Nonroad, <i>loco/marine</i> *	2012	15	35	40

\* Nonroad diesel fuels must comply with ASTM No. 2 diesel fuel specification for aromatic and cetane.

These fuel improvements will result immediate and significant environmental and public health benefits by reducing PM from existing engines. EPA also announced its intent to propose more stringent emission standards for all new commercial, recreational, and auxiliary marine diesel engines except the very large engines used for propulsion on deep-sea vessels. EPA would require the use of advanced emission-control technologies similar to those already upcoming for heavy-duty diesel trucks and buses.

### **1.2.3 California Diesel Fuel Standards**

On November 18 2004, the California Air Resources Board (ARB) approved a regulation that requires harborcraft to use the same cleaner diesel fuel used by on-

road trucks, starting in 2006 for harborcraft operated in the South Coast Air Quality Management District, and starting in 2007 for statewide, as shown in Table 1.2. Harborcraft are defined as all marine vessels except oceangoing ships. Oceangoing ships are distinct from harborcraft because they travel internationally, and would not have access to ARB diesel fuel at ports outside of California. ARB is developing a rule that would require oceangoing ships to use a cleaner marine diesel fuel to power auxiliary engines while in California coastal waters and at dock. ARB is also working with EPA to explore the feasibility of pursuing a West Coast Sulfur Emission Control Area, where ships would be required to burn cleaner fuel. In addition, military vessels are exempted from the California diesel fuel standards.

**Table 1.2 California diesel fuel standards**

Implementation Date	Maximum Sulfur Level (ppmw)	Aromatics Level (% by volume)	Cetane Index
1993	500	10	N/A
2006	15	10	N/A

#### **1.2.4 Recent European Union Action**

On July 1 2000, the European Union approved a regulation that requires the members must stop to use the sulfur content which is more than 2,000 ppmw (0.2%). Starting form January 1 2008, the members would be required to use fuel with maximum sulfur content lower then 1,000 ppmw (0.2%). Moreover, in November

2002, the European Union adopted a new strategy to address sulfur emissions from marine engines by reducing the sulfur content of marine fuels used in the European Union. The proposal has two main provisions. The first is a 15,000 ppmw sulfur content limit that would apply to the fuel used by all oceangoing vessels in the North Sea, English Channel, and Baltic Sea, and to all regular passenger vessels operating in the EU by 2007. This provision is consistent with the SO<sub>x</sub> Emission Control Areas designated under MARPOL Annex VI. The second provision would require ships to use fuel with a maximum sulfur content of 2,000 ppmw (0.2%) while they are at berth in ports inside the European Union. This provision is intended to reduce sulfur and particulate matter emissions in populated areas.

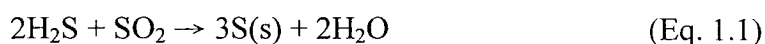
### **1.3 DISULFURIZATION TECHNIQUES**

#### **1.3.1 Hydrodesulfurization (HDS) and Its Limitation**

The hydrodesulfurization (HDS) or distillate hydrotreating is one of the largest scale chemical processes to remove sulfur from diesel and has been carried out in industry today. Traditional HDS is the hydrotreatment process that hydrogen and a catalyst are needed to break up the sulfur-containing compounds in diesel, and hydrogen sulfide is formed. The most commonly used desulfurization catalyst, supported molybdenum sulfide catalyst containing cobalt (Co-Mo/Al<sub>2</sub>O<sub>3</sub>), is operated under high pressures of 100-500 psi of hydrogen and high temperature of 300-400°C. These catalysts interact primarily with the sulfur atom and encourage the



reaction of sulfur with hydrogen to form hydrogen sulfide. The produced gas is then separated from desulfurized distillate and converted to elemental sulfur by the Claus process, where the hydrogen sulfide is oxidized by sulfur dioxide, and sulfur is formed by the overall reaction, shown as Eq. 1.1:



In HDS, organic sulfur compounds exhibit different reactivity. For the sulfur compounds without a conjugation structure between the lone pairs on S atom and the  $\pi$ -electrons on aromatic ring, including disulfides, sulfides, thiols, and tetrahydrothiophene, HDS occurs directly through hydrogenolysis pathway. These sulfur compounds exhibit higher HDS reactivity than that of thiophene by an order of magnitude (Phillipson, 1971), because they have higher the electron density on the S atom and weaker C–S bond. The reactivities of the 1- to 3-ring sulfur compounds decrease in the order: thiophenes (T) > benzothiophenes (BT) > dibenzothiophenes (DBT) (Frye, et al. 1967; Kilanowski, et al. 1978; Houalla et al. 1980; Girgis et al. 1991; Vasudevan, et al. 1996).

In most diesel fuel, alkyl-substituted DBT are the most abundant sulfur species. The position of alkyl substituent has significant effects on the reactivity of alkyl-DBT in HDS process. 4-methyldibenzothiophenes (4MDBT) and 4,6-dimethyldibenzothiophenes (46DMDBT) have much lower reactivities than other sulfur-containing organic compounds. (Kabe, et al. 1992, Ma, et al. 1994, 1995; Gates, et al. 1997; Song, et al. 2003). Moreover, recent studies on HDS indicated that

organic sulfur compounds (OSCs) remaining in diesel fuel at sulfur level lower than 0.1 wt% are alkyl-DBT with alkyl substations at 4- and/or 6- position, whose reactivities are 10 or 40 times lower than the OSCs initially removed in lowering the sulfur level from 1.0 wt% to 0.10 wt%. (Ma, et al. 1994; Mochida, et al. 1996; Gates, et al. 1997). Therefore, to reduce those refractory OSCs based on conventional approaches of HDS of diesel fuel, if reducing the sulfur level from current 0.050 wt% to 0.0015 wt%, the volume of catalyst bed will have to be increased 3.2 times as that for current HDS catalyst bed. If reducing the sulfur to 0.0001 wt% level, the volume of catalyst bed will have to be increased by about 7 times. It might be difficult to meet the demand by making small improvements in existing HDS technology (Song, et al. 2003).

### **1.3.2 Biodesulfurization**

Biodesulfurization (BDS) is using a series of enzyme-catalyzed reactions to remove sulfur from gasoline and diesel. Over the past decade, considerable works have been done to extend the understanding of the enzymology and molecular genetics of the BDS system, and to design and optimize the bioreactor and bioprocess. As the regulations for sulfur in fuels become more and more stringent, BDS is rising as one of the candidates for the “deeper desulfurization” to produce lower-sulfur fuels. Recently, utilization of byproduct from biodesulfurization has also been reported, and the process system is being explored (Lange, et al. 2000). Moreover, certain microbial biocatalysts have been identified that can biotransform

sulfur compounds found in fuels, including ones that selectively remove sulfur from dibenzothiophene heterocyclic compounds (McFarland, et al. 1998).

Generally, there are two primary pathways for BDS of alkyl-DBTs. However, the most attention is that Monticello recently outlined sulfur-specific Cx-DBT metabolism via the hydrocarbon-conserving (4S) pathway first proposed by Campbell and Kee Rhee. Figure 1.1 shows the microbial chemical pathway (4S) of various bacterial species in the BDS system, which can remove sulfur from substituted dibenzothiophenes with alkyl groups that hinder chemical catalysis and that resist removal by hydrodesulfurization (Monticello, 1998).

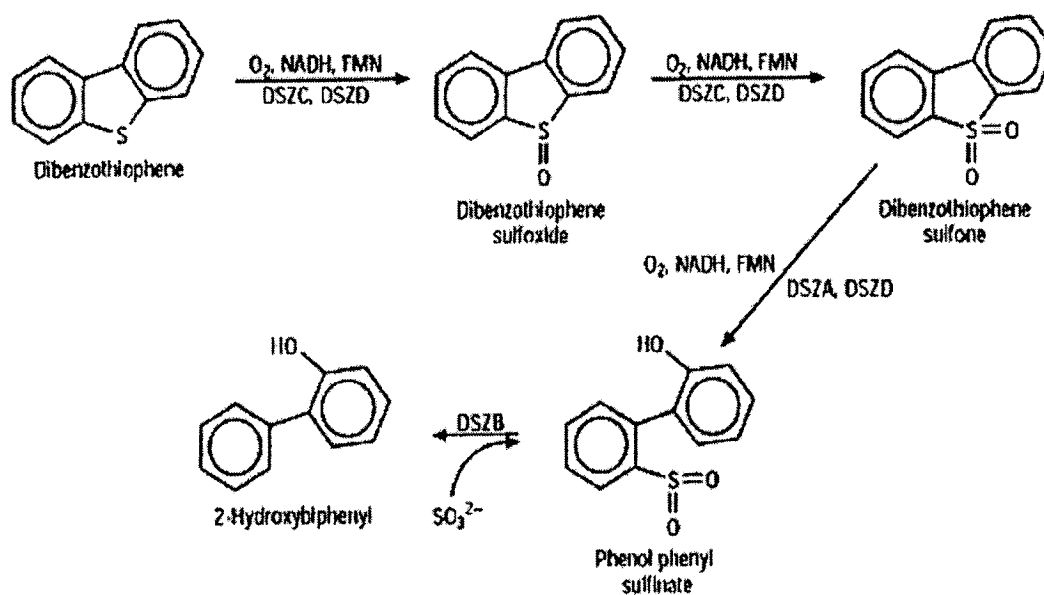


**Figure 1.1 4S pathway of biological desulfurization for model compound dibenzothiophene (Monticello, 2000)**

Although the microbial biocatalysts (microorganisms) have been identified that can biotransform sulfur compounds found in fuels, including any selectively

compounds to form 2-hydroxyl biphenyl and similar compounds, the major obstacle in BDS is still both the limit rate and extent of desulfurization. A study from Energy Biosystems shows that the extensive BDS of hydrodesulfurized diesel led to a 67 % reduction in total sulfur from 1,850 ppm to 615 ppm which can't be further reduced (Folsom, et al. 1999). The recent study indicated that the relative desulfurization activities of various alkyl DBTs were reduced in proportion to the total carbon numbers of alkyl substituent groups. Alkyl DBTs that had a total of six carbons of alkyl substituent groups were not desulfurized. The type or position of alkyl substituent groups had little effect on desulfurization activity. The desulfurization activity of each alkyl DBT, when mixed together, was reduced. This phenomenon was caused by apparent competitive (Kobayashi, 2001).

In summary, although BDS promises mild operating conditions, the biological process proceeds not rapidly enough to remove sulfur at commercially acceptable rate or in the presence of oil. Therefore, bioprocess improvements that enhance biocatalyst stability, achieve faster kinetics, improve mass transfer limitations, temperature and solvent tolerance, as well as broaden substrate specificity to attack a greater range of heterocyclic compounds, are significant issues to achieve the production of low sulfur gasoline (McFarland, et al. 1998; Monticello, 1998; Song, et al. 2003).

### 1.3.3 Sulfur Adsorption

#### 1.3.3.1 Reactive Adsorption for Sulfur Capture from Diesel Stream

A developed desulfurization process called S-Zorb diesel, was recently announced by ConocoPhillips Inc., which is an extension of their S-Zorb Gasoline process for naphtha. S-Zorb diesel contacts diesel fuel streams with a solid sorbent, which attracts sulfur-containing molecules and removes the sulfur atom from the molecule, in a fluid bed reactor at relatively low pressures and temperature in the presence of hydrogen. The sulfur atom is retained on the sorbent while the hydrocarbon portion of the molecule is released back into the process stream. Hydrogen sulfide is not released into the product stream and therefore prevents recombination reactions of hydrogen sulfide and olefins to make mercaptans, which would otherwise increase the effluent sulfur concentration (ConocoPhillips, 2005).

Figure 1.2 illustrates the principle of S-Zorb process.

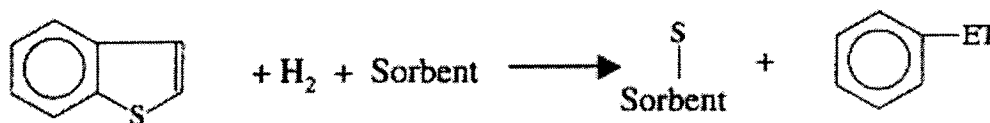


**Figure 1.2 Basic principle of S-Zorb process developed by Phillips Petroleum for sulfur removal from liquid fuel under low  $\text{H}_2$  pressure. (Song, 2003)**

The sorbent (catalyst) is continuously withdrawn from the reactor and transferred to the regenerator section where the sulfur is removed as  $\text{SO}_2$  and sent to an existing sulfur recovery unit. The clean sorbent is reconditioned and returned to

the reactor. The rate of sorbent circulation is controlled to help maintain the desired sulfur concentration in the product (ConocoPhillips, 2005).

Currently, the first commercial S-Zorb unit began operations in April 2001 at ConocoPhillips Refinery in Borger, Texas USA. The unit was designed to treat 6000 barrels per day (bpd) of full range FCC naphtha containing up to 1000 ppmw sulfur, and could reduce the sulfur content down to 10 ppmw or less with little or no octane loss. Moreover, in November 2003, the second commercial S-Zorb unit began operations at ConocoPhillips Refinery in Ferndale, Washington, USA. This unit was designed to treat 20,000 bpd of full range FCC naphtha containing up to 1500 ppmw sulfur, and could reduce the sulfur content down to 10 ppmw or less with little or no octane loss (ConocoPhillips, 2005).

#### 1.3.3.2 Selective Adsorption for Deep Desulfurization

Recently, Song and Ma, 2002 at Pennsylvania State University showed a new desulfurization process by selective adsorption for removing sulfur (PSU-SARS) at ambient temperature without using hydrogen or any other reactive gas. Several adsorbents based on transition metal complexes supported on porous materials, zeolites, supported transition metals, mixed metal oxides, activated carbon, etc. have been developed and used for selective adsorption desulfurization of diesel fuel, gasoline and jet fuel at ambient temperatures. The results from testing various liquid fuels show that selective adsorption of sulfur compounds can be achieved by using a

transition metal compound loaded on a porous support in laboratory scale (Ma, et al. 2002).

Recent work done by Yang and Hernandez-Maldonado, 2003 and 2004 at University of Michigan, Ann Arbors showed that aqueous-phase copper (II)-exchanged Y-zeolites, when autoreduced to Cu (I)-Y, are capable of removing 0.20 mmol of organo-sulfur species from a commercial diesel fuel (297.2 ppmw total sulfur) per gram of zeolite. This corresponds to about 3 thiophenic molecules per unit cell. Afterward, the fuel contained a total sulfur content of less than 1 ppmw. The deep desulfurization levels were obtained because of a  $\pi$ -complexation between the Cu ions ( $1s^2 2s^2 2p^6 3s^2 3p^6 3d^{10} 4s^0$ ) and the thiophenic aromatic rings (Hernandez-Maldonado, et al. 2003, 2004).

As seen in Figure 1.3, through the  $\pi$ -complexation mechanism the cations can form the usual  $\sigma$  bonds with their empty s-orbitals and, in addition, their d-orbitals can back-donate electron density to the antibonding  $\pi$ -orbitals ( $\pi^*$ ) of the sulfur rings. Experimental data and molecular orbital (MO) calculations have shown that  $\pi$ -complexation with cuprous ions is stronger with organo-sulfur molecules (i.e., thiophenic molecules) than with aromatics without sulfur (e.g., benzene) (Yang, et al. 2002, 2003; Takahashi, et al. 2003).

In summary, adsorption of sulfur compounds has been studied and reported in both open literature and patent literature for many years, but not successfully developed for liquid fuels because there are major problems with selectivity towards

sulfur compounds in the presence of many other compounds such as aromatics and polar species in refinery streams. Several researches have been done and showed the optimum results for deep desulfurization of the low sulfur content diesel. However, due to the limitation on adsorption capacity and regeneration rate of adsorbent, adsorption desulfurization can be used as a complementary process to the HDS process.

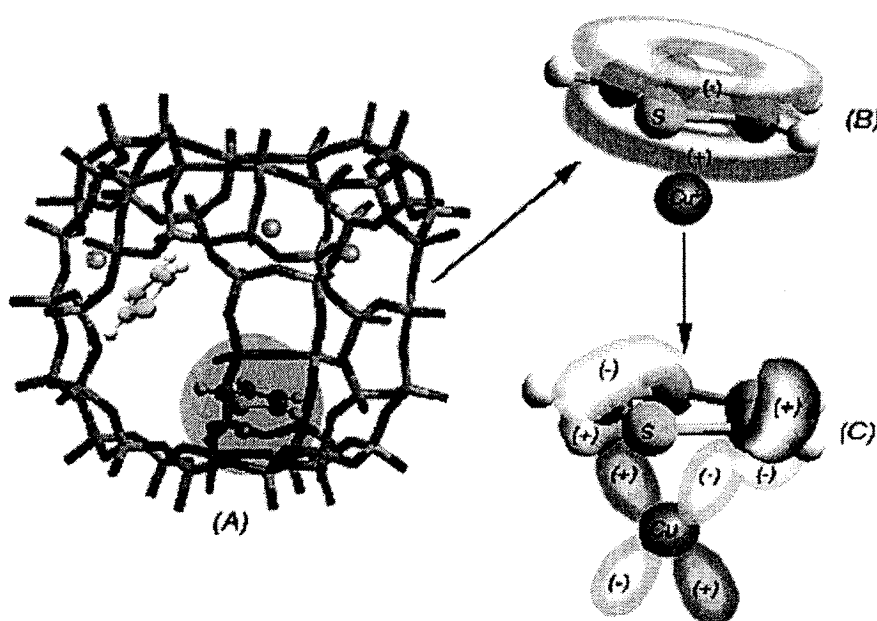


**Figure 1.3 Faujasite supercage with copper ions occupying 6-ring windows sites (A);  $\sigma$ -donation of  $\pi$ -electrons of thiophene to the 4s orbital of copper-(I) (B); d- $\delta^*$  back-donation of electrons from 3d orbitals of copper (I) to  $\pi^*$  orbitals of thiophene. Here 3d represents  $d_{xy}$ ,  $d_{yz}$ , or  $d_{xz}$ , or 3 of the 5 3d orbitals (Hernandez-Maldonado, et al. 2004).**



### 1.3.4 Oxidative Desulfurization

Most of the recent works indicated that the polyoxometalate catalysis such as  $\text{H}_3\text{PM}_{12}\text{O}_{40}$  [ $\text{M} = \text{Mo(VI)}$  or  $\text{W(VI)}$ ] with  $\text{H}_2\text{O}_2$  can produce more effective and selective oxidants as peroxo-metal species for the oxidation of nucleophiles (such as olefins and organic compounds) under phase transfer agent (Venturello, et al. 1985; Hill, et al. 1995). Even organic sulfur compounds with less nucleophilicity such as dibenzothiophene can have high yields of sulfones or sulfoxides under mild conditions (Collins, et. al. 1997; Yen, et al. 2002). It was reported that the desulfurization efficiency of diesel was greatly improved and reach over 95% within four hours. However, the reactivity of sulfur compounds in this system shows that the dibenzothiophene react more quickly then benzothiophene, and that increasing substitution also increases resistance to reaction.

Recently, solid catalysts (Zeolite) have been used for many areas, i.e., oxidation. Zeolite is a crystalline aluminosilicate with a cage structure, and its framework structure encloses cavities (or pores) occupied by cations and water molecules work. In a number of zeolites and silicalites, silicon or aluminum atoms in the framework can possibly be isomorphically replaced with transition metal ions. Titanium silicalite (TS-1) was the first zeolite catalyst that has been developed for liquid phase oxidation reactions.

Shiraishi et al. investigated an oxidative desulfurization process for light oil using a vanadosilicate molecular sieve as the catalyst and  $\text{H}_2\text{O}_2$  as the oxidizing agent. The catalytic activities for three kinds of vanadosilicates (VS-1, VS-2 and VS-

HMS), having different structures and pore size distributions, were compared with those for the corresponding titanosilicates (TS-1, TS-2 and TS-HMS). The oxidation of dibenzothiophene and benzothiophene in acetonitrile was catalyzed more effectively by vanadosilicates than titanosilicates, where the mesoporous vanadosilicate showed the highest activity. The vanadosilicate also accelerated the desulfurization of the actual light oil in an oil/acetonitrile two-phase system: the sulfur content of the oil was decreased successfully from 425 ppm to less than 50 ppm. During the process, nitrogen-containing compounds were also removed successfully from the light oil. However, the vanadosilicate, recovered following the reaction, could not be reused for further treatment of light oil. This is because the catalytic activity of the vanadosilicate decreases significantly during the reaction, owing to the dissolution of vanadium species in the silica framework into the acetonitrile solution (Shiraishi et al. 2003).

## **CHAPTER 2**

### **THEORETICAL BACKGROUND**

#### **2.1 INTRODUCTION**

Ultrasound assisted oxidation desulfurization (UAOD) process is designed to combine three complementary techniques, including ultrasonication, phase transfer catalysis, and transition metal catalyzed oxidation. Ultrasonication is the name given to the study and application of sound waves having frequency higher than the audible frequency of the human (16 kHz), and has been approved to be a very useful tool in increasing reaction rates, clearing, drilling, chemical process, and the production of emulsion. Phase transfer catalysis is a powerful tool in many areas of chemistry. It is often used for conducting reactions between two or more reagents in two or more phases. Transition metal catalyst, known as polyoxometallates (POMs), is a large and fast growing class of metal oxygen clusters that exhibit unique molecular structures, charge densities, and acidic and frequently reversible redox properties. It has wide applications in the field of analytical chemistry, biochemistry, and solid-state device. However, the most important application of POMs is in the field of catalysis as oxygen and multielectron relays (Hill, 1992; Moffat, 2001; Pope and Muller, 2001). This chapter is to describe the basic concepts of these three techniques, which could lead to be a better understanding of their synergistic interaction in UAOD system, are described in the chapter.

## **2.2 SONOCHEMISTRY**

### **2.2.1 Fundamental of ultrasound**

Ultrasonication is the name given to the study and application of sound waves having frequency higher than the audible frequency of the human (16 kHz), which can be divided into two sections, one is dealing with low amplitude vibrations and the other is with high energies. Basically, the low amplitude propagation is concerned with the effect of the medium on the waves, so permanent changes do not take place in the medium. The techniques employed for this purpose are applied to the non-destructive testing of materials. The good examples are determination of elastic constants, thickness measurements, and flaw detection. Reasons for using ultrasonic frequencies, as opposed to audio-frequencies, include: (a) shorter wavelengths occur at higher frequencies so that plane wave conditions are more easily realized. This is especially important for small specimens. (b) absorption coefficients are usually much higher and thus more easily measurable at higher frequencies. (c) frequencies associated with relaxation phenomena often fall within the ultrasonic range (Blitz, 1967).

High energy application is concerned with changes brought about by the waves in the medium. Its applications include cleaning, drilling, chemical processes, and the production of emulsions. These are carried out either directly by the agitation of the waves or through the phenomenon of cavitation. An important advantage of using higher frequency waves is that they are more easily focused (Blitz, 1967). In

this study, the high energy application of ultrasound was applied to combine other complementary techniques to increase the reaction rate of oxidation desulfurization associated with emulsion phenomena.

#### 2.2.2.1 Cavitation Mechanism

Cavitation is a phenomenon which has been observed in boiling water, and also in sea water in the vicinity of a rotating ship's propeller. It refers to the formation and the subsequent dynamic life of bubbles in liquids. These bubbles can be either gas or vapor filled and form in a wide variety of liquids under a wide range of conditions. Cavitation occurs in water, organic solvents, biological fluids, liquid helium, and molten metals, as well as many other fluids. It may be hydrodynamic, thermal, or acoustic in origin (Suslick, 1988).

In all cases of bubble formation, a nucleus is required. This may take a variety of forms. It may be a very small bubble (1 millionth of an inch in diameter) already existing in the liquid, or it may be a small pocket of gas cracking in the wall of the vessel containing liquid. Moreover, dust particles are good nuclei. Some defect or void in the structure of the liquid may act as a center around which a bubble will grow. Therefore, when ultrasound is used, the cavitational activity is directly proportional to the number density of particles present in the medium (Madanshetty and Apfel, 1991). Chemical effects due to ultrasound are not observed when there are no dissolved gases in the system, when the sound intensity is not greater than the cavitation threshold of the system (Fitzgerald et al., 1956), or when the reactant is

not volatile enough to enter the cavitation bubble during its formation (Griffing, 1952). Moreover, the nuclei remain after a bubble collapses. They will then serve again as nuclei for new bubbles.

Ultrasonic waves are a mechanical disturbance which consists of pressure fluctuations, positive and negative, above and below the pressure of the liquid in which they are traveling. A reduction in pressure encourages a submicroscopic bubble to grow. A pressure above that of the pressure in the liquid will discourage bubble growth or cause the collapse of one that has started to grow (Suslick, 1988).

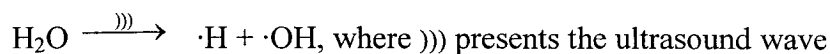
The sudden collapse of bubbles which have started to grow produces the characteristic effects usually associated with cavitation. Growth of the bubble occurs in a time interval corresponding to one-fourth of the period of the sound wave. Collapse occurs in a small fraction of that time period. Because of the rapidity of the collapse, large instantaneous pressures and temperatures are developed at the center of the bubble. Theoretically, a bubble may grow under influence of sound wave and reach a size of  $10^{-3}$  or  $10^{-2}$  inch. However, when it collapses, its size is about  $10^{-5}$  or  $10^{-6}$  inch. This is another reason that the localized pressure is so high. The total force in the collapsing bubble is applied over a minute area (Suslick, 1988).

The cavitation force is greatest at the center of the collapsing bubble. Its effect is formed in the vicinity because a liquid transmits shock waves readily. The intensity of the radiated shock wave decreases with the square of the distance from the sound source, but the pressure decreases only in inverse proportion to the distance. Therefore, in most ultrasonic liquid processing operations, it is essential to

indicate that it is not the sound wave that does the work. It is the high instantaneous pressure created by the catastrophic collapse of a cavitation bubble. Truly, the sound wave helps to form the cavitation bubble, but its role is to supply energy at a relatively slow rate. This energy will be released suddenly when the negative pressure disappears.

#### 2.2.2.2 Cavitation Chemistry

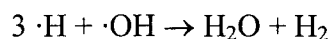
It is also known that under ultrasonic cavitation sites aqueous sonochemistry leads to the free radicals formed



under a reducing atmosphere, for example if sodium borohydride is added



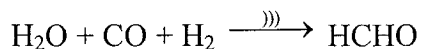
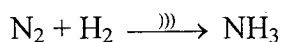
production of  $\text{H}_2$  will eliminate water recombination



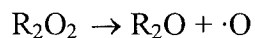
Therefore the H atoms are abundant and hydrogenation will occur because the H is more than the reverse formation of water by



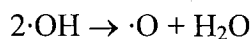
Further, it has been documented that



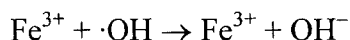
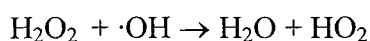
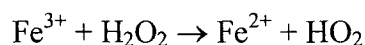
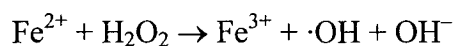
Furthermore, in the oxidation condition in the presence of peroxide, hydroperoxide, or hydrogen peroxide,  $R_2O_2$  where R could be hydrogen, then the release of O as



and at site of cavitation



Thus, oxygen will be abundant and the oxidative rendition proceeds. If water contains transition ion, such as iron, then Fenton type reaction will proceed. Usually this is termed as the metal ion catalyzed decomposition of hydrogen peroxide



Both OH and  $HO_2$  are strong oxidants. In this case a source of  $H_2O_2$  must be supplied, especially for a polyperoxometallate used as a catalyst (Yen, 1999).

### 2.2.2 Factors Affecting Sonochemistry

It is well known that cavitation is the sonochemistry and the origin of sonochemical effect. The ambient conditions of the reaction system can greatly influence the intensity of cavitation, which directly affects the reaction rate and/or yield. These conditions include the reaction temperature, external pressure, irradiation frequency, ultrasonic intensity, and choice of solvent.



#### 2.2.2.1 Temperature

The cavitation process is temperature-dependent because several of the important characteristics of a liquid that affect cavitation intensity are themselves temperature-dependent. The principal ones are vapor pressure, surface tension, the diffusion rates of gases that are dissolved in the liquid, and the solubility of air and other gases in the liquid (Thompson and Doraiswamy, 1999).

It is well known that the kinetics of most chemical reaction increases with increasing temperature, however, an increase in the ambient reaction temperature results in an overall decrease in the sonochemical effect. As the reaction temperature is raised, the equilibrium vapor pressure of the system is also increased, which decreases the cavitation threshold and leads to easier bubble formation. However, the cavitation bubbles are formed contain more vapor. The collapse of vapor-filled bubbles cushions the implosion and reduces the ultrasonic energy. In general, the largest sonochemical effects are observed at lower temperature when a majority of the bubble contents is gas. Therefore, to determine the extent to which changes in temperature are asparate to affect the cavitation intensity, it is necessary to consider its relative effect on reaction kinetics, vapor pressure, surface tension, and other characteristics such as ultrasonic intensity (Thompson and Doraiswamy, 1999).

#### 2.2.2.2 External Pressure

Increasing the ambient reaction pressure generally results in an overall increase in the sonochemical effect because of the decrease in the vapor pressure of the mixture. Decreasing the vapor pressure increases the intensity of the implosion, thus increasing the ultrasonic energy produced for cavitation (Thompson and Doraiswamy, 1999). However, ultrasonically induced cavitation can be suppressed completely by the application of sufficient external pressure. It appeared that operating at pressures of 200 psig and above increased the cavitation threshold in the system to a level where the cavitation bubbles could not be produced or were produced in such small quantities (Moulton et al. 1983, 1987). Moreover, a reduction in the static pressure in a liquid results in surface tension forces becoming predominate in determining the critical bubble size for cavitation.

#### 2.2.2.3 Ultrasonic Frequency

The most important effect of frequency on the cavitation process is to determine the maximum size of a bubble nucleus. Those will grow to a size which results in a catastrophic collapse. Bubbles larger than this size will not grow. At very high frequencies, the cavitation effect is reduced because either (1) the rarefaction cycle of the sound wave produces a negative pressure which is insufficient in its duration and/or intensity to initiate cavitation or (2) the compression cycle occurs faster than the time required for the micro-bubble to collapse (Thompson and Doraiswamy, 1999). Therefore, an increase in the frequency of the applied sound

wave requires an increase in its intensity in order to remain above the threshold value needed for cavitation. Most sonochemical reactions are carried out in the low frequency range between 20 kHz to 50 kHz.

#### 2.2.2.4 Ultrasonic Intensity

Generally, the sonochemical effects will increase with increasing ultrasonic intensity. However, there is a threshold level of intensity for the sound field. The intensity of ultrasound should be larger than this threshold to occur the cavitation. Moreover, high intensities of impressed sound are accompanied by all alteration of the wave shape. Due to high vibration amplitude of sound wave, decoupling occurs when the source of ultrasound does not contact with the medium, particularly if large numbers of cavitation bubbles build up at or near the emitting source of the transducer. It results in a heavy loss of power transferring from the source to the medium (Mason, 1999). Therefore, it is difficult to obtain significantly more vigorous cavitation by an increase in the level of the applied sound field. There usually exists an optimum ultrasonic intensity in most sonochemical systems.

#### 2.2.2.5 Choice of Solvent

The properties of solvent include vapor pressure, surface tension, and viscosity, which can significantly affect the occurrence and intensity of cavitation. Cavities are more readily formed when a solvent with a high vapor pressure, low viscosity, and low surface tension is used. However, the intensity of cavitation is

benefited by using solvents with opposing characteristics which is low vapor pressure, high viscosity, and high surface tension (Thompson and Doraiswamy, 1999). Moreover, when using the extremely volatile solvent, diethyl ether, which has a vapor pressure of 0.73 atm at 25 °C, the cavitation was inhibited (Luche, 1998). Therefore, to achieve higher sonochemical effects as a result of more intensive collapsed of cavitation bubbles, selecting of solvent is frequently dictated by the type of chemistry involved.

### **2.2.3 Ultrasound and Phase Transfer Catalysis**

It is well known that phase transfer catalysis (PTC) is a powerful tool in many areas of chemistry. It is often used for conducting reactions between two or more reagents in two or more phases. The use of ultrasound can significantly improve the reaction efficiency under phase transfer conditions (Thompson and Doraiswamy, 1999, Shah, et al. 1999).

Most phase transfer catalysis is surface-active species that lowers surface tension and permits easy formation of micro-bubbles under ultrasound. Ultrasound helps to improve the liquid-liquid interfacial area through emulsification, which is important for viscous films containing gas-filled bubbles and cavitation bubbles. Gas-filled bubbles are within the films, oscillating because of ultrasound, mobilized by acoustic streaming, and entraining some of the film. Simultaneously, cavitation bubbles spray solvent on the film that covers the pulsing gas bubble. The pulsing action of the gas bubble is therefore disrupted and the liquid is scattered on its

surface, leading to highly dispersed emulsions (Shah, 1999, Mai et al. 2003). Therefore, the addition of PTC to ultrasonic systems reduces the surface tension of the liquid, thus reducing the cavitation threshold and facilitating the generation of bubbles. Finally, it results significantly in improving the reaction efficiency.

### **2.3 HYDROGEN PEROXIDE AS OXIDANT**

Oxidation of sulfides is the most straightforward method for the synthesis of sulfides and sulfones. A large number of oxidants, particular those with oxygen and donor capabilities, have been extensively studied in context with transition metal catalyzed oxidation process. The primary criteria in choosing an appropriate oxidant for a large-scale operation includes the active oxygen content, the selectivity ability in its application, and the environmental effects. The active oxygen content is calculated as the ratio between the weight of oxygen that can be transferred to a suitable substrates and the molecular weight of the oxidant (Strukul, 1992). Table 2.1 summarizes the active oxygen content and the product of some common oxidants.

As is clear from Table 2.1,  $\text{H}_2\text{O}_2$  largely exceeds all the others with the exception of ozone which is highly noxious and requires costly equipment for its generation. Hydrogen peroxide is a clear, colorless liquid that is completely miscible with water. Crystal structure determination of pure  $\text{H}_2\text{O}_2$  shows that H-O and O-O bond distances is 1.01 and 1.453 , respectively, while the corresponding H-O-O-H. The dihedral angle of H is close to  $90^\circ$ . Another interesting structure feature of  $\text{H}_2\text{O}_2$

is the presence of hydrogen bonding through the peroxy oxygens indicating significant Lewis basicity (Strukul, 1992).

**Table 2.1 Single oxygen atoms donors (Strukul, 1992)**

Donor	% Active oxygen	Product
H <sub>2</sub> O <sub>2</sub>	47.0 <sup>a</sup>	H <sub>2</sub> O
O <sub>3</sub>	33.3	O <sub>2</sub>
<i>t</i> -BuOOH	17.8	<i>t</i> -BuOH
NaClO	21.6	NaCl
NaBrO	13.4	NaBr
HNO <sub>3</sub>	25.4	NO <sub>x</sub>
KHSO <sub>5</sub>	10.5	KHSO <sub>4</sub>
NaIO <sub>4</sub>	7.2 <sup>b</sup>	NaIO <sub>3</sub>
PhIO	7.3	PhI

a: Calculated on 100% H<sub>2</sub>O<sub>2</sub>. b: Assuming only one oxygen atom is utilized.

Hydrogen peroxide is quite stable in neutral aqueous solution and resists, to decomposition for a long time if kept from light, any impurities, and higher temperature (Moiseev, 1999). Industrially, hydrogen peroxide is employed mainly as a non-selective oxidant in operations like the bleaching of paper, cellulose and textiles, water purification, and in the formulation of detergents (Strukul, 1992).

H<sub>2</sub>O<sub>2</sub> is also a powerful oxidant with a high oxidation potential. However, it reacts very slowly with organic compounds such as organic sulfides and alkenes. In

order to take advantage of its power, it is required to “active” H<sub>2</sub>O<sub>2</sub> with transition metal catalyst. Therefore, the activation of H<sub>2</sub>O<sub>2</sub> is able to improve its reactivity through the formation of intermediate peroxides, which are more effective oxidants than hydrogen peroxide.

## 2.4 POLYOXOMETALATE CATALYSIS

### 2.4.1 Polyoxometalates

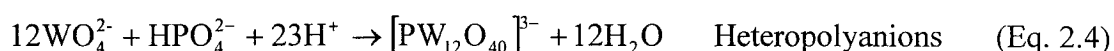
Polyoxometalates (POMs) containing early transition-metal oxygen-anion clusters are a large and rapidly growing class of compounds. The majority of the applications of POMs are found in the area of catalysis. About 80-85% of patent and applied literature claims or investigates POMs for their catalytic activity. The remaining 15-20% of the applications can be grouped in the categories of biochemistry, analytical chemistry, and solid-state device (Katsoulis, 1998).

Polyoxometalates consist of isopolyanions and heteropolyanions. Isopolyanions contain only one metal and oxide ions. Heteropolyanions contain one or more p or d block elements as “heteroatom(s)”, typically tetrahedral, about which the metal-oxo framework is built (Pope, 1983; Hill, 1995; Barker and Glick, 1998). These complexes can be represented by the general formulas as Eq. 2.1 and Eq. 2.2.



Where M is usually tungsten (VI), molybdenum (VI), vanadium (V), niobium (V), tantalum (V), and Titanium (IV) in their d<sup>0</sup> electron configuration are usually

referred as “addenda ions” (Hill, 1995; Barker and Glick, 1998). Moreover, isopolyanions and heteropolyanions are usually prepared and isolated from aqueous solution during acidification. In aqueous solution of oxoanion such as  $\text{WO}_4^{2-}$ , isopolyanions in cluster form of  $\text{W}_{10}\text{O}_{32}^{4-}$  are formed (Eq. 2.3). Furthermore, in the presence of two types of oxoanions such as  $\text{WO}_4^{2-}$  and  $\text{HPO}_4^{2-}$ , heteropolyanions such as  $\text{PW}_{12}\text{O}_{40}^{3-}$  are produced (Eq. 2.4) (Pope, 1983).



The structures of isopolyanions and heteropolyanions appear to be governed by the well-known electrostatic and radius-ratio principles observed for extended ionic lattices, and have sizes of a few nm. Basically, they are customarily described in terms of assemblages of metal-centered  $\text{MO}_n$  polyhedra that are linked by shared corners, edges, and faces (Pope, 1983). POMs are composed primarily of  $\text{MO}_6$  octahedra but in some case by  $\text{MO}_5$  pentahedra and  $\text{MO}_4$  tetrahedra. The most common types of  $\text{MO}_6$  octahedra are those containing one terminal oxo group and five bridging oxo groups (Type I octahedra), and those containing two terminal oxo groups and four bridging oxo groups (Type II octahedra) (Hill, 1995).

#### 2.4.2 Heteropoly Acids – Keggin Heteropolyanions

Catalysis by heteropoly acids (HPAs) and related polyoxometalate compounds is rapid growing within the last four or five decades. HPAs are efficient oxidants and



exhibiting fast reversible multielectron redox transformation under mild condition. The first characterized and the best known of these is the Keggin heteropolyanion which is the tetrahedrally-coordinated heteroatoms and typically represented by the formula structure  $[XM_{12}O_{40}]^{x-8}$ , where X is the central atom ( $Si^{4+}$ ,  $P^{5+}$ , etc.), X is its oxidation state, and M is the metal ion ( $Mo^{6+}$  or  $W^{6+}$ ). The  $M^{6+}$  ions can be substituted by many other metal ions, e.g.,  $V^{5+}$ ,  $Co^{2+}$ ,  $Zn^{2+}$ , etc. The Keggin anion is composed of a central tetrahedron  $XO_4$  surrounded by 12 edge- and corner-sharing metal-oxygen octahedra  $MO_6$ , shown as Figure 2.1. The octahedra are arranged in four  $M_3O_{13}$  groups. Each group is formed by three octahedra sharing edges and having a common oxygen atom which is also shared with the central tetrahedron  $XO_4$  (Kozhevnikov, 1998).

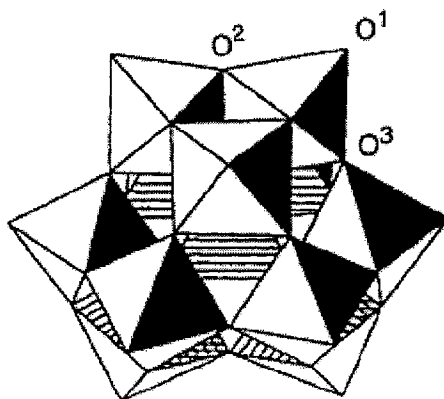


**Figure 2.1** The Keggin structure of the  $[XM_{12}O_{40}]^{x-8}$  anion ( $\alpha$ -isomer); terminal ( $O^1$ ), edge-bridging ( $O^2$ ), and corner-bridging ( $O^3$ ) oxygen atoms. (Kozhevnikov, 1998)

HPAs catalysis in homogeneous liquid phase has exhibited more efficient and cleaner processing compared to conventional mineral acids. Being stronger acids, HPAs will have significantly higher catalytic activity than mineral acids. Particularly in organic media, the molar catalytic activity of HPA is often 100-1000 times higher than that of H<sub>2</sub>SO<sub>4</sub>. This makes it possible to carry out the catalytic process at a lower catalyst concentration and/or at a lower temperature (Kozhevnikov, 1998).

The relative activity of Keggin HPAs primarily depends on their acid strength. Other properties such as the oxidation potential which determines the reducibility of HPA by reaction medium, as well as the thermal and hydrolytic stability are also important. The properties for the most common HPAs are summarized in Table 2.2.

**Table 2.2 The order of different properties for the most common HPAs (Kozhevnikov, 1998)**

Properties	The order of common HPAs
Acid strength	PW > SiW ≥ PMo > SiMo
Oxidation potential	PMo > SiMo >> PW > SiW
Thermal stability	PW > SiW > PMo > SiMo
Hydrolytic stability	SiW > PW > SiMo > PMo

Usually, tungsten HPAs are the catalysts of choice because of their stronger acidity, higher thermal stability, and lower oxidation potential compared to molybdenum HPAs. Generally, if the reaction rate is controlled by the catalyst acid strength, PW shows the highest catalytic activity in the Keggin series (Kozhevnikov, 1998).

The major problem and limitation in the utility of homogeneous catalysis processes is the difficulty in catalyst recovery and recycling. However, the separation of products and recovery and recycling of catalyst often becomes much easier, if a homogeneously catalyzed reaction can be performed in a biphasic system. The biphasic system consists of two immiscible phases including liquid catalyst phase and a product/reactant phase with intense mass transfer between them. Furthermore, due to their high solubilities in a variety of polar solvents and insolubility in nonpolar solvents, HPAs are suitable catalysts for operating under phase-transfer conditions (Kozhevnikov, 1998).

#### 2.4.3 Ishii-Venturello Expoxidation

Duncan et al. have reported a more comprehensive kinetic and spectroscopic study on Ishii-Venturello expoxidation, which has thoroughly investigated 1-octene conversions and 1,2-epoxyoctane selectivities under biphasic conditions:  $\text{H}_2\text{O}_2$ /1-octene in  $\text{CHCl}_3$ , with 21 different polyoxometalates and cetylpyridinium chloride as the phase transfer agent. In this work, it was established that only  $[\text{PW}_{12}\text{O}_{40}]^{3-}$  and  $[\text{PW}_{11}\text{O}_{39}]^{3-}$  which rapidly form the polyperoxometalate  $\{\text{PO}_4[\text{WO}(\text{O}_2)_2]_4\}^{3-}$ , the effective species for expoxidation. It is because both POMs are labile and can degrade rapidly in aqueous  $\text{H}_2\text{O}_2$  to form the active epoxidizing agent PPM (Duncan et al. 1995, Yadav, et al. 2000).

The  $\{\text{PO}_4[\text{WO}(\text{O}_2)_2]_4\}^{3-}$  peroxotungstate was isolated and characterized crystallographically by Venturello et al. 1983 and Ishii et al. 1985. The anion

consisted of the  $\text{PO}_4^{3-}$  anion and two  $[\text{W}_2\text{O}_2(\text{O}_2)_4]$  species, shown as Figure 2.2. Moreover, The spectroscopic and kinetic investigations by Brégeault et al. 1991, Griffith et al. 1993, Thouvenot et al. 1994, and Hill et al. 1995 show that the  $\{\text{PO}_4[\text{WO}(\text{O}_2)_2]_4\}^{3-}$  is a catalytically important species among various peroxotungstates generated by the reaction of  $\text{H}_3[\text{PW}_{12}\text{O}_{40}]$  with excess hydrogen peroxide.

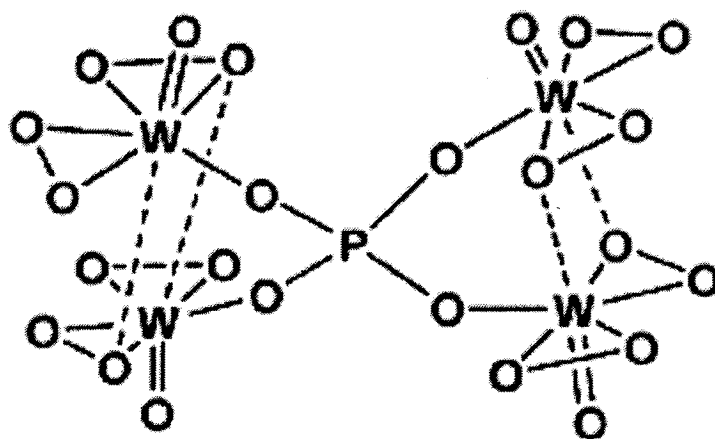


**Figure 2.2** Molecular structure of  $\{\text{PO}_4[\text{WO}(\text{O}_2)_2]_4\}^{3-}$

The general mechanism of Ishii - Venturello epoxidation proposed by Duncan (1995) is shown in Figure 2.3. The initial addition of  $\text{H}_2\text{O}_2$  leads to the gradual conversion of  $[\text{PW}_{12}\text{O}_{40}]^{3-}$  to a number of intermediate peroxo species (IPS) as  $[\text{P}_m\text{W}_n\text{O}_o(\text{O}_2)_p]^{X-}$  (Step 1). Further addition of  $\text{H}_2\text{O}_2$  will convert those intermediate peroxo species into the so-called subsequent peroxo species (SPS) as  $[\text{P}_q\text{W}_r\text{O}_s(\text{O}_2)_t]^{Y-}$  (Step 2). In presence of excess  $\text{H}_2\text{O}_2$ , SPS were oxidized into the

epoxidizing species PPM (Step 3). In the epoxidation reaction, two dominant steps exist: a slow epoxidation,  $\text{PPM} + \text{Alkene} \rightarrow \text{SPS} + \text{epoxide}$  (Step 4), followed by a rapid regeneration of PPM with  $\text{H}_2\text{O}_2$  (Step 5) (Duncan et al. 1995, Mai et al. 2003). Therefore, the most remarkable catalytic activity in the Ishii-Venturello system is the formation in situ of polyperoxometalate (PPMs), which are much more active and selective oxidant than hydrogen peroxide.

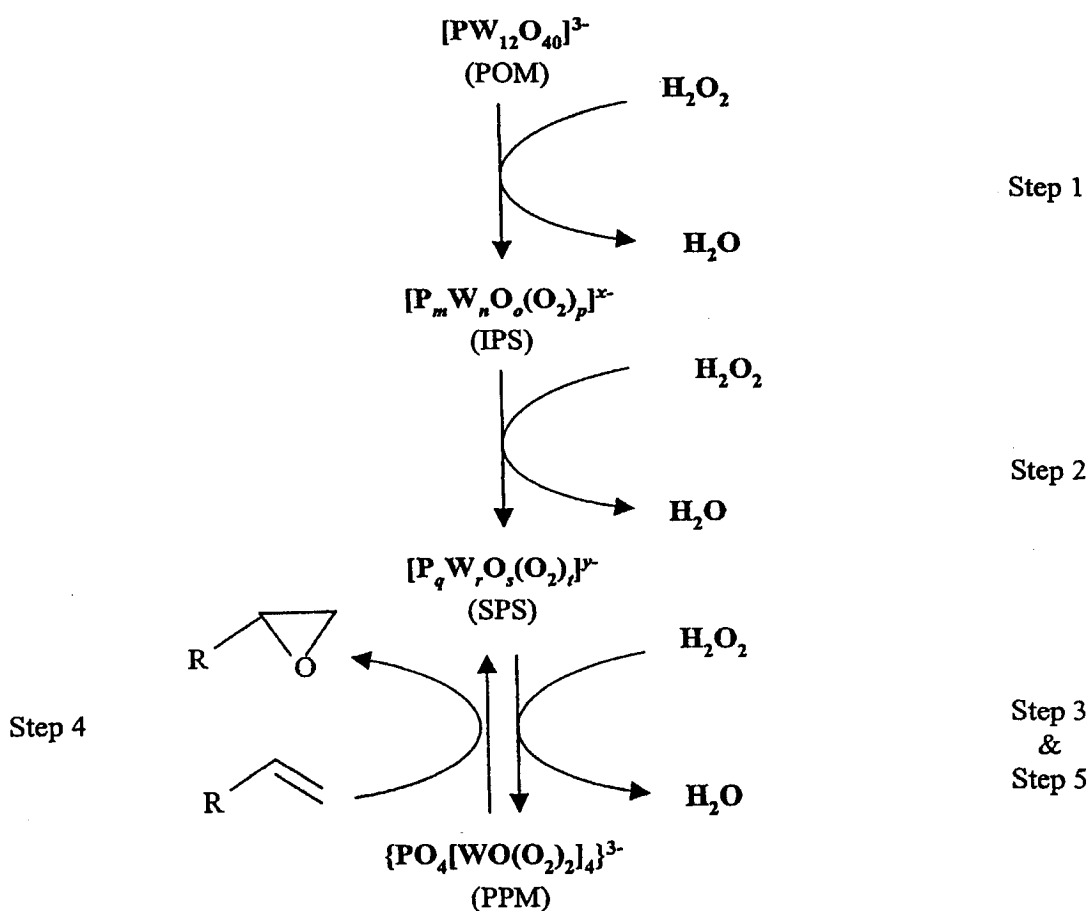


Figure 2.3 Dominant processes in Ishii-Venturello epoxidation (Duncan, 1995)

## 2.5 PHASE TRANSFER CATALYSIS

### 2.5.1 Quaternary Ammonium Salts

Phase transfer catalysis (PTC) is a powerful tool to improve process efficiency, product selectivity and providing mild reaction conditions in organic chemical reactions. It is often used for conducting reactions between two or more reagents in two or more phases. The most commonly used phase-transfer catalysis is quaternary ammonium salts. Among those, tetrabutylammonium salts, tetraoctylammonium salts, benzyltriethylammonium chloride, and tricaprylmethylammonium chloride (Aliquat 336 or Adogen 464) are more frequently applied and commercially available (Stark, et al. 1994; Sasson and Neumann, 1997).

Quaternary ammonium salts consist of a central nitrogen atom which is joined to four organic radicals and one and various hydrophilic anions. Figure 2.4 exhibits their general structure. "R" represents alkyl, aryl, or heterocyclic radical substitutes containing 4 to 60 carbon atoms bound to a nitrogen atom. Usually, the total cationic portion is associated with a halide ion. Moreover, quaternary ammonium salts are generally stable under neutral or acidic conditions up to 150 °C. In basic media, the ammonium salts are generally far more susceptible to degradation, but are more stable than the corresponding phosphonium salts (Jones, 2001).

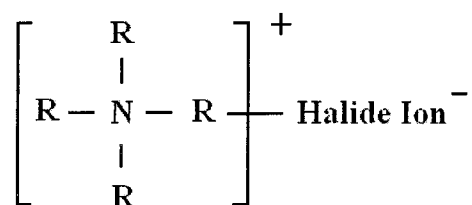


**Figure 2.4 General structure of quaternary ammonium salts (Jones, 2001)**

### 2.5.2 Starks' Extraction Mechanism

In its simplest form, the phase-transfer catalyzed nucleophilic substitution reaction,  $\text{RX} + \text{Y}^- \rightarrow \text{RY} + \text{X}^-$ , in which the active nucleophile  $\text{Y}^-$  is transferred from the aqueous into the organic phase, can be depicted by Figure 2.5. The mechanism requires the 'extraction' of the nucleophilic anion by the quaternary ammonium cation  $\text{Q}^+$  as the ion-pair  $[\text{Q}^+\text{Y}^-]$  into the organic phase, where the nucleophilic reaction can take place. Subsequent to the reaction the 'spent' catalyst forms an ion pair with the released anion  $\text{X}^-$  and equilibration of  $[\text{Q}^+\text{X}^-]$  between the two phases establishes a cycle, which will continue until all the nucleophilic species  $\text{Y}^-$  or the organic substrate  $\text{RX}$  is consumed (Jones, 2001).

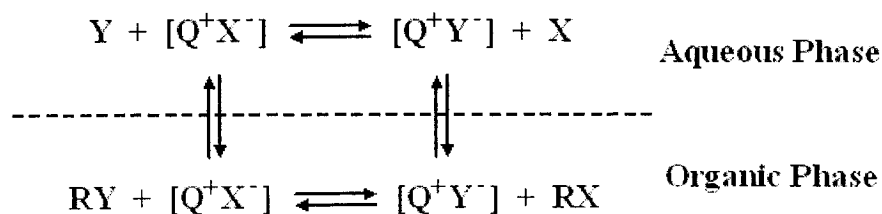


**Figure 2.5 Starks' extraction mechanism (Jones, 2001)**

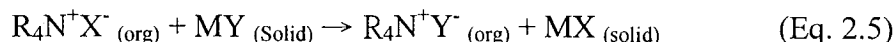
The thermodynamic of the 'extraction' mechanism is extremely complex. In the initial equilibration of the ion pairs, reaction has to be taken not only because of the relative stabilities of the ion-pairs but also of the relative hydration of the anionic species. Assuming the complete non-solvation of the ion-pairs, the formation of the ion-pair  $[Q^+Y^-]$  will generally be favored when the relative hydration of  $X^-$  is greater than that of  $Y^-$ . However, in many cases, the anion of the ion-pair is hydrated, which has a significant effect both on equilibrium between the ion-pairs in the aqueous phase and the relative values of the partition coefficients of the two ion-pairs  $[Q^+X^-]$  and  $[Q^+Y^-]$  between the two phases (Jones, 2001).

### **2.5.3 Solid-Liquid Anion Exchange**

Originally, the crystalline sodium or potassium formates are not accessible to quaternary ammonium salts in organic solution, and therefore direct solid-liquid anion exchange is not possible. However, when a small amount of water is added, a thin aqueous film is formed on the surface of the solid crystals and anion transport is possible. Moreover, it was shown that with a limited amount of water, the transfer of the formate anion from the solid state into the water thin film is the rate-determining step for the entire process. In contrast to liquid-liquid exchanges, in solid-liquid systems the nature of the cation, M, has a profound effect on the exchange process. The exchange rate and the maximum conversion obtained were found to depend on the aqueous solubility ratio  $MY/MX$  (Eq. 2.5). Thus, for solid-liquid anion exchange,



the order of reactivity (solubility ratio at 100 °C in parentheses) is exhibited as  $\text{Ca}^{2+} < \text{Li}^+ < \text{Na}^+ < \text{K}^+$  (Sasson and Neumann, 1997).



Dermeik and Sasson have demonstrated that the maximum conversion of the fluoride-chloride exchange reaction:  $\text{RCl} + \text{KF} \rightarrow \text{RF} + \text{KCl}$  catalyzed by quaternary onium salts was found to be strongly dependent on the water content of the inorganic salt. A maximum conversion was obtained when the potassium fluoride contained 0.33 mol of water per mol of KF. This phenomenon is due to better extraction of the fluoride anion when the KF is drier, offset by decomposition of the catalyst in the absence of water. It was shown that the selectivity constant is dependent on composition of the inorganic salt and on temperature (Dermeik and Sasson, 1985)

#### 2.5.4 The Design of Catalytic System

The factors that should be considered when choosing a phase transfer catalyst include reactivity, selectivity, and ease of separation from product and catalyst decomposition. In industry, one should additionally consider the availability, cost and toxicity of the catalyst. Reactivity is usually the primary criterion. Generally, the reactivity of QAS is subject to such factors as the lipophilicity of the quaternary ammonium cation, the degree of hydration of its anion and its stability under the reaction conditions (Sasson and Neumann, 1997).

One of the PTC features is the strong effect of the catalyst structure on the reaction rate. The cation of QAS consists of ammonium fragment (hydrophilic) and carbon chain fragment (lipophilic). It is obvious that increasing the length of carbon chain will increase its lipophilicity, thus improve the extraction or transfer rate of the active ion pair to the organic phase. However, the optimum size of the cation should be determined by the nature of the PTC reaction and the distribution equilibrium of the QAS and reactive species in both organic and aqueous phase (Sasson and Neumann, 1997; Dehmlow and Dehmlow, 1993).

The great influence of the catalyst anion on the reaction rate has been shown in numbers of publications. Dehmlow and Dehmlow have represented a general list of anions with decreasing order extractability for a given quaternary cation (anion lipophilicity) in liquid-liquid systems:  $\text{picrate} \gg \text{MnO}_4^- > \text{SCN}^- > \text{I}^- \approx \text{ClO}_3^- \approx \text{ArSO}_3^- > \text{NO}_3^- > \text{Br}^- \approx \text{CN}^- \approx \text{BrO}_3^- \approx \text{ArCOO}^- > \text{NO}_2^- \approx \text{Cl}^- > \text{HSO}_4^- > \text{HCO}_3^- \approx \text{CH}_3\text{COO}^- > \text{HCOO}^- > \text{F}^- \approx \text{OH}^- > \text{SO}_4^{2-} > \text{CO}_3^{2-} > \text{PO}_4^{2-}$ . It indicates that the anion with lower lipophilicity has higher ability for hydration, thus permits the faster transfer rate of the active ion pair into the organic phase (Sasson and Neumann, 1997; Dehmlow and Dehmlow, 1993).

Currently, the use of ultrasound with phase transfer catalyst has attracted considerable interests and has led to promising developments (Mason, 1990; Luche, 1998; Shah, et al. 1999). With the help of ultrasound, the two phase system with PTCs can perform the emulsions. Most of PTCs are surfactants which can lower the interfacial tension and allow emulsification to very small droplet size (10 nm in

fiameter or smaller) under the ultrasonication (Schramm, 1992). When very fine emulsions are formed, the interfacial area available for PTC reactions is significantly increased, thus increasing the rate of the reaction. Furthermore, ultrasound can also enhance the efficiency of PTC reactions by generating more reactive intermediates so that the reaction proceeds in a short time and under mild conditions.

#### **2.5.5 Phase Transfer Agent**

In this study, Phase transfer catalyst can react as phase transfer agent (PTA) which is used to aid the oxygen transfer in both aqueous and organic phases. When the reaction is inhibited in aqueous/organic system, a “phase transfer agent” con brings the complex into an organic phase for the oxygen transfer to take place in the target compound, allowing the target compound to be oxidized. Usually PTA is equivalent to surfactant. Furthermore, Selection of a phase transfer agent is usually the most important step in design and development of PTA reaction system. Quaternary ammonium salts (QAS) are least likely to interfere in chemical reaction (Dehmlow and Dehmlow, 1993).

## **CHAPTER 3**

### **ULTRASOUND IN INDUSTRIAL APPLICATION**

#### **3.1 INTRODUCTION**

Due to the stringent rules requiring ultra-low sulfur content in diesel fuels, it is necessary to develop alternative methods of desulfurization of fossil fuel derived oil, such as diesel. Current technology is not sufficient to solve this problem. The ultrasound assisted oxidative desulfurization (UAOD) system was first adopted by Dr. Mai at Dr. Yen's group at USC. High sulfur removal has been accomplished by a probe type ultrasound unit. However, the probe type unit is merely at a batch scale. This is sufficient for research purposes but inadequate for large-scale commercial production. A continuous flow system can fulfill the needs of practical application. Therefore, a continuous-flow reactor will be operated as a modular unit. Based on this concept, a tubular reactor (sonoreactor) attached to a pump station will be developed and operated to reduce any type of diesels to an ultra low-sulfur requirement. Different tubular reactors will be assembled based on the composition of the sulfur compounds in different diesels. Optimization of the treatment procedure will be simplified into a tubular reactor treatment. Furthermore, other impurities will be minimized.

Among all manufactories, only Branson Inc. could provide us with a commercial unit that met our requirements. However, because of the inappropriate

frequency and large capacity, this unit couldn't achieve the best results. After consulted with many ultrasound experts and transducer specialists, Dr. Shung, a Professor from the Department of Biomedical Engineering at USC, kindly provided us with a lot of valuable suggestions and strongly recommended the Blatek Tech. at Penn State University. Therefore, a tailor-made module reactor (sonoreactor) was successfully assembled by Dr. Geng, the senior engineer at Blatek Tech. It is also the first time for Dr. Geng to construct a unit designed specifically for oil industries. After overcame a lot of difficulties, this portable unit, which contains an RF amplifier, a function generator, a pretreatment tank, and a pipeline system, was finally developed and operated in ambient environment. This chapter will introduce the ultrasound in industrial applications and the design of this tailor-made tubular reactor - the sonoreactor.

## **3.2 ULTRASONIC TRANSDUCER**

### **3.2.1 Transducer**

Transducer is a device that converts variations in one energy form into corresponding variations in another, usually electrical form (Payne, 2002). One widely used class of transducers consists of devices that produce an electric output signal, e.g., microphones, phonograph cartridges, and photoelectric cells. Other widely used transducers accept an electric input, e.g., loudspeakers, light bulbs, and solenoids. Moreover, transducer is sometimes applied to devices producing an output in the same form as their input, e.g., transformers and filters. Theoretically, ultrasonic transducers convert energy in one form to another into acoustic energy and can be roughly divided into two types – mechanical transducers and electromechanic transducers.

### **3.2.2 Mechanical Transducer**

Mechanical transducers convert the kinetic energy of stream of fluid into acoustic energy. The best example is whistle.

#### **3.2.2.1 Whistle**

Sound may be generated by passing a gas or liquid through an orifice or over an edge, which can be known as whistle and satisfactory for generation of energy in suitable materials. The passage of the gas generates vortices, spaced periodically, which propagate the sound wave. While a simple circular hole applied for this

purpose, more stable results may be obtained in various ways. Those devices may be used in either gas or liquids, where their low impedance allows better coupling (Calin, 1960)

*Galton whistle* is basically consists of a jet which sends out a stream of gas against a small cavity. The principle of Galton's whistle is shown diagrammatically in Figure 3.1. A stream of compressed air is pumped through a passage formed by the gap between two concentric cylinders A and B. After it impinges on to the wedge-shaped edge, resonate cavity is formed by a cylinder C and plunger D. The air stream sets the cylinder end into oscillation. This small ultrasonic whistle produces high intensity sounds at frequencies that are essentially inaudible to humans.

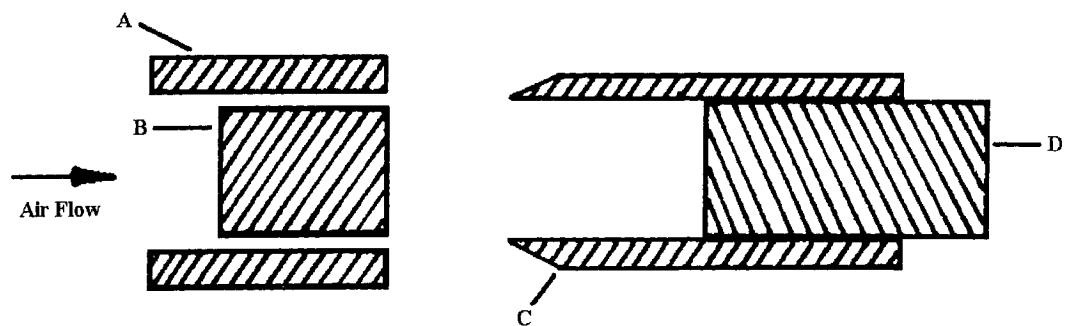


**Figure 3.1 Cross-section through Galton's whistle (Gooberman, 1969)**  
(A and B – Concentric Cylinders, C – Wedge, D – Plunger)

*Hartmann whistle* is similar to Galton whistle but works on a different principle. Figure 3.2 shows a schematic cross-section of the whistle. A jet of air flows through the cylinder A, which consists of a nozzle (cylinder A) where a jet of

compressed air emerges. At the exit, the air velocity increases and exceeds that of sound giving rise to a shock wave a short distance out from the end of the cylinder. At this point, the shock wave is unstable and causes the air within cavity to oscillate. This device is capable of producing high frequency, high amplitude pressure and velocity perturbations. Therefore, the Hartmann generator has been suggested as a precipitator of dust or fog, and also been used for signaling and active flow control applications.

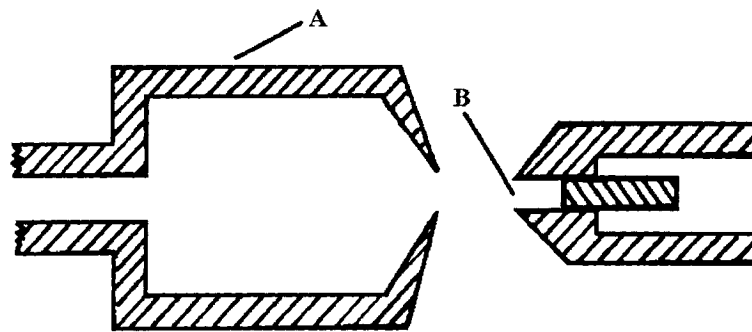


**Figure 3.2 Cross-section through Hartmann's whistle (A- Cylinder, B-Resonant cavity) (Gooberman, 1969)**

#### 3.2.2.2 Jet-edge Devices

The principle of Jet-edge device is shown diagrammatically in Figure 3.3. A stream of fluid is pumped through a circular hole in a plate of thickness. Because of viscous forces at the fluid and solid boundary, vortices are set up which travel with a velocity until they reach the far side of the plate where they radiate a pressure pulse in all directions. The pressure pulse radiated by one such vortex will travel back to the other side of the plate where it will provoke another vortex to form. Because the



jet is convective unstable, the interaction between jet and wedge produces a dipole pressure field on the nozzle. Therefore, the oscillating jet produced by the orifice causes sound produced by the blade. Furthermore, the stability of this system can be improved by placing a suitably resonant wedge-ended plate near the hole.

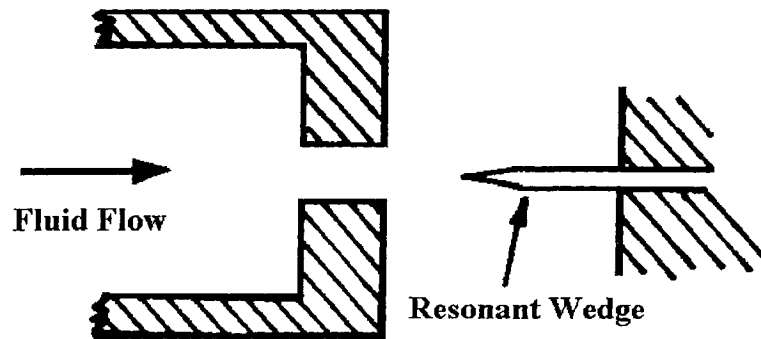


**Figure 3.3 Cross-section through a jet-edge system (Gooberman, 1969)**

Jet-edge generators are suitable for both gases and liquids and provide a stable and simple means for generating fairly high powers suitable for bulk processing of fluids by ultrasonic energy such as manufacturing emulsions and dispersions (Gooberman, 1969).

### **3.2.3 Electromechanic Transducers**

Electromechanical transducers convert electrical into acoustic energy. There are five types of such transducers in current use: moving coil, electrostatic, piezoelectric, ferroelectric and magnetostrictive types. Piezoelectric and

magnetostrictive types are the commonest in commercial use, and will discuss in following two sections.

#### 3.2.3.1 Piezoelectric Transducer

Certain polar molecules form crystals which lack centers of symmetry. If a plate cut from such a crystal is mechanically deformed a voltage develops between two faces of the plate and this phenomenon is known as the direct piezoelectric effect. Conversely, if a voltage is applied between the two faces the plate will deform because of the inverse piezoelectric effect.

The conversion of electrical pulses to mechanical vibrations and the conversion of returned mechanical vibrations back into electrical energy are the basis for ultrasonic testing. The active element is the heart of the transducer as it converts the electrical energy to acoustic energy, and vice versa (Gooberman, 1969). Theoretically, there are two general classes of piezoelectric materials: those that are naturally piezoelectric and those that are piezoelectric only after they have received special treatment. Examples of the first class are naturally occurring crystals of quartz and tourmaline, artificially grown crystals of ammonium and hydrogen phosphate, Rochelle salt, lithium sulfate and lead niobate. The other class of materials is those that possess an enhanced electrostrictive effect and can be made to show piezoelectric properties after being subjected to a special treatment which causes them to become polarized. Barium titanate and lead zirconate-titanate are examples of electrostrictive materials.

Piezoelectric transducers are not frequency limited. The active element of most acoustic transducers used for commercial applications is a piezoelectric ceramics, which can be cut in various ways to produce different wave modes. A large piezoelectric ceramic element can be seen in the image of a sectioned low frequency transducer. Piezoelectric crystals made from quartz crystals and magnetostrictive materials were primarily used in early 1950. (Gooberman, 1969) When piezoelectric ceramics were introduced they soon became the dominant material for transducers, because they have good piezoelectric properties and easy to manufacture into a variety of shapes and sizes. They also operate at low voltage and are usable up to about 300°C. Figure 3.4 shows a schematic diagram of an ultrasonic transducer made by piezoelectric ceramics.

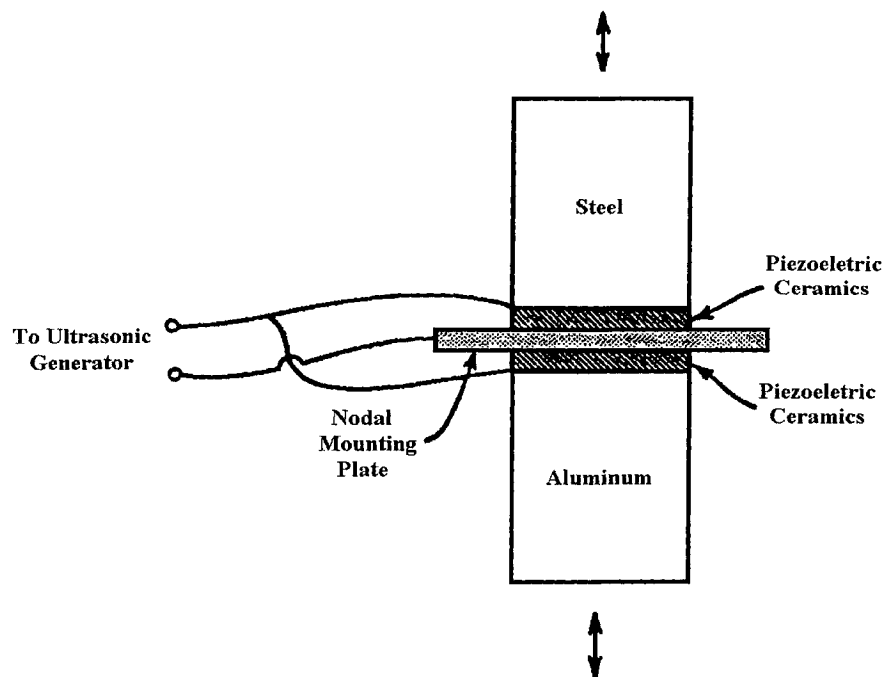


**Figure 3.4 Schematic diagram of piezoelectric transducer (Gooberman, 1969)**

Today's piezoelectric ultrasonic transducers are reliable, efficient devices which can be used with confidence in all power ultrasonic applications. The fact is that piezoelectric transducers are capable of providing a wider range of frequency and waveform characteristics and higher electrical conversion efficiency. Figure 3.5 shows the design diagram and product of its commercial application. Therefore, piezoelectric transducers are a good choice for current advanced technology.

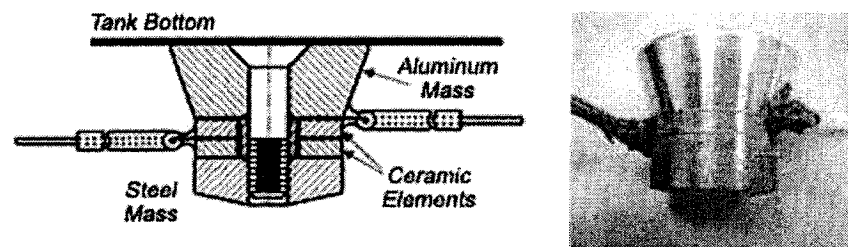


**Figure 3.5 Piezoelectric transducers in commercial application**  
(website: [http://www.blackstone-ney.com/04.TP\\_mag\\_vs\\_piezo.php](http://www.blackstone-ney.com/04.TP_mag_vs_piezo.php))

### 3.2.3.2 Magnetostrictive Transducers

The name magnetostriction or piezomagnetism is given to the phenomenon that when some materials are magnetized a change in dimensions occurs. This change can be either positive or negative in a direction parallel to the magnetic field and is independent of the direction of the field (Gooberman, 1969).

Two materials most commonly used for constructing magnetostrictive transducers are pure nickel and iron-cobalt alloys (49 % iron, 49 % cobalt and 2 % vanadium). Figures 3.6 shows the design of magnetostrictive transducers which

consist of a large number of nickel plates or laminations arranged in parallel with one edge of each laminate attached to the bottom of a process tank or other surface to be vibrated. A coil of wire is placed around the magnetostrictive material. When a flow of electrical current is supplied through the coil of wire, a magnetic field is created. This magnetic field causes the magnetostrictive material to contract or elongate and thereby obtain a usable amount of acoustic power output. However, due to physical size limitations of the magnetostrictive transducer, it is inherently limited to operate at frequencies below approximately 30 kHz. Because frequency is dependent on the length of the transducer, higher frequency requires a shorter and shorter length.

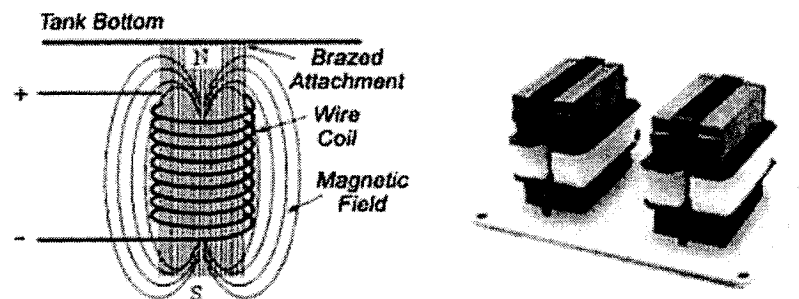


**Figure 3.6 Basic equivalent circuit for a magnetostrictive transducers and it's commercial application**  
(website: [http://www.blackstone-ney.com/04.TP\\_mag\\_vs\\_piezo.php](http://www.blackstone-ney.com/04.TP_mag_vs_piezo.php))

### 3.3 ULTRASONIC SYSTEM TYPES

#### 3.3.1 Ultrasonic Bath

Ultrasonic baths were originally manufactured for cleaning purposes. Typical baths have the transducers attached to the bottom, as shown in Figure 3.7a, although the transducers can be submersed in a conventional tank to obtain similar effects, showed as Figure 3.7b. Bath systems are widely used in sonochemical research, because they are readily available and relatively inexpensive. The reaction vessel is typically immersed in the coupling fluid contained in the bath (indirect sonication). However, the bath itself can be used as the reaction vessel but would require additional mechanical agitation. Moreover, the bath walls would be exposed to the reaction mixture and/or irradiation, making them susceptible to corrosion or erosion (Thompson et al., 1999).

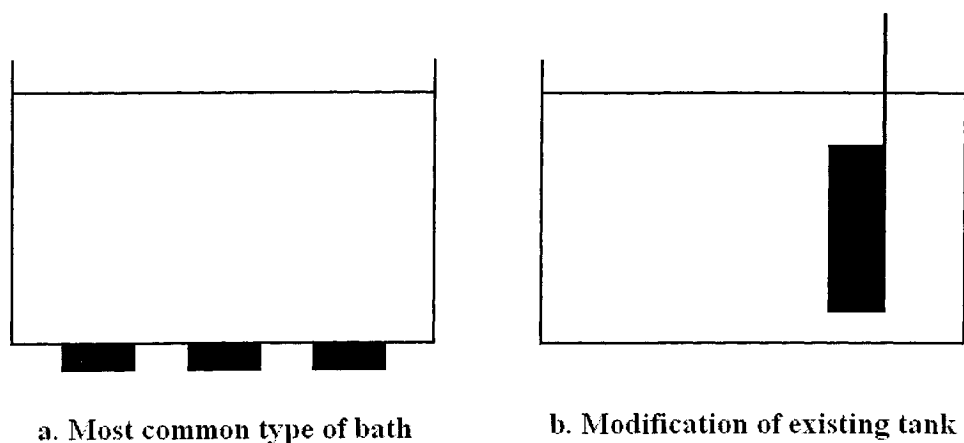


**Figure 3.7** Ultrasonic bath systems with (a) mounted transducers and (b) submersed transducers. (Thompson et al., 1999)

When indirect sonication is used, the ultrasonic power which reaches the reaction vessel is relatively low as compared to other ultrasonic systems, such as a probe. In addition, obtaining reproducible results may be difficult because the amount of power reaching the reaction mixture is highly dependent on the placement of the sample in the bath. The results can also vary with time as the bath warms during operation (Lickiss and McGrath, 1996). Another disadvantage using a bath system is that the coupling fluid surrounding the reaction vessel(s) will eventually increase in temperature, making the maintenance of isothermal conditions difficult. Cooling coils can be placed within the bath, but they will have an effect on the sound field and may reduce the amount of power reaching the vessel (Thompson et al., 1999). Moreover, it is essential to determine the optimum conditions for each bath and to replace the reaction vessel in the same place, due to the different characteristics of every bath.

### **3.3.2 Probe (Horn) Systems**

Probe systems, also called horn systems, are being more frequently used for sonochemical research in the laboratory, because they are possible to achieve much greater vibrational amplitudes. As a result of this, much greater energy densities can be achieved and capable of delivering large amounts of power directly to the reaction mixture, which can be regulated by varying the amplitude to the transducer.

Transducers used in modern power ultrasonic systems are almost without exception based upon the pre-stressed piezoelectric design. In this construction, a

number of piezoelectric elements are bolted between a pair of metal end masses. The piezo elements would be a pre-polarized lead titanate zirconate composition, which exhibit high activity coupled with both low loss and ageing characteristics. They are ideally suited to form the basis of an efficient and rugged transducer.

Several experiments have been carried out to determine the sound field characteristics in a probe system. The localized area of ultrasonic intensity in a fluid is highly dependent on the power delivered to the transducer. Contamine et al. (1994) observed that when the power delivered to the system is low (i.e., 8 W), the distribution of ultrasonic intensity is characteristic of a standing wave in the axial direction. However, as the power delivered to the system increases, the wave pattern dissipates and the intensity becomes higher near the probe tip and decreases axially. In the radial direction, it indicated that at low powers (i.e., 8 W) the intensity is slightly higher at the center of the reactor but is comparable over the cross section of the reactor. However, as the power delivery increases, the ultrasonic intensity increases at the center of the reactor and dissipates in the radial direction. At an input power of 200 W, the active region in the radial direction is equal to that of the horn (the remaining radial direction had negligible activity). A minimum liquid height of 1 cm must be maintained in the reaction vessel, below which the transducer does not function properly (Ratoarinoro et al., 1995)

Using probe systems have following disadvantages: (a) Erosion and pitting of the probe tip may contaminate the reaction solution. (b) Because of geometric losses and acoustic decoupling problems, it is impossible to transmit an intensity cavitation



filed more than 2-5 cm beyond the end of probe. (c) The probe system can not transmit to large process volume. (d) Larger transducer has to displace. (e) The higher intensity increases the stress on material, more likely to fall. Therefore, the probe systems are not suitable for larger commercial scale.

### 3.4 MODULE DESIGN OF CONTINUOUS ULTRASONIC DESULFURIZATION

#### 3.4.1 Module Design

The major effort of this study is to setup a laboratory-size continuous reactor system. A simple sketch of the flow diagram is described in Figure 3.8. The sonoreactor is the heart of this continuous flow system, which can be a chamber mounted with transducers and connected with recirculation loop and pump. Moreover, this sonoreactor can be a module-type representing multiple reactors in series or in parallel mode.

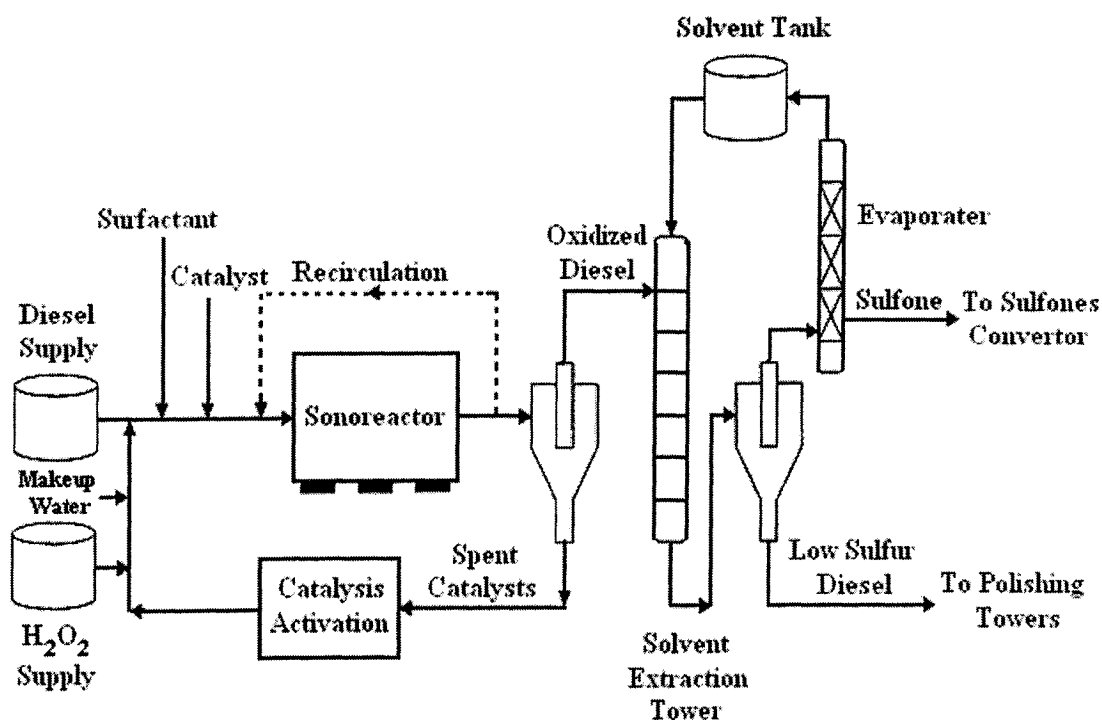


Figure 3.8 Schematic flow diagram of the continuous ultrasound assisted oxidative desulfurization process (Yen, 2003)

The other important portion after the sonoreactor is the two hopper-type cyclones. The first cyclone is used for the de-emulsification or separation of the oil phase from the aqueous phase. The second cyclone is used to receive the oxidized diesel after solvent extraction. Between the two cyclones, there is a solvent extraction tower where the sulfone byproduct and low sulfur diesel are partitioned out, and deliver to the second cyclone. There is an evaporation tower to distill the solvent used for extraction to retrieve the solvent for reuse. In this evaporator, the sulfone byproducts are obtained (Yen, 2003).

### **3.4.2 The Portable Continuous UAOD Unit**

Incorporating ultrasonic technology into current reactor design is becoming increasingly important in today's industries. As discussed in previous chapter, the ultrasound assisted oxidative desulfurization (UAOD) system has accomplished high sulfur removal by a probe type ultrasound unit. However, the probe type unit is merely at a batch scale. This is sufficient for research purposes but inadequate for large-scale commercial production. This study has spent a long time in designing and developing this unique modular of continuous flow system which contains a sonoreactor, a RF amplifier, a function generator, a pretreatment tank and a pipeline system. The detail design of each component in this portable unit will be discussed as following sections.

### 3.4.2.1 The Design of Sonoreactor

The sonoreactor, tailor-made by Blatek Tech., is basically a tubular reactor mounted with electromechanical transducers, which provides the direct sonication to the process stream. The diesel and hydrogen peroxide supply are metered in, and together with the make-up water. Moreover, an appropriate amount of surfactant or PTA, as well as the transition metal catalyst, is to add into the sonoreactor. Figure 3.9 illustrates the flow diagram of sonoreactor combined in a series or parallel. If the quality of fuel is extremely high in certain types of sulfur compounds, more than one module of the sonoreactor are required and can be used in a series. On the other hand, if the quantity of fuel is high, sonoreactors can be used in parallel.

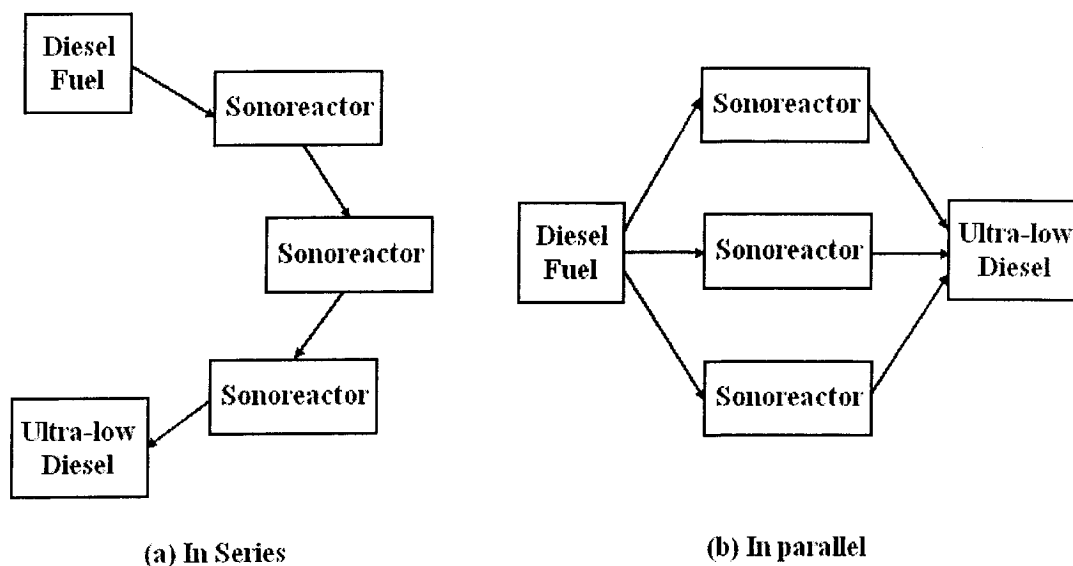


**Figure 3.9 Flow diagram of sonoreactor (a) in series or (b) in parallel**

Transducers used in modern power ultrasonic systems are almost without exception based upon the pre-stressed piezoelectric design. Figure 3.10 shows the schematic diagram of the sonoreactors which was designed with 9.1 inch length and 1 inch inlet diameter, and operated at fixed frequency of 20 kHz with various power intensities from 100 watts to 400 watts. In this construction, four piezoelectric ceramics are bolted between a pair of metal end masses that couple with a coupling cone (horn type taper) made with titanium alloys. The piezo elements would be of a pre-polarized lead titanate composition that exhibits high activity coupled with both low loss and ageing characteristics. The piezoelectric transducers are mounted in a fixture or in a protective case by means of the nodal mounting plate. Figure 3.11 shows the picture of sonoreactor.

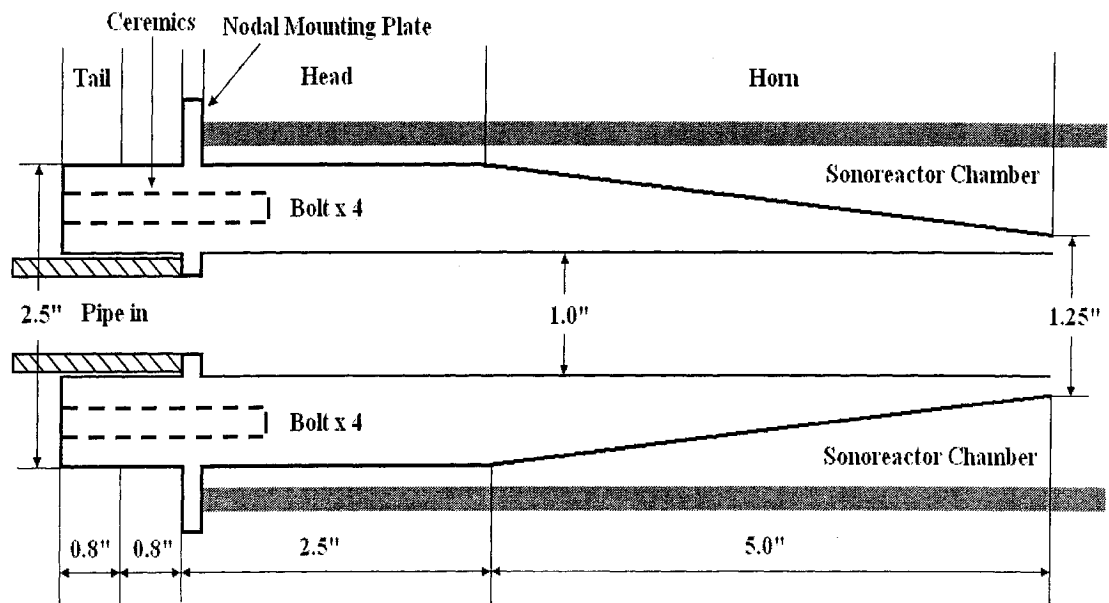


**Figure 3.10 Schematic design diagram of the sonoreactor**

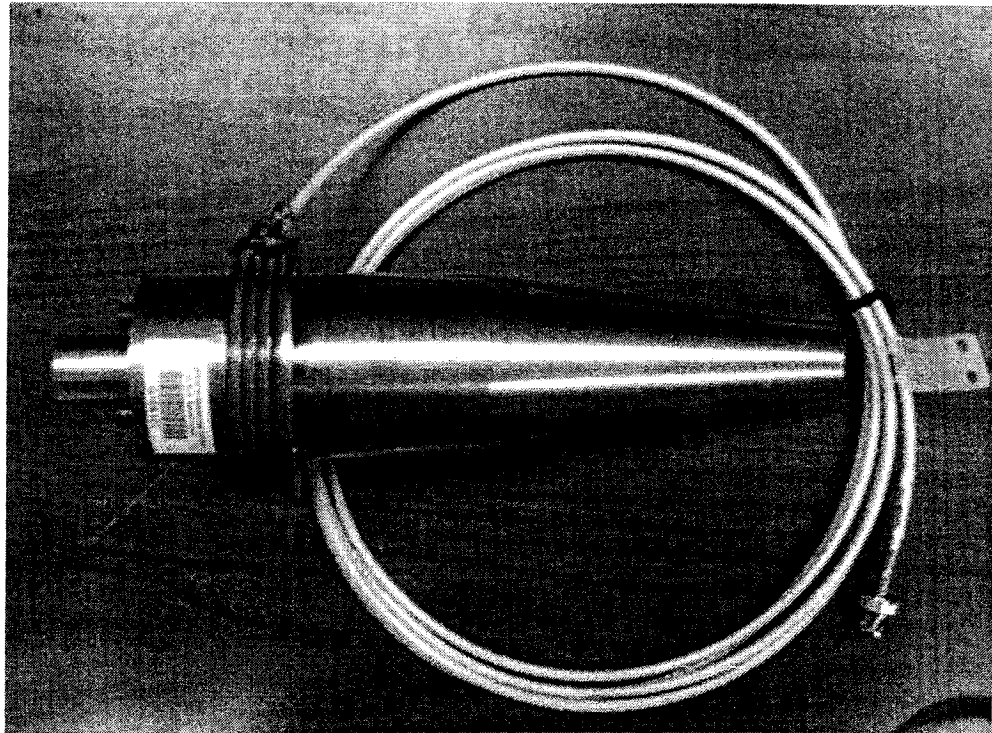


**Figure 3.11 Picture of sonoreactor**

#### 3.4.2.2 RF Amplifier

The radio transmitter is a collection of stages. Each stage modifies the signal in some way to produce the desired output. In the first stage, an oscillator or exciter generates the desired operating frequency. The output from this section is raised to the specified transmitter output value. This power increase may be by means of successively larger amplifying stages or in some cases, where the exciter output is sufficient, directly to the final power amplifier (PA) of the transmitter.

The RF signal transmitted must carry some information. In broadcasting, the transmitted information takes the form of speech or music and is called modulation.

With amplitude modulation (AM), the RF carrier is varied in strength (amplitude) at a rate depending on the frequency of the sound. Regardless of where modulation of the carrier takes place, it is essential that the amplifying stage produces a clean, linearly amplified signal.

Amplifier Research 700A is used to control the power output. Its detailed specifications are described in the following:

- Power Output into 50 ohms  
Maximum: up to 700 watts  
Linear: 250 watts @ less than 1dB gain compression
- Frequency: 10 kHz to 250 kHz useful range from 8 kHz to 450 kHz at reduced gain
- Gain: 60 dB minimum
- Input Attenuator: Continuously adjustable over greater than an 18 dB range
- Input Impedance: 50 ohms nominal
- Output Impedance (Switch Selectable) 12.5, 25, 50, 100, 150, 200, 400, 600, 1000 ohms nominal
- Connectors: type BNC
- Power Meter: Directional power meter and front panel selector switch allows separate measurement of the forward power leaving the amplifier and the power reflected by the load
- Primary Power: 115 VAC, 50/60 Hz, 15 Amp

#### 3.4.2.3 Function Generator

A function generator is used to generate repetitive waveforms which can be injected into a device under test and analyzed as they progress through the device to confirm the proper operation of the device and/or pinpoint a fault in the device. Moreover, function generators usually generate a triangle waveform as their basic output. The triangle is generated by repeatedly charging and discharging a capacitor from a constant current source. This produces a linearly-ascending or descending voltage ramp. As the output voltage reaches upper and lower limits, the charging and discharging are reversed, and producing the linear triangle wave. By varying the current and the size of the capacitor, different frequencies may be obtained.

#### 3.4.2.4 Portable Continuous Desulfurization Unit

Based on the concept of module design, this portable unit of continuous flow system, which consists of a sonicator, an RF amplifier, a function generator, a pretreatment tank, and a pipeline system, was operated at room conditions for a given time. The size for a single unit is 2' x 4' x 1', as shown in Figure 3.12. This portable unit of continuous flow system can demonstrate the feasibility of large-scale operation even in a relatively small installation with low capital investment and maintenance cost. It also ensures the safety considerations by operating under ambient temperature and pressure conditions, and the addition of the dilute hydrogen peroxide. Moreover, this system permits a multistage process for the best quality or quantity purpose and performance.



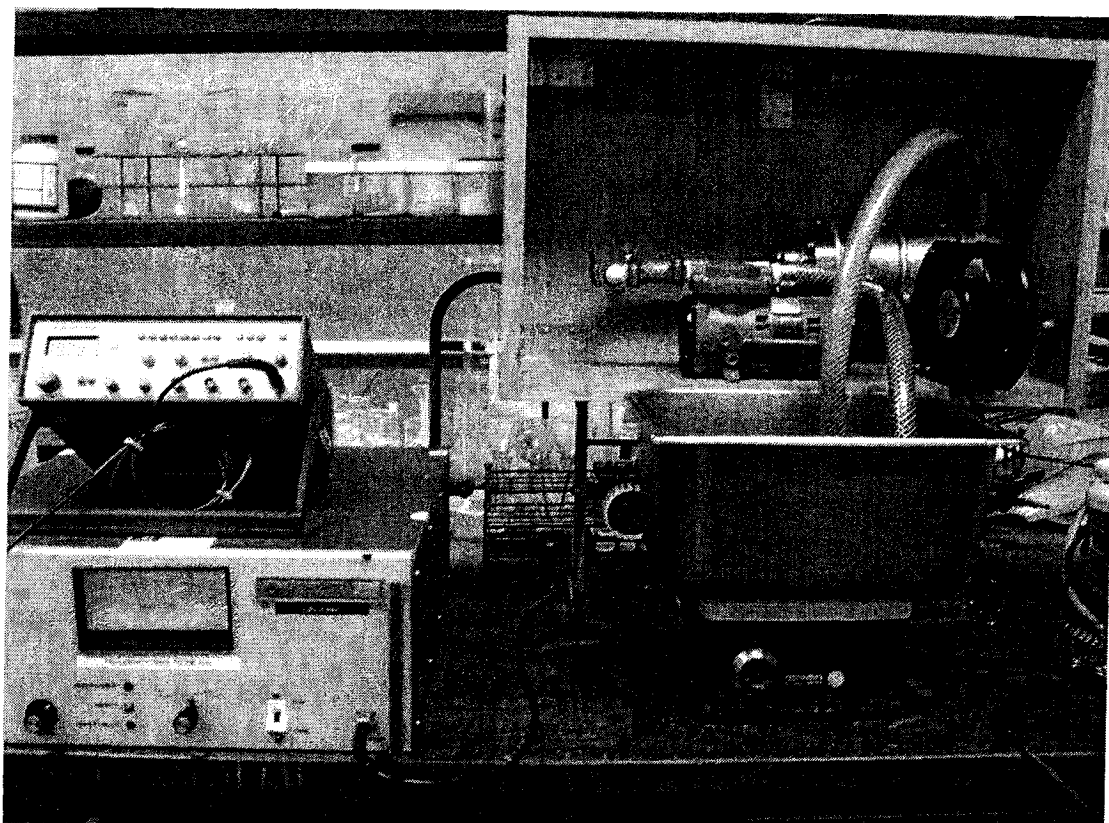


**Figure 3.12 Portable continuous desulfurization unit**

## CHAPTER 4

### UAOD ON MODEL SULFUR COMPOUND

#### 4.1 INTRODUCTION

It is evident from the work discussed in pervious chapter that the greatest advantages of the oxidative desulfurization (ODS) process are low reaction temperature and pressure, and that expensive hydrogen is not used in the process. Another advantage of ODS is that the refractory sulfur compounds in HDS are easily converted by oxidation (Collins, et al. 1997). Therefore, ODS has great potential to be a complementary process to traditional HDS for producing deeply desulfurized diesel fuel. Dibenzothiophene, 4-methyl-dibenzothiophene, and 4,6-dimethyldibenzothiophene are typical refractory sulfur compounds in diesel and other fuel oils. It is well known that the HDS reactivity of dibenzothiophenes decreases dramatically with the increase of methyl substitutes at the sterically hindered positions (positions 4 and 6).

The applicability of an oxidation desulfurization scheme depends on the kinetic and selectivity of the oxidation of organic sulfide to sulfones. Polyoxometalates have long been studied for oxidation reactions, particularly, the polyoxometalate/hydrogen peroxide system for organic substrate oxidations (Kozhevnikov, et al. 1998). It has been well documented in the previous oxidation work that the tungsten and molybdenum polyoxometalates with a Keggin structure

converted to polyoxoperoxo species in the presence of hydrogen peroxide. Species have been spectroscopically identified and their structures have been determined (Venturello, et al. 1985; Ballistreri et al. 1992). Even sulfur compounds with low nucleophilicity such as dibenzothiophene can be oxidized under mild condition to sulfoxides or sulfones in high yields (Collins, et al. 1997; Yen, et al. 2002; Mai, et al. 2003).

Mai, et al. 2003 has demonstrated the high yields of DBT and its families by UAOD process. However, the problems of bromo-byproducts and low oxidation efficiency of BT and its families exhibited serious drawbacks to enhance the deep desulfurization. In this chapter, the performance of UAOD process on model sulfur compounds (mainly focused on BT and its families) was evaluated. A series of experiments were carried out to optimize the reaction conditions, in which the type and amount of phase transfer agents and transition metal catalysts were carefully evaluated. Finally, the results were characterized by instrumental analysis.

## **4.2 MATERIALS AND EXPERIMENT METHODS**

### **4.2.1 Materials**

Model compounds and chemicals, including Benzothiophene (BT), benzothiophene sulfone (BTO), 2-methylbenzothiophene (2MBT), dibenzothiophene (DBT), dibenzothiophene sulfone (DBTO), 4-methyldibenzothiophene (4MDBT), 4,6-Dimethyldibenzothiophene (46DMDBT), methyltributylammonium hydroxide (MBAH), tetraoctylammonium bromide (TOAB), tetraoctadecylammonium bromide

(TODAB) tetraoctylammonium fluoride (TOAF), tetrabutylammonium bromide (TBAB), tetramethylammonium fluoride (TMAF), methyltributylammonium chloride (MTAC), phosphotungstic acid hydrate ( $\text{H}_3\text{PW}_{12}\text{O}_{40}\cdot 20\text{H}_2\text{O}$ , HPW), sodium phosphotungstic hydrate ( $\text{Na}_3\text{PW}_{12}\text{O}_{40}\cdot 14\text{H}_2\text{O}$ , NaPW), phosphomolybdic acid hydrate ( $\text{H}_3\text{PMo}_{12}\text{O}_{40}\cdot 15\text{H}_2\text{O}$ , HPMo), sodium phosphomolybdic hydrate ( $\text{Na}_3\text{PMo}_{12}\text{O}_{40}\cdot 20\text{H}_2\text{O}$ , NaPMo), Tween 80, and 1-Octanesulfonic Acid, were obtained from Aldrich Chemical, Milwaukee, Wisconsin. Solvent (toluene) for experiments and analysis and hydrogen peroxide (30 vol %) were obtained from VWR Inc, Los Angeles, California.

#### 4.2.2 Experimental Method

Model sulfur compounds were dissolved in toluene as the stock solution with the given sulfur content. An appropriate volume of the stock solution containing the phase transfer agent and an equal volume of hydrogen peroxide (30 vol % solution) containing transition catalyst metal were added into the glass reactor. The mixture was irradiated by ultrasound at a frequency of 20 kHz. During the period of ultrasonication, the mixture was emulsified. The temperature in the reactor was controlled by using a 5-L thermal water bath. Upon cooling and centrifuging, the emulsion was broken and benzothiophene sulfone was formed at upper layer.

The sulfur compounds in the feed and product were analyzed by Varian gas chromatograph (Varian 3400) equipped with a pulsed flame photometric detector (PFPD) and an ion trap mass spectrometer (Saturn 2000, MS). A fused-silica

capillary column DB-5 ms (30 m x 0.25 mm I.D.) with 0.25  $\mu$ m film thickness (J & W Scientific, Folsom, CA USA) was used. The column temperature program was first retained at 100 °C for 3 minutes, and was heated at the increasing rate of 6 °C /min to 275 °C , and kept at 275 °C for 10 minutes. Benzothiophene (BT), Benzothiophene Sulfone (BTO) and their families were identified and quantified with the standard samples. The other major peaks shown in GC-PFPD were identified using selected ion monitoring or comparing molecular ions in GC/MS.

In the study, different types of surfactants were selected to exam the reaction rate in presence of surface-active agents. Different cationic surfactants, such as quaternary ammonium salts (QASs), and some additives were considered to test the highest sulfur reduction with byproduct free. Different types of transition metal catalyst were also selected to exam the highest efficiency for the oxidation of organic sulfur compounds. Finally, diluted hydrogen peroxides were tested to ensure the safety consideration.

### **4.3 QUANTIFICATION OF ORGANIC SULFUR COMPOUND ANALYSIS**

#### **4.3.1 Total Sulfur Content**

Based on method ASTM D4294-83, non-dispersive X-ray fluorescence (NDXRF) was used to determine the total sulfur content in the model compounds system. The Sulfur-in-Oil Analyzer (SLF A-20, Horiba Inc., California), was

employed to determine any sample with total sulfur content range from 0.002 to 5 wt. % of sulfur.

#### 4.3.2 Low Sulfur Content Determination

Based on our previous quantitative sulfur analysis studies of low-sulfur hydrocarbon in using GC-PFPD, the response of PFPD for sulfur compounds is inherently nonlinear. The intensity of the blue light emission is theoretically proportional to the square of the sulfur concentration in the flame. This result has been evidenced in published paper (Hutte, et al. 1992) and presented in American Chemical Society, Division of Petroleum Chemistry, 2004 (Ma, et al. 2004). Therefore, for samples with total sulfur content below 20 ppm, the concentration of each sulfur compound was quantified by GC-PFPD according to the following equation (Eq. 4.1), and the results are shown in Table 4.1 and Figure 4.1:

$$C_i \text{ (ppm)} = m A_i \quad (\text{Eq. 4.1})$$

where  $C_i$  is the sulfur concentration of organic sulfur compound  $i$ ,  $A_i$  is the peak area of organic sulfur compound  $i$ , and  $m$  is the calibration factor. The value of  $m$  and  $n$  were determined by standard samples. This procedure is used throughout this chapter and will be used for future work.

**Table 4.1 Peak area of low sulfur contained compounds**

<b>Concentration (ppm)</b>	<b>Peak Area</b>
1	16057
2	42567
5	255901
7	506812
10	1034682

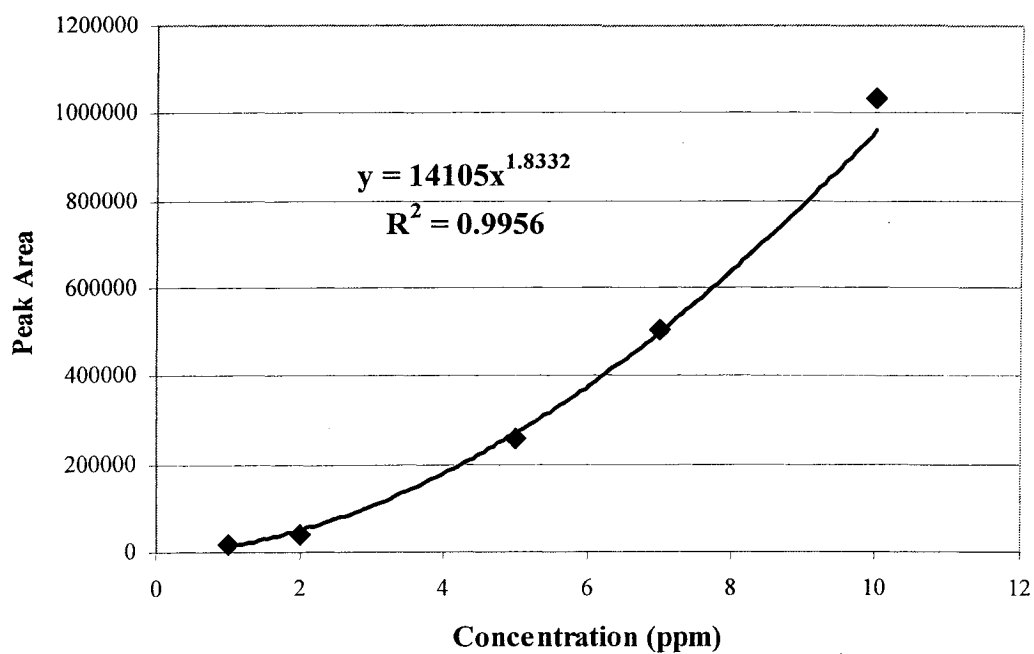


**Figure 4.1 Calibration curve for quantification of sulfur concentration**

## 4.4 RESULTS AND DISCUSSION

### 4.4.1 Process Optimization

#### 4.4.1.1 Effect of the Structure of QASs as Phase Transfer Agent

Phase Transfer catalysis (PTC) is a powerful tool in many areas of chemistry. It is a technique for conducting reactions between two or more reagents in two or more phases, when reaction is inhibited because the reactants cannot easily come together. A phase transfer agent is added to transfer one of the reagents to a location where it can conventionally and rapidly react with another reagent. It is also necessary that the transferred species are in a highly active state when transferred; otherwise large amounts of phase-transfer agent will be required. This activation function, with the transfer function, allows phase-transfer catalysis to occur with only a catalytic amount of phase-transfer agent (Starks, et al. 1994; Dehmlow and Dehmlow, 1993; Sasson and Neumann, 1997).

Choosing a phase transfer agent is usually the most important step in design and development of the UAOD process. Table 4.2 shows the oxidation of BT to BTO, which proceeds at very low or high reaction rate in presence of surface-active agents using quaternary ammonium salts (QASs) as cationic surfactants. It indicates that the effective oxidant in the reaction system is in the form of peroxo metal anion and cationic surfactants. QASs can especially function as a phase transfer agent and



deliver the anion into organic phase or the interfacial region, thus facilitating the oxidation of organic sulfur compounds.

**Table 4.2 Effect of different types of surfactants on UAOD process**

Type	Surfactant	Desulfurization
Cationic	Tetraoctylammonium Bromide (TOAB)	+
	Tetrabutylammonium Bromide (TBAB)	+
	Methyltributylammonium Chloride (MBAC)	+
	Methyltributylammonium Hydroxide (MBAH)	+
	Tetramethylammonium Fluoride (TMAF)	+
Anionic	1-Octanesulfonic Acid, Sodium Salt	—
Nonionic	Tween 80	—
Control	No Surfactant	—

Note: + indicates that there is reaction occurring under reaction conditions.  
 - indicates that there is no reaction occurring under reaction conditions.

It is known that the structure of the QAS cation not only influences its ability to transfer ion from the aqueous to organic phase but also strongly affects the rate of the organic phase reaction. In this study, several QASs with different cation structures were employed to evaluate their catalytic activities on the oxidation of BT to BTO. Figure 4.2 shows that the oxidation rate of BT to BTO increased with increasing the carbon chain length of QAS cations. The catalytic activities follow the

order:  $(\text{C}_8\text{H}_{17})_4\text{N}^+\text{Br}^-$  (TOAB) >  $(\text{C}_4\text{H}_9)_4\text{N}^+\text{Br}^-$  (TBAB) >  $(\text{C}_4\text{H}_9)_3\text{MeN}^+\text{Cl}^-$  (MBAC) >  $(\text{C}_4\text{H}_9)_3\text{MeN}^+\text{OH}^-$  (MBAH) >  $(\text{CH}_3)_4\text{N}^+\text{F}^-$  (TMAF). It indicated that QASs with smaller number of carbon number connected to nitrogen cation such as TMAF, MBAH and MBAC are not lipophilic enough to transfer the heteropolyperoxo metal anion into organic phase or interfacial region. However, TOAB and TBAB, which have larger lipophilic cation, can easily transfer the metal anion into organic phase and thus permit faster reaction.

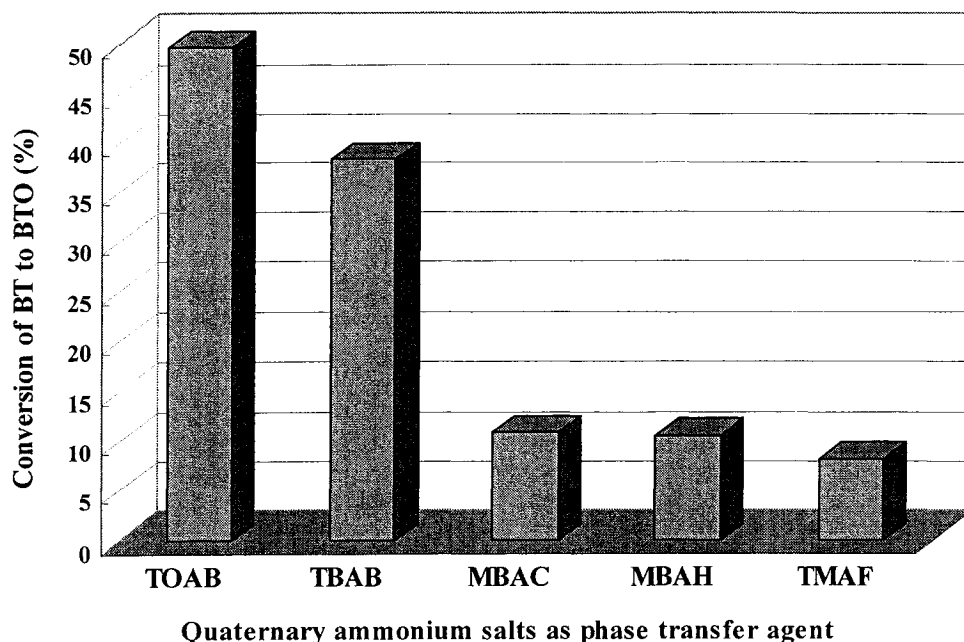


**Figure 4.2 Effect of different structure of QASs on oxidation of BT to BTO**

#### 4.4.1.2 Effect of the amount of QASs as Phase Transfer Agent

Based on previous studies, the required catalyst quantities of QAS range from less than one mole percent to several moles with various systems. In most cases, 1-3 mol % can be regarded as normal dosage (Sasson and Neumann, 1997; Dehmlow and Dehmlow, 1993).

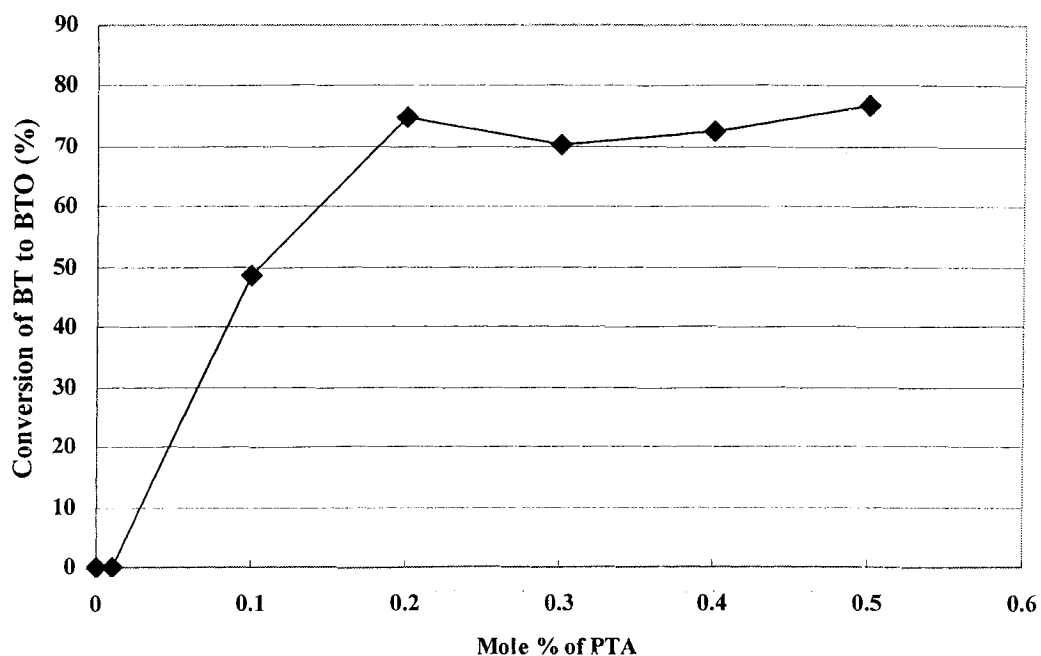
In this study, it indicated that the QASs, especially with longer carbon chain, were considered to be used in a very small amount under the UAOD conditions. For example, the addition of TOAB should not exceed 0.5 mol% in order to prevent a few side effects under ultrasound, including foaming and excessive decomposition of hydrogen peroxide in the reaction.

Table 4.3 and Figure 4.3 shows that the oxidation efficiency of BT to BTO generally increased with increasing amounts of TOAB as PTA. There was no oxidation with the concentration of TOAB less than 0.01 mol% due to insufficient transfer of oxidized metal anion into organic phase or O/W interface. The oxidation efficiency reached 49% with the concentration of TOAB at 0.1 mol%. As the addition of TOAB increased, the oxidation efficiency increased drastically and reached 74.87 % with the concentration of TOAB at 0.2 mol%. Further increasing the concentration of TOAB was not resulted in increasing the conversion of BT to BTO (nearly 75 %). In some literatures, it was a phenomenon typically occurring where the reaction rates are liner dependent on the concentrations of phase transfer catalyst (Dehmlow and Dehmlow, 1993). However, in the case of micellar catalysis, there is generally a pronounced acceleration in the rate near the critical micelle

concentration followed by a flat or decreasing rate at higher concentrations (Neumann and Hhenlin, 1994; Mai, 2003).

**Table 4.3 Oxidation efficiency of different amount of phase transfer agent**

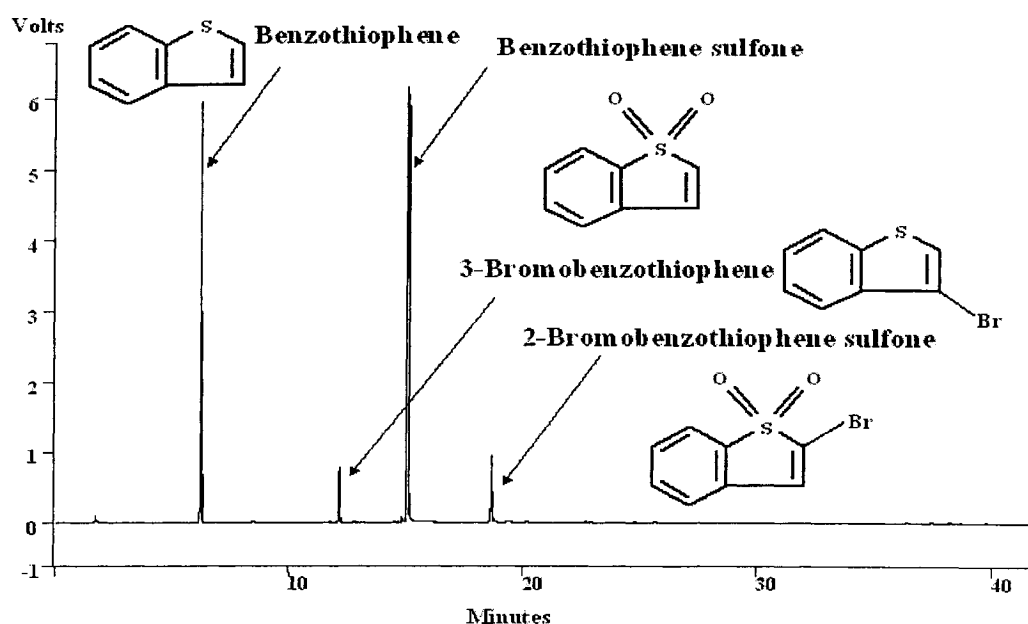
Amount Conversion	Phase Transfer Agent (mol%)						
	0	0.01	0.1	0.2	0.3	0.4	0.5
BT to BTO (%)	0.00	0.00	48.53	74.87	70.37	72.72	76.70



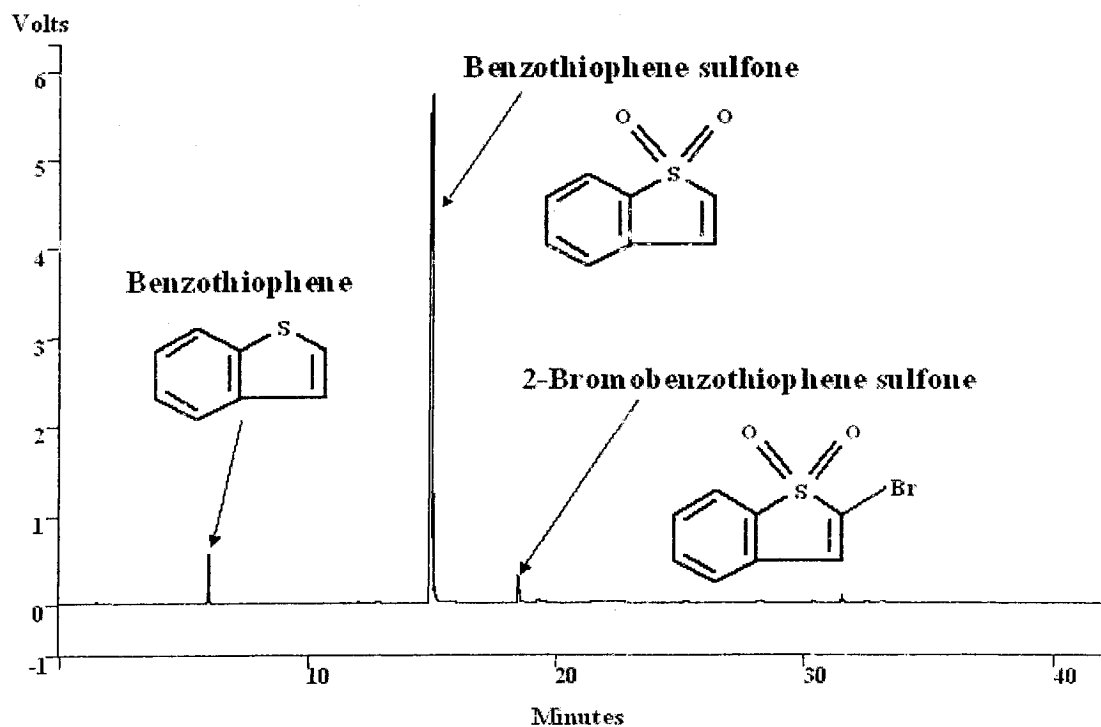
**Figure 4.3 Effect of amount of PTA on conversion of BT to BTO**

Figure 4.4 shows that there were three sulfur products left in the desulfurized BT solution (0.1g PTA). Based on the retention time, these three sulfur compounds were categorized as BTO, 3-bromobenzothiophene and 2-bromobenzothiophene sulfone. Figure 4.5 shows that there were two sulfur products left in the desulfurized BT solution (0.2g PTA), which were categorized as BTO and 2-bromobenzothiophene sulfone and permitted the 74.87 % oxidation efficiency of BT to BTO.

Benzothiophene sulfone and 2-bromobenzothiophene sulfone produced are known as polar organic compounds, and can be easily extracted by solvent extraction or removed by silica or alumina adsorption (Satoru, et al. 2004). Therefore, it indicated that the real removal percentage could be estimated to increase 10% from current BT to BTO conversion percentage.



**Figure 4.4 GC-PFPD chromatograms of BT after UAOD process under 0.1 g PTA**

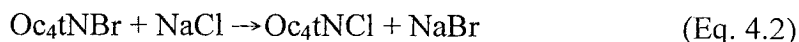


**Figure 4.5 GC-PFPD chromatograms of BT after UAOD process under 0.2 g PTA**

#### 4.4.1.3 Solid-Liquid Anion Exchange on Phase Transfer Agent

Sodium chloride (NaCl) is an ionic crystal at room temperature, with its sodium and chlorine atoms arranged in almost a regular array, which can be called as lattice. Originally, the crystalline sodium or potassium formates are not accessible to quaternary ammonium salts in organic solution, and therefore direct solid-liquid anion exchange is not possible. However, when a small amount of water is added, a thin aqueous film is formed on the surface of the solid crystals and anion transport is possible.

Table 4.4 and Figure 4.6 show the oxidation of BT to BTO, which executed at various reaction rates in presence of sodium chloride. The oxidation efficiency of BT to BTO generally increased with increasing amount of NaCl, because the formation of solid-liquid anion exchange executed.



Due to the better phase transfer ability of TOAC than that of TOAB, the oxidation efficiency reached 61.13% with the weight of NaCl at 0.5 g. Moreover, an important observation was that when the weight of NaCl was smaller than 0.5g, the aqueous phase was a clear homogeneous solution under the reaction conditions. If larger amount of NaCl added, the NaCl-H<sub>2</sub>O<sub>2</sub> phase existed initially as slurry. As the reaction proceeded, the precipitated solid sodium bromide could not be extracted and thus the reaction was shifted to the right, which inhibited the produce of TOAC and reduced the efficiency of phase transfer reaction.

**Table 4.4 Oxidation efficiency on different amount of sodium chloride**

Amount Conversion BT to BTO (%)	Weight of Sodium Chloride (g)							
	0	0.1	0.3	0.5	0.7	0.9	1.2	1.5
	48.53	51.47	56.71	61.13	50.40	46.99	41.85	38.15

Figure 4.7 shows that there were two major sulfur products left in the desulfurized BT solution (0.5g NaCl). Based on the retention time, these two sulfur compounds were categorized as BTO and 2-bromobenzothiphenesulfone. There was

no chlorine compound after the oxidation desulfurization. This result also can be evidenced by GC-MS analysis. Figure 4.8 shows the GC/MS chromatograms of BT as model sulfur compound after UAOD process under different conditions, including using 0.1g PTA, 0.2g PTA, and 0.1 g PTA with 0.5g NaCl as additive.

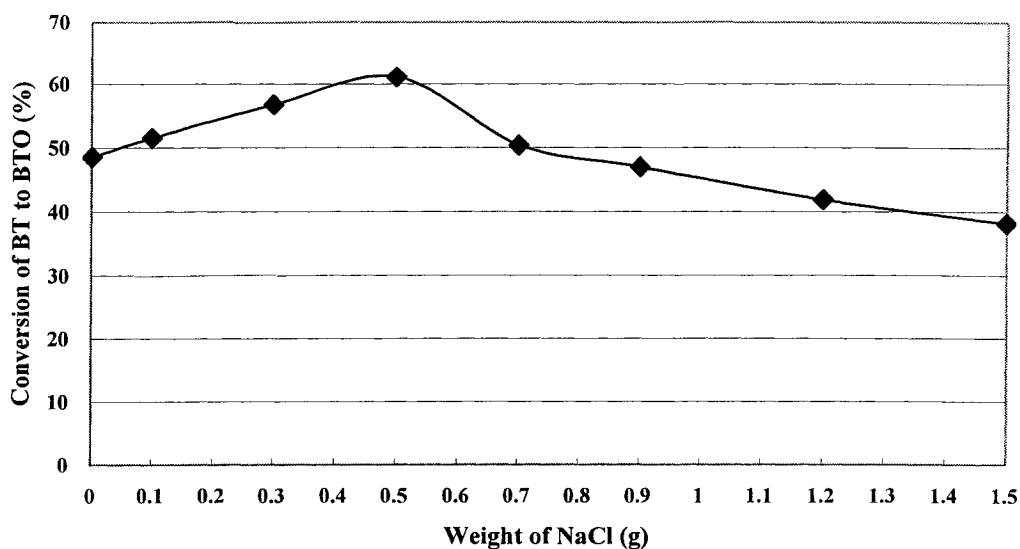


**Figure 4.6 Effect of amount of NaCl on conversion of BT to BTO**

Through the formation, growth, and collapse of cavitation bubbles, the low-energy density of sound wave is converted into high-energy characteristic of the interior and surrounding of collapsing gas bubble (Mason, 1991). Because of the cavitation process of ultrasound, high energy was generated in order to cleave the bonds of some molecules. It was thought that the anion of PTA can interchange with added amount of chloride and therefore decreased the amount of bromo by-products, but the results did not support this. Therefore, this study indicated that the ionic



effect of the sodium chloride can increase and decrease the oxidation efficiency of BT to BTO. The optimum amount of NaCl has been evidenced at the weight of 0.5 g to reach 61.13 % oxidation efficiency.

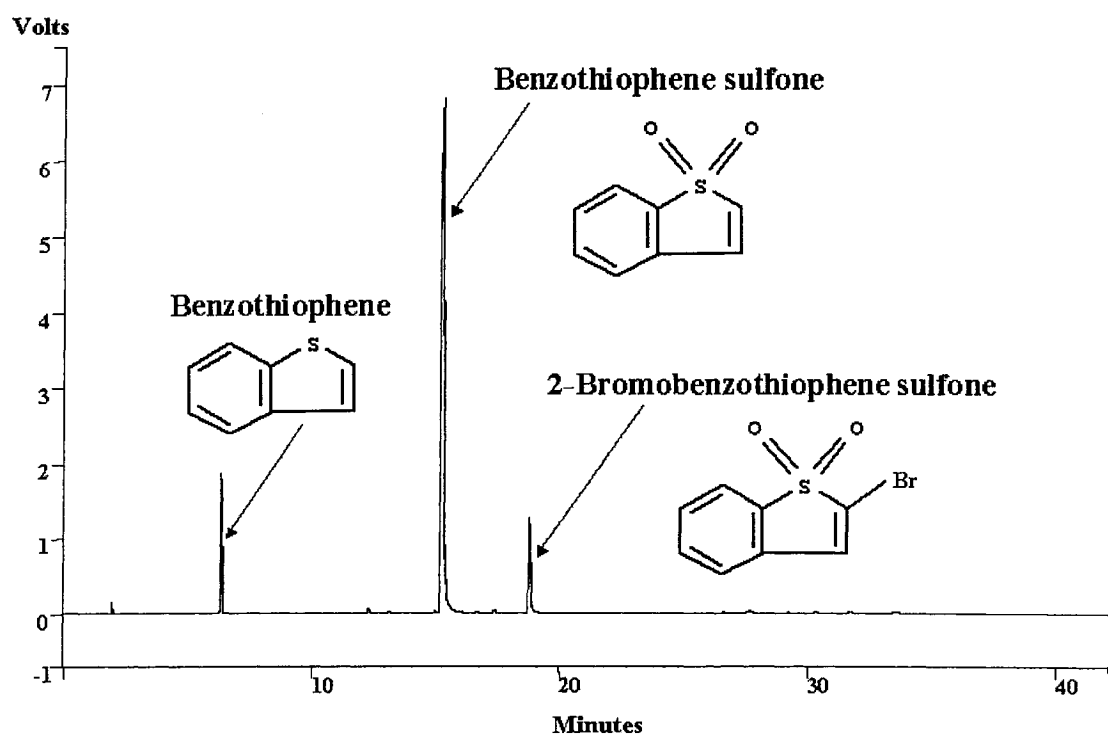


**Figure 4.7 GC-PFPD chromatograms of BT after UAOD process with 0.5 g NaCl**

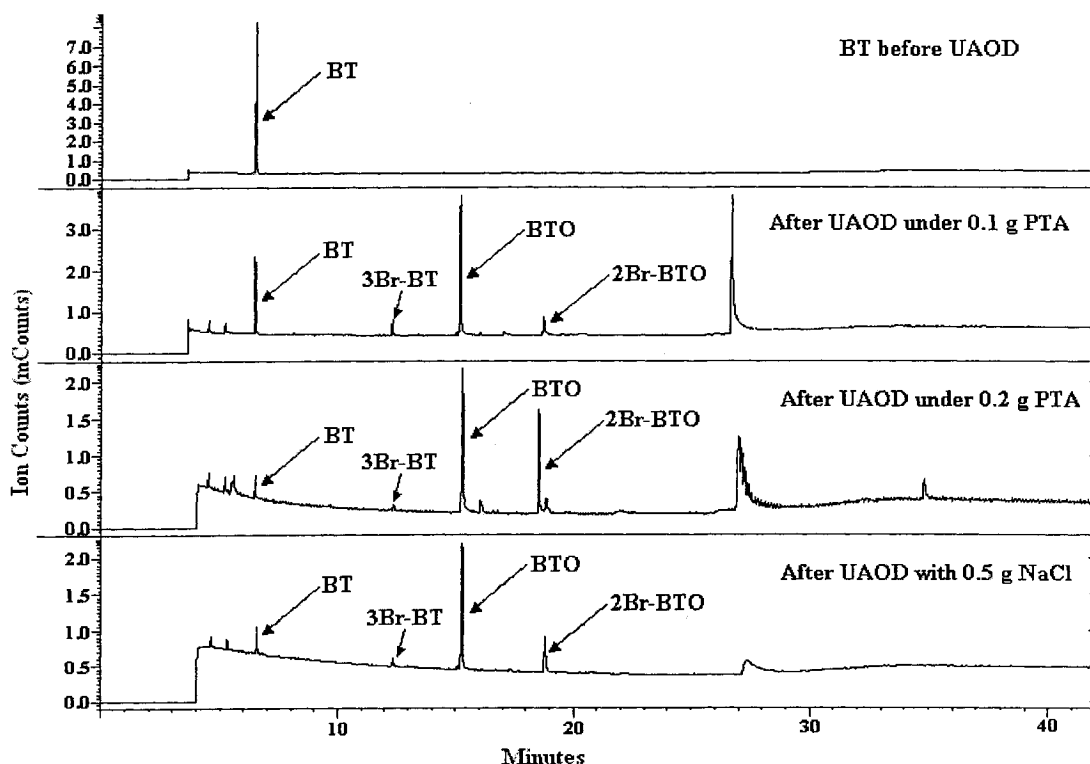


**Figure 4.8 GC-MS chromatograms of BT after UAOD with different conditions**

#### 4.4.1.4 High Yield of Benzothiophene Sulfone from Fluoride containing Phase Transfer Agent

As discussed in previous section, choosing a phase transfer agent is usually the most important step in design and development of a UAOD process. Tetraoctylammonium fluoride was first used as PTA to optimize the oxidation efficiency. Both benzothiophene (BT) and 2methyl-benzothiophene (2MBT) have been obtained with high yield. Even dibenzothiophenes (DBT) were cleaned from any contamination of bromo compounds. The results from fluoride containing PTA were satisfactory – high yield and free of any by-products.

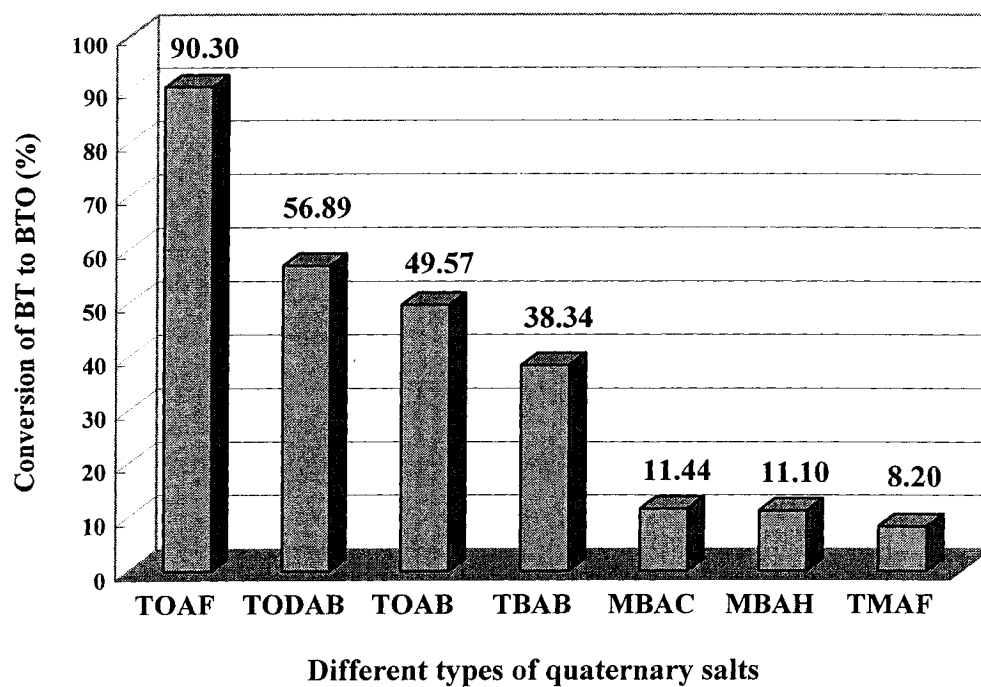
Table 4.5 illustrates the percentage conversions of BT to DBT with different quaternary ammonium salts. TOAF has the highest yield. Again, the chain length of the substituents had a positive effect on the yield. The conversions are illustrated in Figure 4.9. Moreover, further experiments were carried out with TOAF for 20 mins sonication time. Figure 4.10 shows that the BT to BTO conversion further improved to 97.55%. The spectra were free of any bromo by-products.

Figure 4.11 indicates the results of 2MBT by using the TAOF as PTA. The bromo compounds didn't appear, whereas with the TAOB as PTA had a bromo by-product resulted. Figure 4.12 indicates that the oxidation of DBT using the same conditions as BT and 2MBT. The results show that the new quaternary salt with fluoride had similar results.

Figure 4.13 shows the comparison of different model sulfur compounds by using TOAB and TOAF as PTA. TOAF showed better oxidation efficiency in all kinds of model sulfur compounds than TOAB. Therefore, comparing the result of previous section, the longer carbon chain length of QASs with smaller anion had better efficiency to transfer metal anion into organic phase and thus permit faster oxidation reaction ( $F^- > Cl^- > Br^- > I^-$ ). Based on the results, TOAF is selected as phase transfer agent because of its high conversion efficiency and relative low cost, which is the same price of TOAB and 10% of the price of TODAB.

**Table 4.5 Oxidation efficiency on different phase transfer agents**

List of PTA	BT to BTO Conversion %
TOAF ((CH <sub>3</sub> (CH <sub>2</sub> ) <sub>7</sub> ) <sub>4</sub> N <sup>+</sup> F <sup>-</sup> )	90.30
TODAB ((CH <sub>3</sub> (CH <sub>2</sub> ) <sub>17</sub> ) <sub>4</sub> N <sup>+</sup> Br <sup>-</sup> )	56.89
TOAB ((C <sub>8</sub> H <sub>17</sub> ) <sub>4</sub> N <sup>+</sup> Br <sup>-</sup> )	49.57
TBAB ((C <sub>4</sub> H <sub>9</sub> ) <sub>4</sub> N <sup>+</sup> Br <sup>-</sup> )	38.34
MBAC((C <sub>4</sub> H <sub>9</sub> ) <sub>4</sub> MeN <sup>+</sup> Cl <sup>-</sup> )	10.94
MBAH ((C <sub>4</sub> H <sub>9</sub> ) <sub>3</sub> MeN <sup>+</sup> OH <sup>-</sup> )	10.60
TMAF ((CH <sub>3</sub> ) <sub>4</sub> N <sup>+</sup> F <sup>-</sup> )	8.20



**Figure 4.9 Comparison of yields of different quaternary salts**

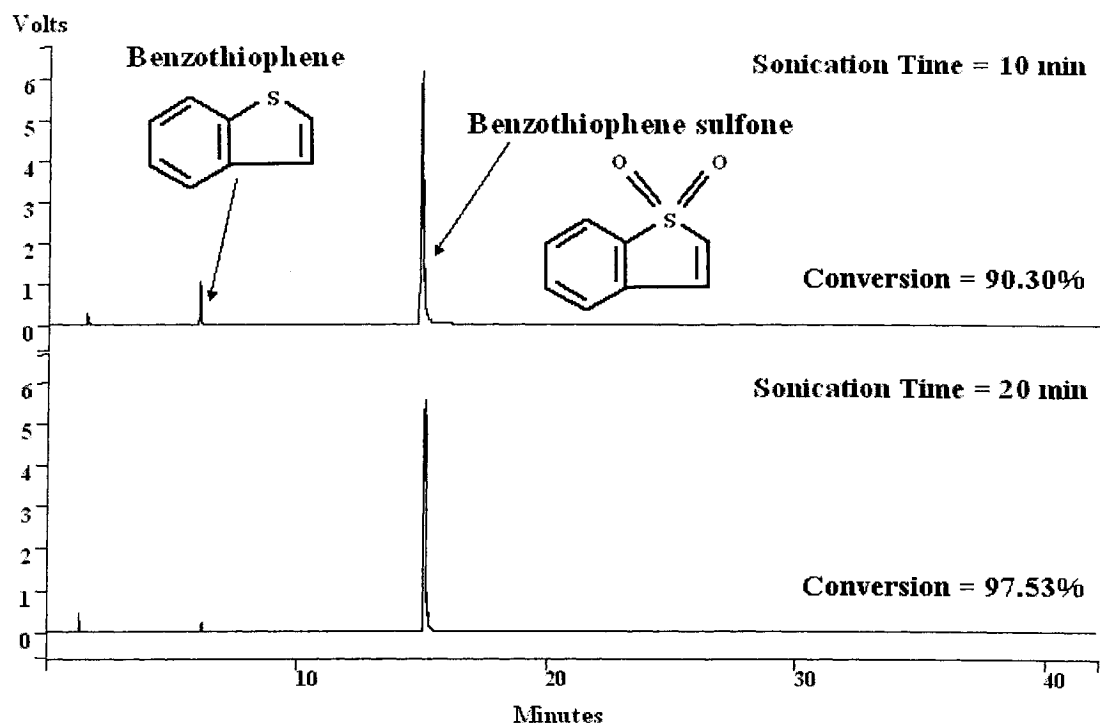


**Figure 4.10 GC-PFPD chromatograms of BT using TOAF as PTA in different sonication time**

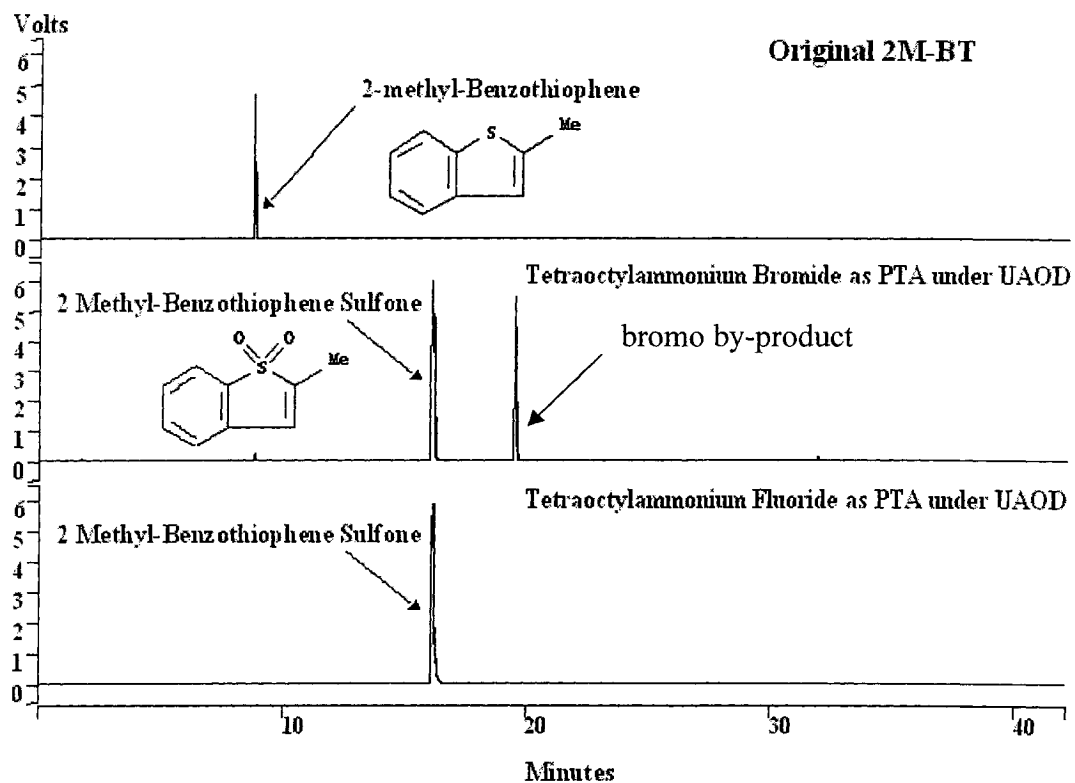


**Figure 4.11 GC-PFPD chromatograms of comparison of 2MBT after UAOD process by using different PTA**

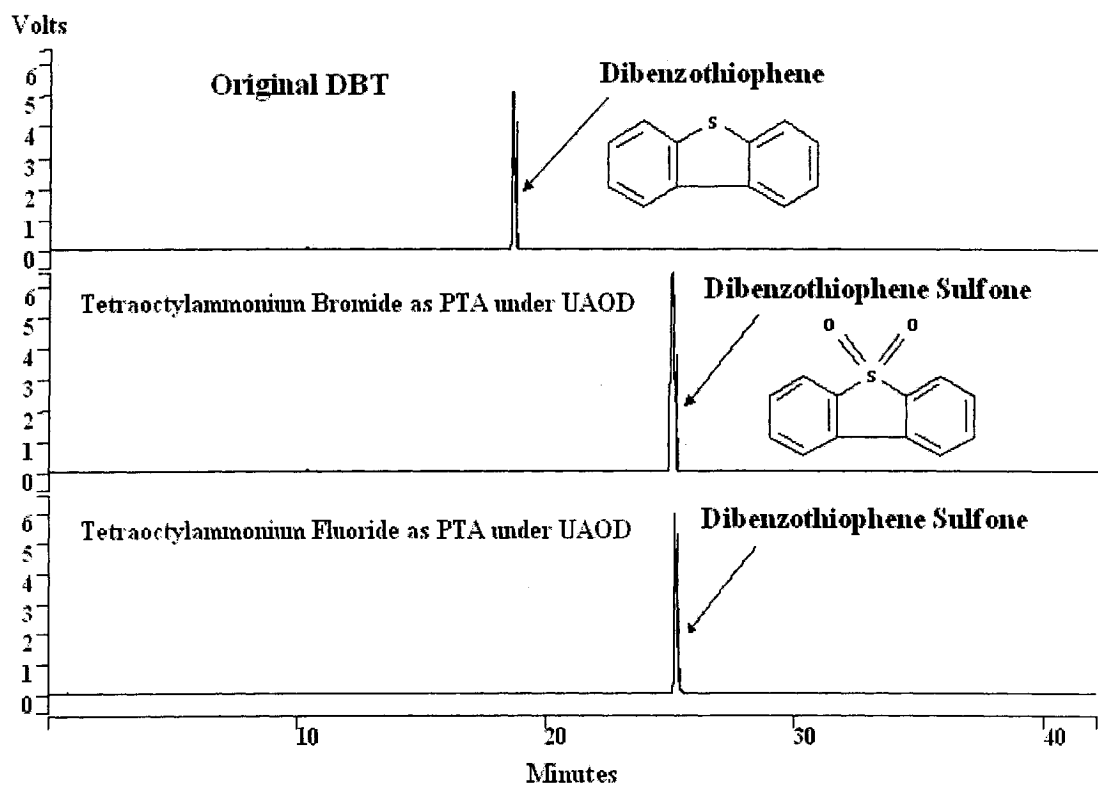


**Figure 4.12 GC-PFPD chromatograms of comparison of DBT after UAOD process by using different PTA**

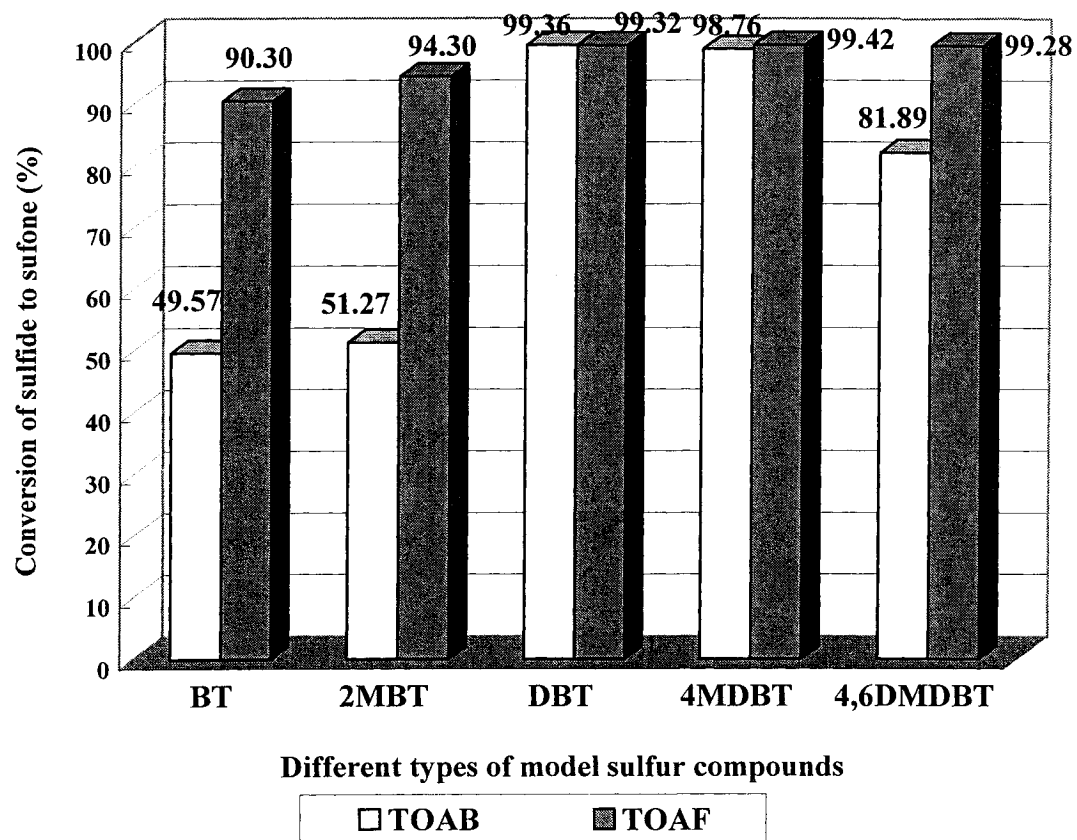


**Figure 4.13** Comparison of yields of model sulfur compounds using different PTA



#### 4.4.1.5 Effects of the Transition Metal Catalyst

Based on previous studies, it is well known that the addition of some metal ion derivatives such as W(VI) and Mo(VI), react with  $\text{H}_2\text{O}_2$  to form more effective and selective oxidants such as oxo- and peroxo-metal complex, results in high rate and high selectivity in oxidation of nucleophilic substrates such as organic sulfides or alkenes. (Sheldon and Kochi, 1981; Patai, 1983; Bortolini et al, 1985, 1987; Strukul, 1992b; Murahashi and Davies, 1999)

Te et al. (2001) has studied the oxidation efficiency of various model sulfur compounds (DBT, 4MDBT and 4,6DMDBT) by polyoxometalate/ $\text{H}_2\text{O}_2$  systems. The  $\text{H}_2\text{O}_2$  solutions of phosphotungstic acid and its salt were very active catalyst systems for the model compound oxidation, while their tungsten counterpart systems were more active than molybdenum counterpart systems. It was found that oxidation reactivities decreased in the order of DBT > 4MDBT > 4,6DMDBT, the same reactivity trend that exists in HDS.

It is known that the phosphotungstic and phosphomolybdic Keggin ions convert to polyoxoperoxo species in the presence of hydrogen peroxide (Venturella, et al, 1985; Ballistreri, et al, 1994; Salles, et al, 1994). Therefore, simple experiments were performed to test the presence of the Keggin unit in the oxidation reaction. A number of commercially available polyoxometalate compounds were examined under UAOD condition, such as phosphotungstic acid hydrate (HPW), sodium phosphotungstic hydrate (NaPW), phosphomolybdic acid hydrate (HPMo), and sodium phosphomolybdic hydrate (NaPMo).

Figure 4.14 shows the comparison of yields of BTO and DBTO by using different TMCs. It is clear that phosphotungstic compounds were better catalyst precursors compared to molybdenum counterparts. The acid form of phosphotungstic anion performed slightly higher in oxidation activity compared to its sodium salt, suggesting that the acidic function of the catalyst was playing a significant role in oxidation process. Usually, tungsten HPAs are the catalysts of choice because of their stronger acidity, higher thermal stability, and lower oxidation potential compared to molybdenum HPAs. Generally, if the reaction rate is controlled by the catalyst acid strength, PW shows the highest catalytic activity in the Keggin series (Kozhevnikov, 1998).

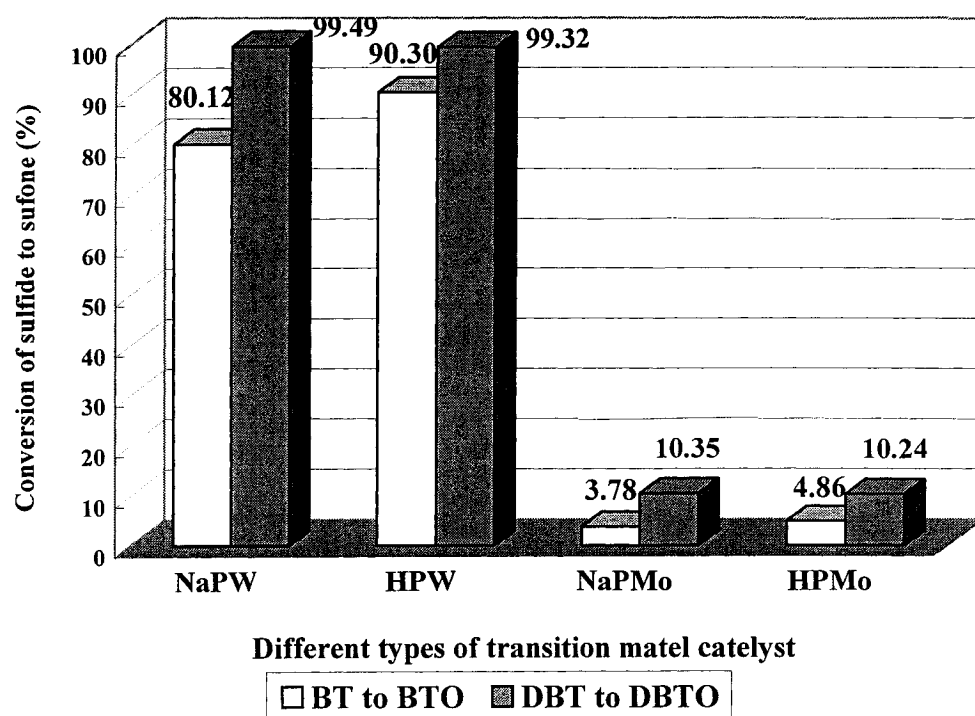


**Figure 4.14 Comparison of yields of BT and BTO by using different TMC**

In this reaction, phosphotungstic compounds with hydrogen peroxide exhibited the highest activity. It is because the formation of the polyoxoperoxo species in this system, where the activities are not dictated by the original Keggin structure (and its redox potential) but by the oxidative activities of the derived polyoxoperoxo species, such as,  $\{\text{PO}_4[\text{WO}(\text{O}_2)_2]_4\}^{3-}$ . This result is consistent with what was reported for the oxidation of other organic substrates in polyoxometalate/ $\text{H}_2\text{O}_2$  systems (Salles, et al, 1994; Te. et al, 2001). In the future work, phosphotungstic acid is selected as transition metal catalyst because of its highest conversion efficiency.

#### **4.4.2 UAOD on Other Model Sulfur Compounds and Kinetic Study**

In most of the available literatures, the mechanisms, and kinetics of Ishii – Venturello system dealt with epoxidation of olefins or olefinic compounds. Limited work has been reported on mechanistic and kinetic studies for oxidation of organic sulfur compounds in a polyoxometalate/PTA/ $\text{H}_2\text{O}_2$  system. However, since many aspects of the reaction remain essentially the same, especially the in-situ formation of polyperoxometalate  $\{\text{PO}_4[\text{WO}(\text{O}_2)_2]_4\}^{3-}$ , which has been isolated and identified in our experiments, the results obtained from studies on Ishii-Venturello epoxidation could be extended to other systems including ultrasound-assisted oxidative desulfurization (UAOD) process.

This study was conducted by using series of model molecules representative of the different class of sulfur compounds presented in diesel fuels. These

compounds, either reactive or resistant to hydrodesulfurization, are all susceptible with different reaction rate for oxidation. It is known from literature that only sulfides with an electron density on the sulfur atom higher than 5.73 can be oxidized in the conditions adopted in this work (Otsuki, et al. 2000). Therefore, thiophene and alkylated thiophenes were not considered in this study.

Several studies indicated that in presence of an excess of  $H_2O_2$ , the oxidation of organic sulfur compounds follows pseudo first order kinetics in carboxylic acid/ $H_2O_2$  and polyoxometalate/ $H_2O_2$  systems (Te, et al. 2001; Otsuki, et al. 2000; Collins, et al. 1997). In the experiments, conversion of sulfur compounds was calculated using their initial concentration ( $C_0$ ) and after t min reaction ( $C_t$ ). Conversion X is expressed as Eq. 4.3:

$$X = \frac{C_0 - C_t}{C_0} \quad (\text{Eq. 4.3})$$

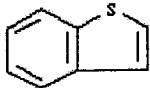
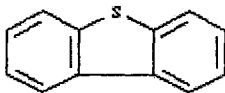
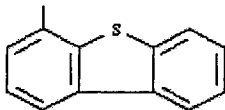
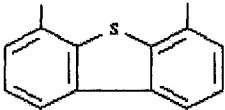
Assuming that the volume and mass of the reaction mixture were constant, only small amounts of liquid sample were withdrawn during the reaction. If BT and DBT oxidation follows pseudo first order reaction kinetic, then the rate constant and reaction time t can be described using the following equation (Eq. 4.4):

$$\ln\left(\frac{C_t}{C_0}\right) = -kt \quad (\text{Eq. 4.4})$$

A plot of  $\ln(C_t/C_0)$  versus t should be linear, and the value of the apparent rate constant, k, can be obtained by the slope of the linear relationship.

The electron density on the sulfur atom of sulfur compounds and their reaction rate, including benzothiophen, dibenzothiophen, and their methyl-substituted derivatives, are shown as Table 4.6 (Otsuki, et al. 2000). The electron densities were in the range of 5.739 to 5.760. The relationship between the sulfone conversions of model compounds and reaction time is showed as Figure 4.15. Since  $\text{H}_2\text{O}_2$  was present in excess amount, the reaction data was fitted to a first-order rate equation. A plot of  $\ln(C_t/C_0)$  versus reaction time showed as Figure 4.16. The result displayed a linear relationship that confirmed the pseudo-first-order reaction kinetics.

**Table 4.6 Electron density on sulfur atom and rate constants**

Sulfur Compounds	Structure	Electron Density	Rate Constant ( $\text{min}^{-1}$ )
Benzothiophene		5.739	0.1795
Dibenzothiophene		5.758	0.3073
4-Methyldibenzothiophene		5.759	0.3353
4, 6-Dimethyldibenzothiophene		5.760	0.3412

Note: Electron density was provided by Otsuki, et al. 2000.

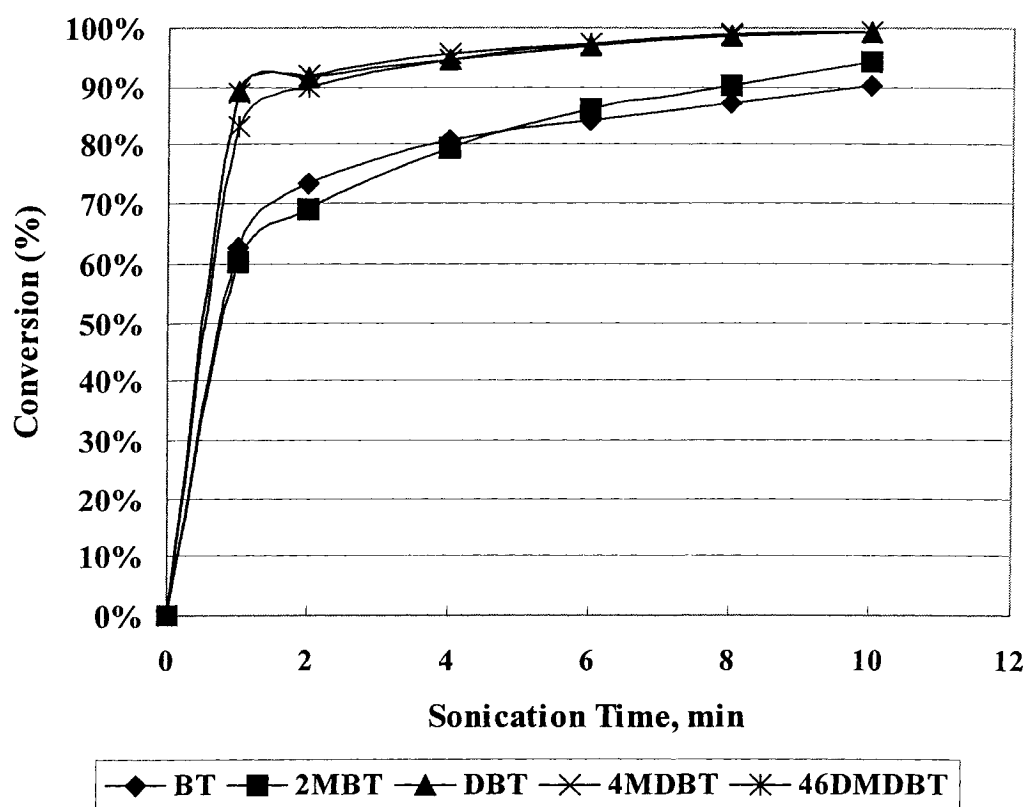
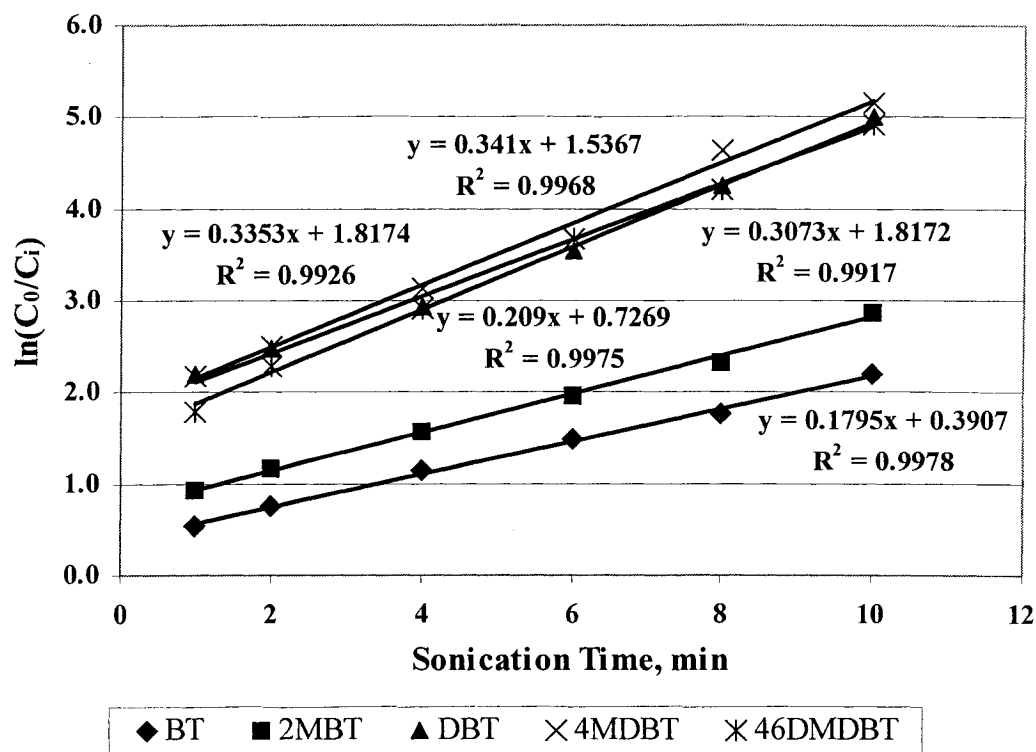
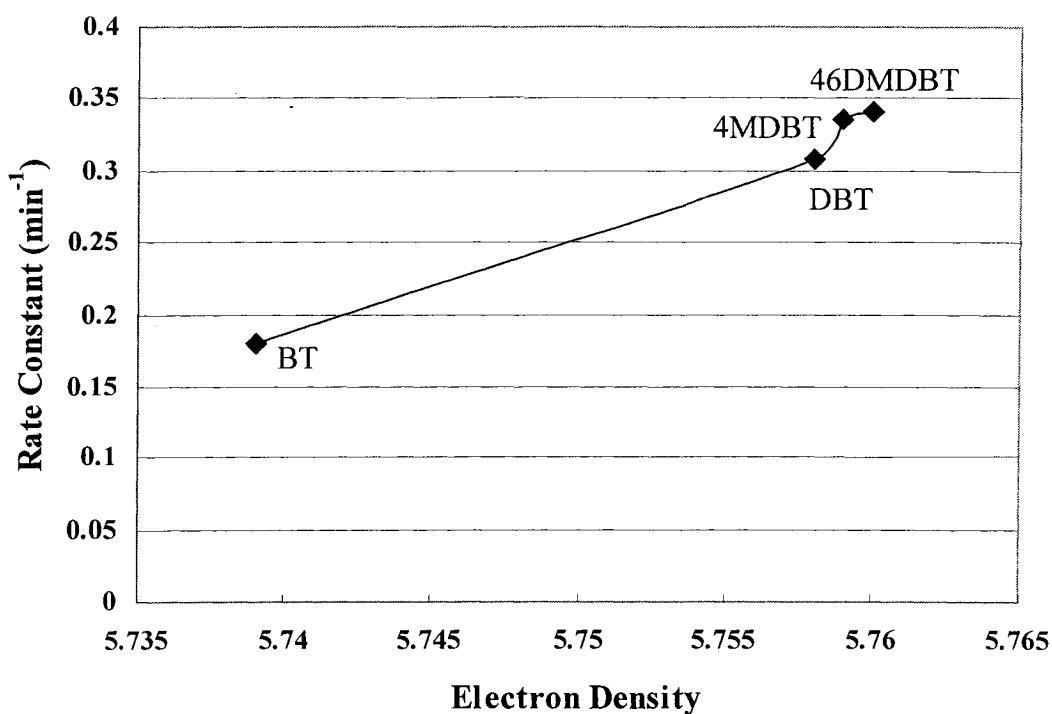


Figure 4.15 Conversion of BT, 2MBT, DBT, 4MDBT and 46DMDBT at different sonication time



**Figure 4.16 Plot of  $\ln (C_0/C_i)$  versus time for oxidation of BT, 2MBT, DBT, 4MDBT and 46DMDBT under pseudo first order condition**

The oxidation reactivity of these sulfur compounds was found in a decreasing order of 46DMDBT > 4MDBT > DBT > 2MBT > BT. The relationships between the rate constants of the oxidation of these model sulfur compounds to corresponding sulfones and the electron densities are shown in Figure 4.17. The reactivity of sulfur compounds for oxidation was increased with the increase of electron density on sulfur atom. The reactivities of BT and DBT derivatives were influenced by the electron donation of substituted methyl groups.



**Figure 4.17 Comparison of the rate constants ( $k$ ) with the electron densities for different model compounds**



## 4.5 SUMMARY

These studies aimed to develop an oxidative desulfurization process with higher reaction rate and higher selectivity, while the UAOD process was designed to combine three complementary techniques, including transition metal catalyzed oxidation, phase transfer catalysis, and ultrasonication. In general, benzothiophene, dibenzothiophene, and their methyl-substituted derivatives are typical thiophenic sulfur compounds that exist in diesel and jet fuels. Using toluene solutions with the model compounds, experiments were performed to compare the reactivities of the different PTA and TMC in oxidation reactions. The series of polyoxometalate/PTA/H<sub>2</sub>O<sub>2</sub> systems were evaluated for the oxidations of model sulfur compounds.

This study has identified that phase transfer agent, especially the quaternary ammonium salts, played a significant role in UAOD process due to sufficient transfer of oxidized metal anion into organic phase or oil/water interface. Moreover, the structure of the QAS cation influenced its ability to transfer ion from the aqueous to organic phase. Based on the experimental results, the oxidation rate of BT to BTO increased with increasing the carbon chain length of QAS cations. Under the same length of carbon chain, the oxidation rate of BT to BTO increased with decreasing the molecular size of QAS anions.

In those experiments, longer carbon chain and smaller anion of QASs were used as phase transfer agent in order to prevent a few side effects under ultrasound, including foaming and excessive decomposition of hydrogen peroxide in the reaction.

A group of typical sulfur compounds in diesel were studied to evaluate the effectiveness of UAOD process and to determine their relative reactivity by using TAOF as PTA. The oxidation reactivities of these OSCs were found in very high yield and free of any by-products. Moreover, 4,6-dimethyldibenzothiophene is a typical refractory sulfur compounds in diesel and other gas oils during the HDS. The optimal oxidation efficiency of 46DMDBT reached 99.28% in 10 minutes by using TAOF as PTA under UAOD condition.

Bromo by-products were formed by using TAOB as PTA during the desulfurization process. 2-bromo and 3-bromo compounds were formed and their sulfones as well. This is caused by the bromide used as PTA, which is the anion of the quaternary salt. These bromo compounds are polar and can be readily separated from the sulfide. If the both position 2 and 3 are blocked in the starting material, there will be no bromo compounds. However, using TAOF as PTA permitted the free of any by-products.

Simply transferring the  $\text{H}_2\text{O}_2$  into organic phase is not sufficient for the oxidation reaction to occur. The addition of polyoxometalate as catalyst precursor, which reacts with  $\text{H}_2\text{O}_2$  to form rather selective oxidants as peroxo metal complex in the form of  $\{\text{PO}_4[\text{WO}(\text{O}_2)_2]_4\}^{3-}$ , results in high selectivity and conversion in the reaction. The phosphotungstic compounds performed much better catalyst precursors compared to molybdenum counterparts. The acid form of phosphotungstic acid performed slightly higher in oxidation activity compared to its sodium salt,

suggesting that the acidic function of the catalyst was playing a significant role in oxidation process.

A group of typical sulfur compounds in diesel were studied to evaluate the performance of UAOD process and to determine their relative reactivities under UAOD conditions. The oxidation reactivities of these OSCs were found in a decreasing order of 46DMDBT > 4MDBT > DBT > 2MBT > BT. This result indicated that rate constant increased with the increase of electron density. Moreover, the oxidation of OSCs under UAOD process followed the pseudo-first-order reaction kinetics.

This information is essential to understand the reactivities of various QASs and TMCs under oxidative conditions, and to optimize the reaction parameter under UAOD process. It also provides a direction to the module study of continues flow desulfurization system as well as the process evaluation of UAOD on diesel fuels.

## CHAPTER 5

### UAOD ON COMMERCIAL DIESEL FUELS

#### 5.1 INTRODUCTION

Diesel fuels are complex mixtures of alkanes, cycloalkanes, and aromatic hydrocarbons with carbon numbers in the range of C<sub>9</sub>-C<sub>28</sub> and with a boiling-range of 150-390 °C. Their relative distribution depends on the feedstock, refining process, and blending schemes based on commercial demand. Due to the higher boiling range, the sulfur compounds in diesel are mostly alkylbenzothiophenes (BTs) and alkyldibenzothiophenes (DBTs). Recent studies on HDS indicated that organic sulfur compounds (OSCs) remaining in diesel fuel at sulfur level lower than 0.1 wt% are alkyl-DBT with alkyl substations at 4- and/or 6- position. These compounds are lower in HDS reactivity and are classified as the most refractory compounds in conventional HDS.

Sulfur compounds are known to be slightly more polar than hydrocarbons. However, oxidized sulfur compounds such as sulfons or sulfoxides are substantially more polar than sulfides. More importantly, the oxidation of sulfides to sulfoxides or sulfones is usually much easier and faster than the oxidation of most hydrocarbons (Bortolini, et al. 1985; Campestrini, et al. 1988; Ballistreri, et al. 1992). Therefore, ultrasound-assisted oxidative desulfurization (UAOD) process operating at ambient temperature and atmospheric pressure permits the selective removal of sulfur

compounds from hydrocarbons by a combination process of selective oxidation and solvent extraction or solid adsorption (Mai, 2003). For convenience, solvent extraction was used as the separation method in this study.

Before fully investigating the desulfurization process, this study first examined whether this process can damage other fuel components. This was essential since many processes end up destroying hydrocarbons, which ultimately affects the performance and energy content of the fuel. Therefore, a study of the selectivity of this oxidative process is very significant, since the UAOD process cannot remove any other hydrocarbons in the diesel fuels.

In this chapter, an ultrasound-assisted oxidative desulfurization (UAOD) process operating at low temperature and atmospheric pressure for given time was executed. The effect of this process on commercial diesels, which include marine logistic fuels (F76, MGO and JP5) and transportation fuel (76 diesel), were evaluated. The selectivity of the oxidation of organic sulfur compounds to sulfones was characterized by GC-PFPD and GC/MS analysis.

## **5.2 MATERIALS AND EXPERIMENT METHODS**

### **5.2.1 Materials**

Three marine logistic fuels with sulfur content of 4,222 ppm (F76), 1,710 (MGO) and 113.7 ppm (JP5), respectively, were received from Long Beach. The jet fuel (JP8) with sulfur content of 863 ppm was received from Army Research Laboratory. Moreover, the transportation diesel with sulfur content of 259 ppm was purchased from 76-gas station, Los Angeles. These diesel fuels were used as the feedstock in this study. Phosphotungstic acid (TMC) and tetraoctylammonium fluoride (PTA) were obtained from Aldrich Chemical. Acetonitrile, the polar solvent for extraction, and hydrogen peroxide (30 vol% solution) were obtained from VWR Inc.

### **5.2.2 Experimental Method**

The oxidation procedure of commercial diesel is described as follows. An appropriate volume of the diesel oil containing tetraoctylammonium fluoride (0.1 g) and an equal volume of hydrogen peroxide (30 vol. % solution) containing phosphotungstic acid (0.2 g) were added to the glass reactor. The mixture was irradiated by 20 kHz ultrasound for 10 min with temperature at  $70^{\circ}\text{C} \pm 2^{\circ}\text{C}$ . After cooling and separation of oil/water, the oxidized diesel was extracted with acetonitrile four times. Acetonitrile was chosen because it has a relatively low boiling point at 355 K and can be easily separated by distillation from the sulfones

with boiling point ranging from 550 K to 950 K. Each time the solvent-to-oil (S/O) ratio was kept at 1:1 by weight (i.e., 5 g diesel per 5 g acetonitrile) and the mixture was shaken vigorously for 1.5 min at room temperature before the oil and solvent layers were separated.

In order to study the effect of oxidation on the efficiency of liquid/liquid (L/L) extraction, original diesel samples were also extracted by acetonitrile using the same procedure as described above. Original diesel, oxidized diesel, extracted diesel, and oil extracted from each extraction step were collected and prepared for GC/PFPD and GC/MS analysis.

### **5.2.3 Selective Ion Monitoring (SIM) Technique**

The selective ion monitoring (SIM) technique in GC/MS analysis was employed to trace the change of organic sulfur compounds (OSCs) and hydrocarbons in diesels throughout the UAOD process. Four types of compounds including *n*-paraffins, *n*-alkyl cyclohexanes, *n*-alkyl benzenes, and alkyl-naphthalenes were selected to present both saturated and aromatic hydrocarbons. The changes of these compounds in UAOD process were monitored at molecular level by using SIM technique in Varian, Saturn GC/MS workstation.

### **5.2.4 Tungsten Analysis**

In UAOD process, the reduced subsequent peroxo species dissociated with phase transfer agent and returned into aqueous phase which was analyzed by

Inductively-Coupled Plasma (ICP) spectrophotometer (Perkin Elmer Plasma 40) for spent tungsten concentration.

## 5.3 ANALYTICAL METHODS

### 5.3.1 Total Sulfur Content

Based on the method ASTM D4294-83, non-dispersive X-ray fluorescence (NDXRF) was used to determine the total sulfur content in the model compounds system. The Sulfur-in-Oil Analyzer (SLF A-20, Horiba Inc., Irvine, CA) was employed to determine any sample with total sulfur content range from 0.002 to 5 wt. % of sulfur. The detection limit is 20 ppm. For samples with total sulfur content below 20 ppm, the concentration of each sulfur compound was quantified by GC-PFPD according to the following equation:

$$C_i \text{ (ppm)} = m A_i^n \quad (\text{Eq. 5.1})$$

where  $C_i$  is the sulfur concentration of sulfur compound  $i$ ,  $A_i$  is the peak area of sulfur compound  $i$ , and  $m$  is the calibration factor. The value of  $m$  and  $n$  were determined by standard samples.



### **5.3.2 Identification of Organic Sulfur Compounds in Diesel**

The sulfur compounds in the diesel fuels were analyzed by Varian gas chromatograph (Varian 3400) equipped with a pulsed flame photometric detector (PFPD) and an ion trap mass spectrometer (Saturn 2000). A fused-silica capillary column DB-5 ms (30 m x 0.25 mm I.D.) with 0.25  $\mu$ m film thickness (J & W Scientific, Folsom, CA USA) was used and the GC oven temperature was initially hold at 100 °C for 3 minutes, then heated up to 275 °C at rate of 6 °C/min, and remained at 275 °C for 10 minutes. Moreover, the model sulfur compounds were used as standard peak in GC-PFPD. The selected ion monitoring (SIM) in GC/MS was used to identify the major peaks in GC-PFPD.

## **5.4 RESULT AND DISCUSSION**

### **5.4.1 Characterization of Diesel Fuels**

Diesel fuels consist mainly of saturated paraffins and naphthens, and aromatic hydrocarbons. Their relative distribution depends on the feedstocks, refining process and blending schemes based on market demand. Basically, there are two types of sulfur compounds with different aromatic skeletons in diesel fuels. Figure 5.1 showed the composition and distribution of organic sulfur compounds (OSCs) in GC-PFPD chromatograms. The first type was the compounds with retention time before 20 minutes, which is alkyl-benzothiophenes (BTs) with alkyl

carbon from 0 to 5. The second type was the compounds with retention time after 20 minutes, which is alkyl- dibenzothiophenes (DBTs) with alkyl carbon varying from 0 to 6.

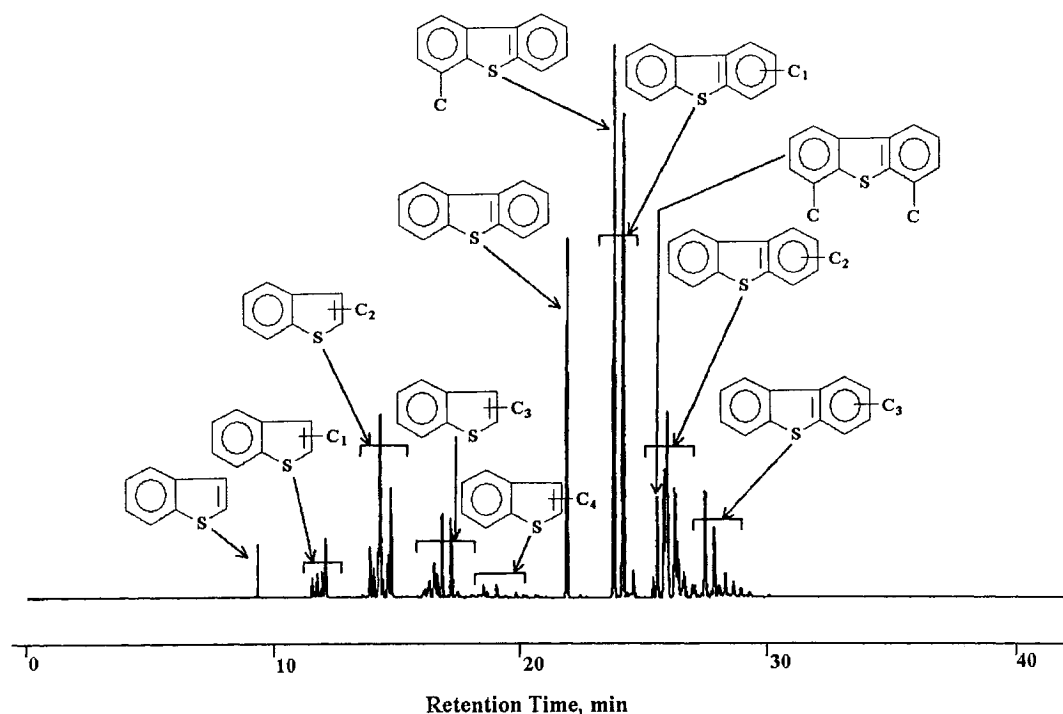


**Figure 5.1 Composition and distribution of organic sulfur compounds in diesel fuels in GC-PFPD chromatogram**

Primary fuel supported for sea-based aircraft is high flash point kerosene-based fuel, designated JP5 and JP8. Conventional powered ships use a distillate-type fuel, such as F76 for propulsion. Military Sealift ships may apply commercial marine fuels for propulsion, such as MGO. Moreover, most of commercial trucks need the transportation diesels as their fuel supplies. In order to differentiate basic compositions of different diesels, The GC-PFPD graph of F76, MGO, JP5, JP8 and

transportation diesel are showed as Figure 5.2. It is estimated that F76 had 45% BTs and 55% DBTs of total sulfur content, while MGO had 30% BTs and 70% DBTs of total sulfur content. However, unlike F76 and MGO, BT and methyl-BTs were the most abundant species in JP5 and JP8, while the DBT and methyl-DBTs were the most abundant species in transportation diesel. Neither sulfides nor alkylthiophene were found in original diesel sample.

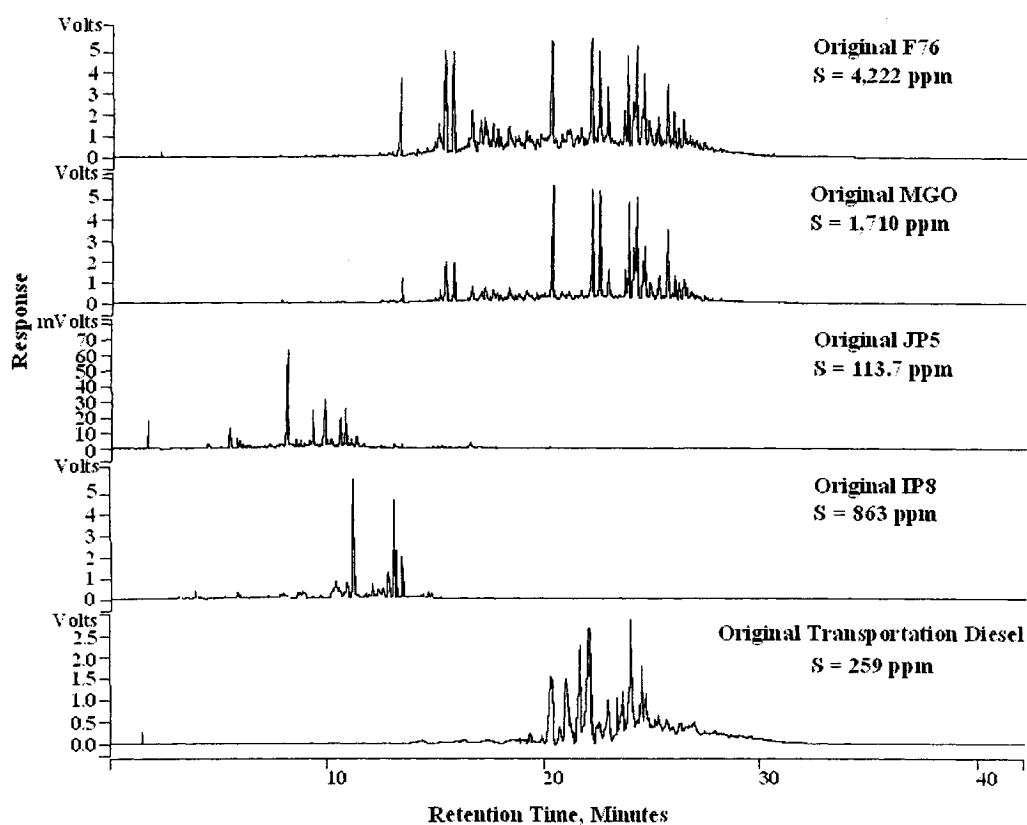


**Figure 5.2 Composition and distribution of organic sulfur compounds in F76, MGO, JP5, JP8 and transportation diesel**

#### 5.4.2 The UAOD on F76 Marine Logistical Diesel

The total sulfur content of the F76 marine diesel was 4,222 ppm. Comparison of GC-PFPD chromatograms of original F76, oxidized F76, and desulfurized F76 in UAOD process was shown in Figure 5.3. Two main groups of sulfur compounds, BTs and DBTs, were oxidized to form benzothiophene sulfones (BTOs) and dibenzothiophene sulfones (DBTOs), respectively. After extracted by acetonitrile, the sulfones in oxidized diesels partitioned into solvents and produced a diesel with total sulfur content of 211.4 ppm. The overall sulfur removal of UAOD on F76 was close to 95 %.

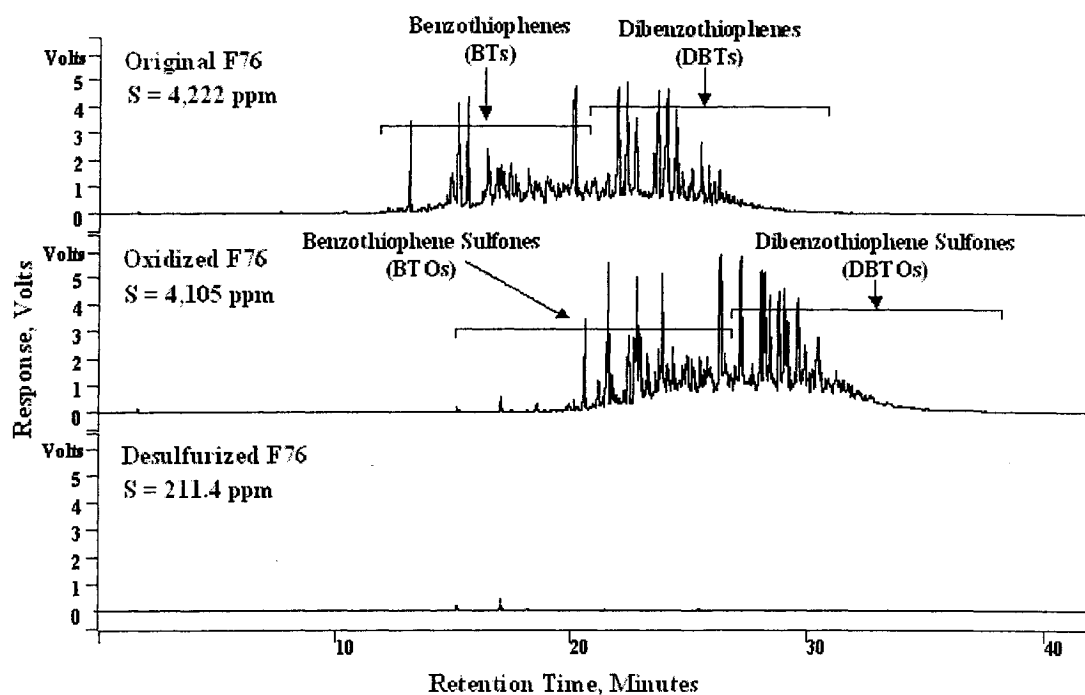


**Figure 5.3** GC-PFPD chromatograms of F76 marine diesel under UAOD process

Organic Sulfur Compounds (OSCs) have different reactivity in oxidation and the extractability of their oxidized products also varies in solvent extraction. Figure 5.4 shows that there were few unreacted BTs (with retention time before 20 mins) remained in the desulfurized F76. For those peaks with retention time after 20 mins were characterized as unreacted DBTs and unextracted BTOs and DBTOs. Base on the retention time, those four major compounds were categorized as compounds in the groups of C<sub>3</sub>-BTs, C<sub>4</sub>-BTs, C<sub>5</sub>-BTs and C<sub>3</sub>-DBTs. It is believed that further identification and quantification of individual OSC would be useful to process the kinetics study of individual OSCs in diesel fuels under UAOD conditions.

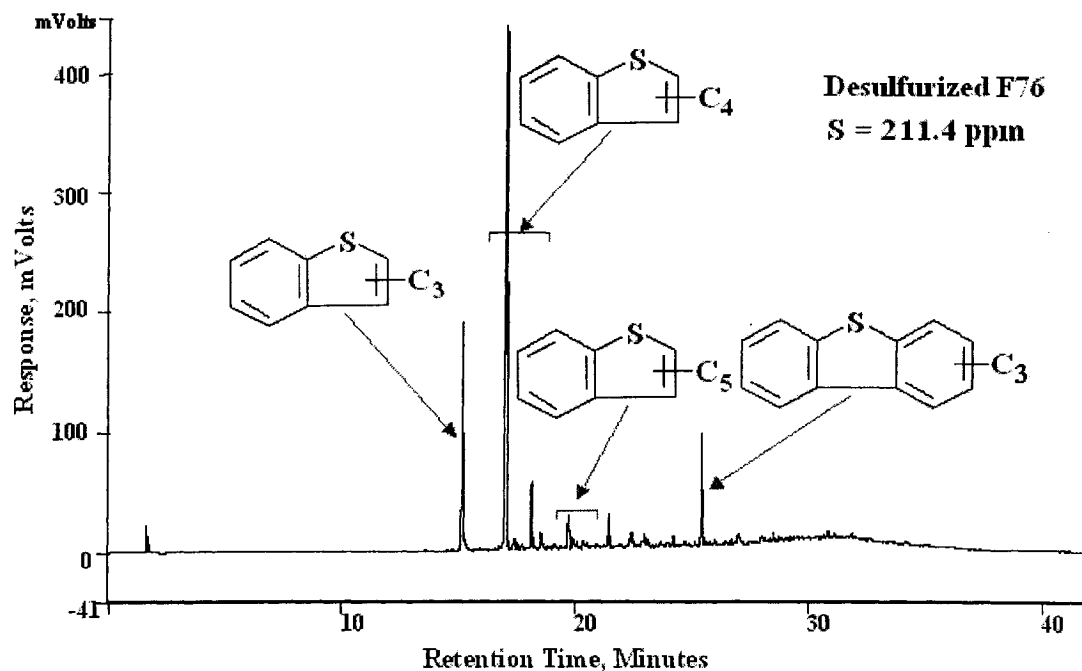


**Figure 5.4 Organic sulfur compounds remain in the desulfurized F76 after UAOD process**

### 5.4.3 The UAOD on MGO Marine Logistical Diesel

The total sulfur content of the MGO marine diesel was 1,710 ppm. Figure 5.5 shows the distribution of OSCs in the original MGO. It is seen that the major types of OSCs were still BTs and DBTs, and the concentrations of BTs were lower than that of DBTs. Unlike F76, DBT and methyl-DBT were the most abundant species in MGO. It is estimated that MGO had 30% BTs and 70% DBTs of total sulfur content. Again, neither sulfides nor alkylthiophene were found in the original MGO.

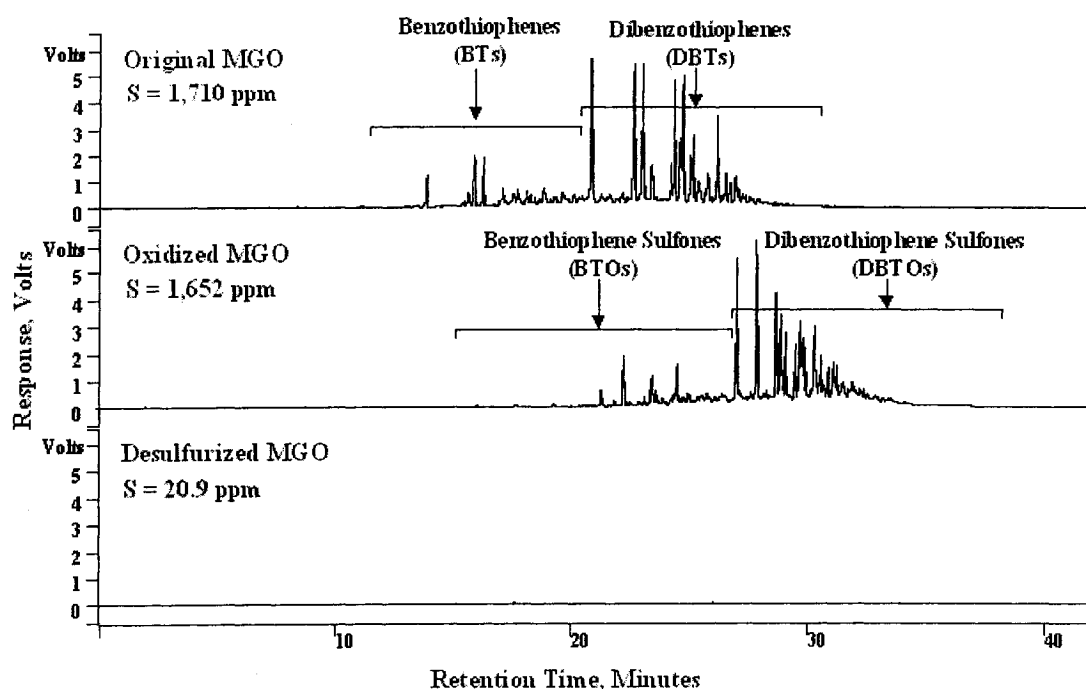


**Figure 5.5 GC-PFPD chromatograms of MGO Marine diesel under UAOD process**

Figure 5.5 also shows the changes of organic sulfur compounds in MGO after oxidation and solvent extraction. It is demonstrated that both BTs and DBTs

oxidized to form BTOs and DBTOs, respectively. After solvent extraction by acetonitrile, the sulfones in the oxidized MGO were essentially removed. As a result, the total sulfur content of desulfurized MGO was 20.9 ppm. The overall sulfur removal of UAOD on MGO was 98.8 %.

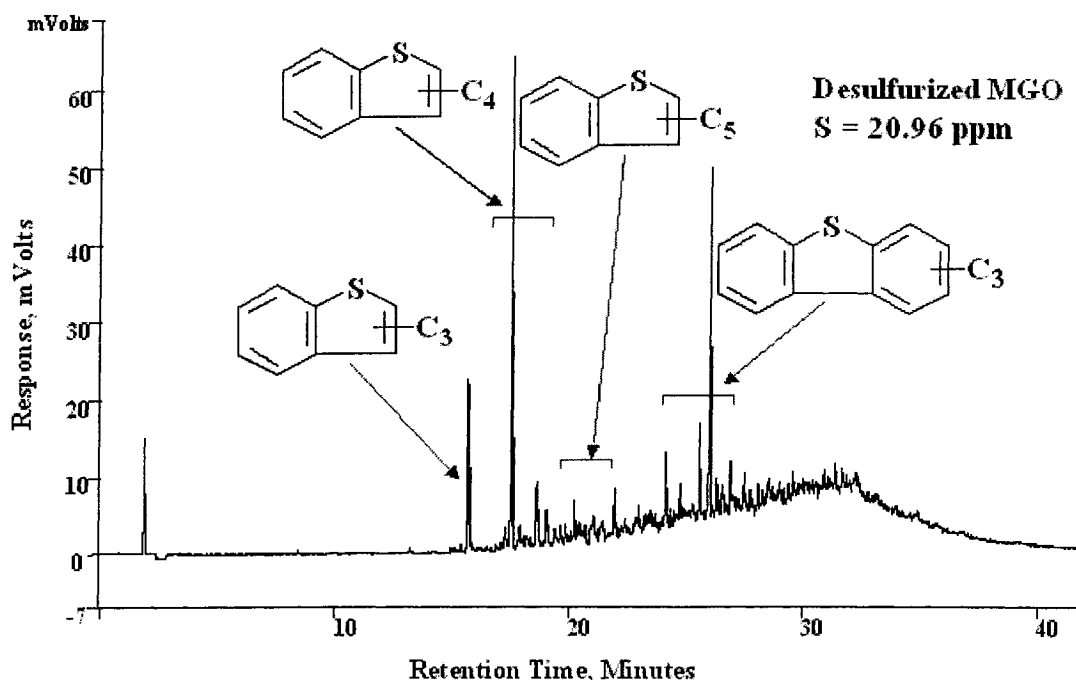


**Figure 5.6 Organic sulfur compounds remain in the desulfurized MGO after UAOD process**

Figure 5.6 indicates that there were four major sulfur compounds left in the desulfurized MGO. Based on the retention time in GC chromatogram, these four sulfur compounds were categorized into four groups of C<sub>3</sub>-BTs, C<sub>4</sub>-BTs, C<sub>5</sub>-BTs and C<sub>3</sub>-DBTs. It is believed that further structural characterizations of these four Sulfur compounds were essential to process design and optimization.

#### 5.4.4 The UAOD on JP5 Marine Logistical Diesel

The total sulfur content of the JP5 Marine diesel was 113.7 ppm. Figure 5.7 shows the distribution of organic sulfur compounds in the original JP5. Clearly, unlike F76 and MGO, BT and methyl-BTs were the most abundant species in JP5. Again, neither sulfides nor alkylthiophene were found in the original JP5. Moreover, as shown in Figure 5.7, most BTs in the JP5 were oxidized into corresponding sulfones within 10 min and subsequently removed by solvent extraction. The total sulfur content in the desulfurized JP5 was 27.7 ppm. The overall sulfur removal of UAOD on JP5 was close to 87.5 %.

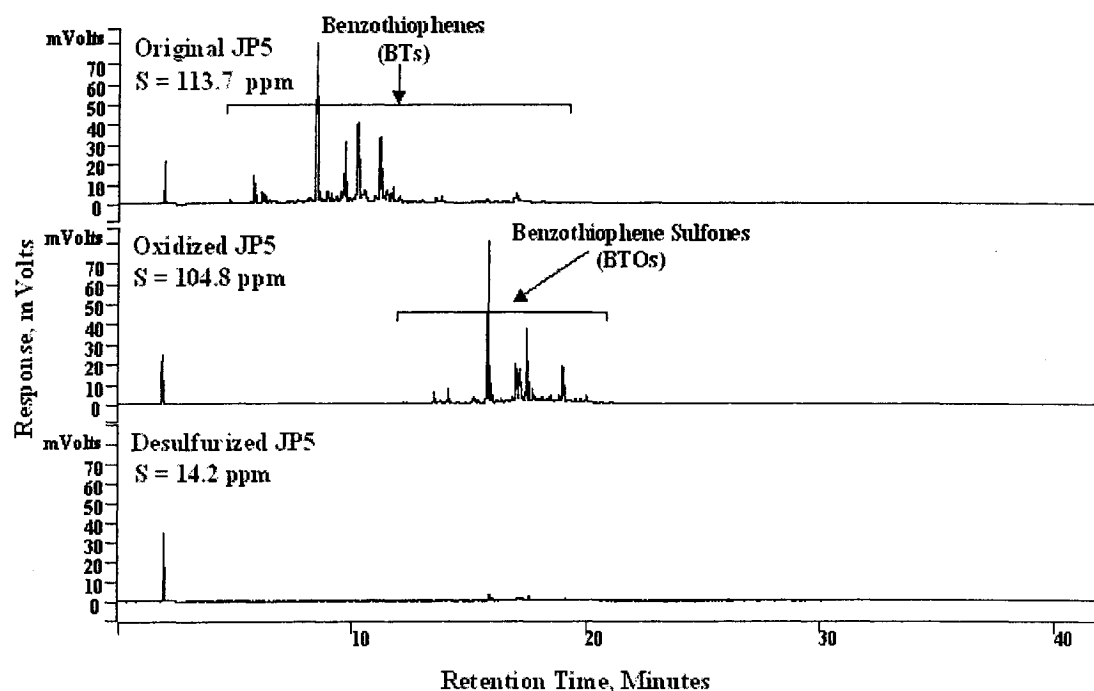
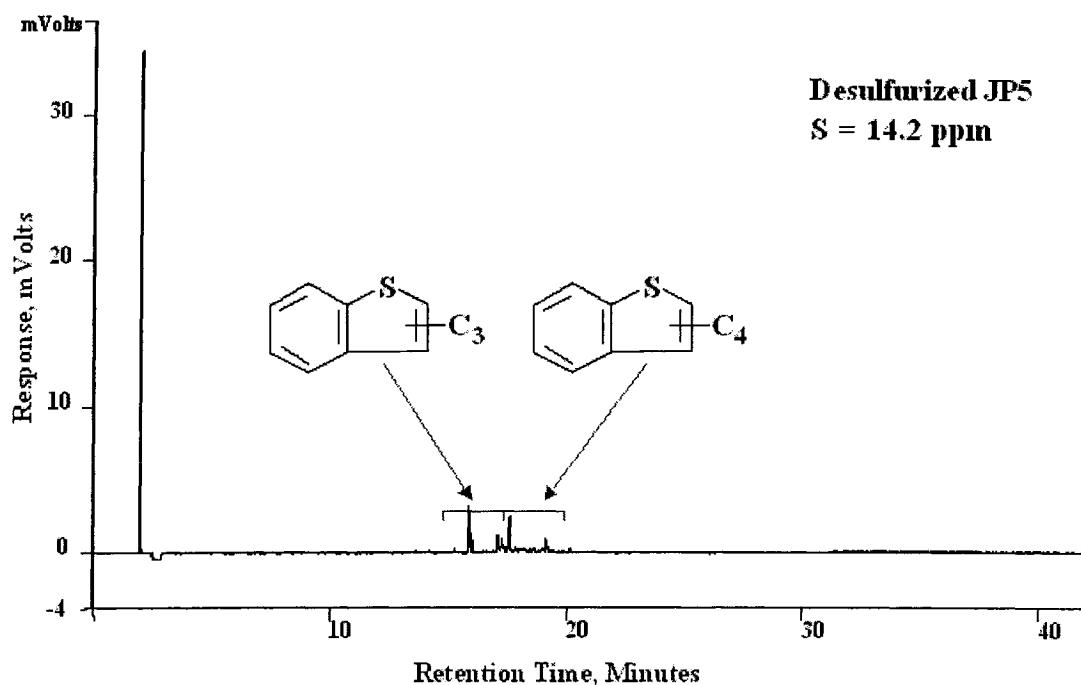


Figure 5.7 GC-PFPD chromatograms of JP5 marine diesel under UAOD process



Figure 5.8 indicates that there are two major BTs left in the desulfurized JP5, including C<sub>3</sub>-BTs and C<sub>4</sub>-BTs groups. These two BT compounds in the desulfurized JP5 were identified as the same sulfur species in the desulfurized F76 and desulfurized MGO. Therefore, It indicates that marine diesel fuels, with different composition, distribution of OSCs, and total sulfur content, may lead to very similar low sulfur diesels (LSD) with respect to the remaining sulfur species after UAOD process.



**Figure 5.8 Organic sulfur compounds remain in the desulfurized JP5 after UAOD process**

#### 5.4.5 The UAOD on JP8 Jet Fuel Diesel

The total sulfur content of the JP8 jet fuel was 863 ppm. Figure 5.9 shows the distribution of organic sulfur compounds in the original JP8. Clearly, unlike F76 and MGO, methyl-Ts, BT and methyl-BTs are the most abundant species in JP8. Moreover, as shown in Figure 5.9, most Ts and BTs in the JP8 were oxidized into corresponding sulfones within 10 min and subsequently removed by solvent extraction. The total sulfur content in the desulfurized JP8 was 1.0 ppm. The overall sulfur removal of UAOD on JP8 was achieved at 99.9 %. Figure 5.10 indicated that there were no organic sulfur compounds left in the desulfurized JP8 (Ultra-low diesel.).

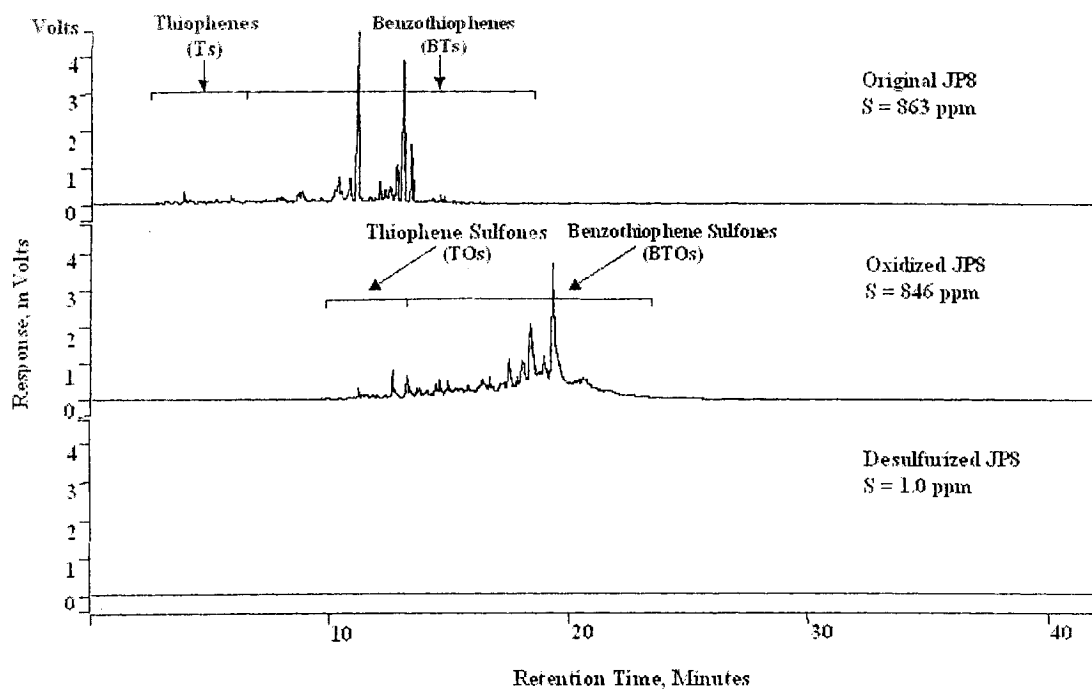
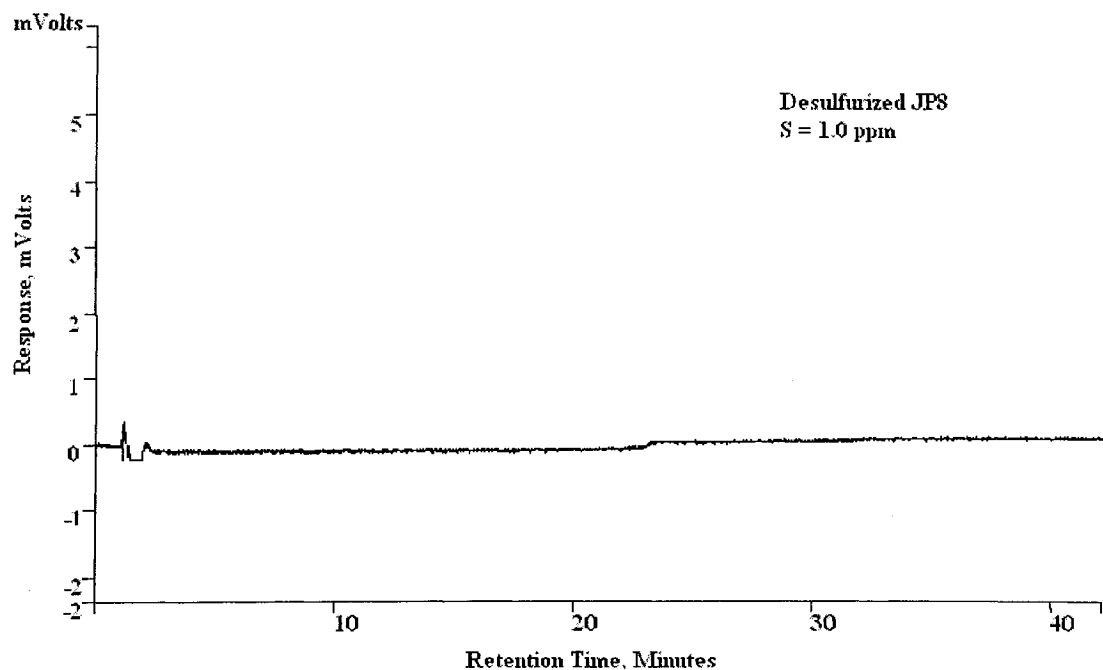


Figure 5.9 GC-PFPD chromatograms of JP8 Jet fuel diesel in UAOD process



**Figure 5.10 Organic sulfur compounds remain in the desulfurized JP8 after UAOD process**

#### **5.4.6 The UAOD on Transportation Diesel**

The total sulfur content of transportation diesel was 259 ppm. Comparison of GC-PFPD chromatograms of original diesel, oxidized diesel, and desulfurized diesel in UAOD process is shown as Figure 5.11. Two main groups of sulfur compounds, BTs and DBTs, were oxidized to form benzothiophene sulfones (BTOs) and dibenzothiophene sulfones (DBTOs), respectively. After being extracted by acetonitrile, the sulfones in oxidized diesel partitioned into solvents and produced a diesel with total sulfur content of 10 ppm. The overall sulfur removal of UAOD on transportation diesel was close to 96.1 %.

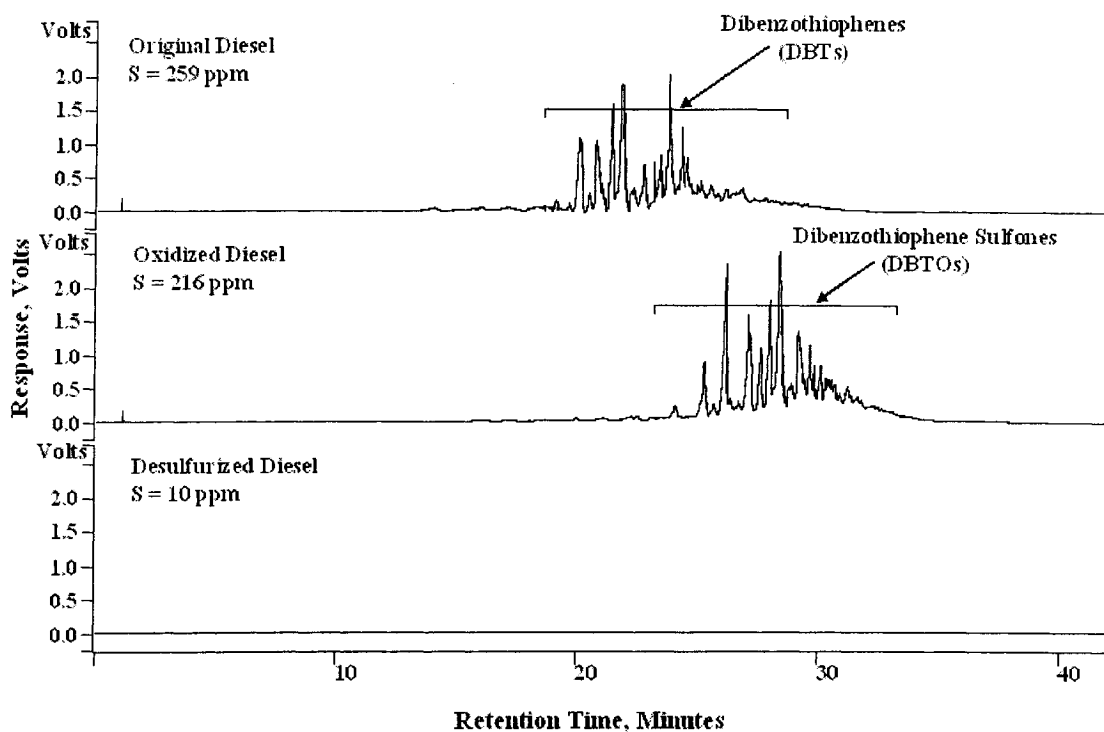


**Figure 5.11 GC-PFPD chromatograms of transportation diesel under UAOD process**

Organic Sulfur Compounds (OSCs) have different reactivities in oxidation and the extractability of their oxidized products also varies in solvent extraction. Figure 5.12 shows that there were some small amounts of unreacted BTs and DBT that remained in the desulfurized diesel, including the groups of C<sub>4</sub>-BTs and C<sub>3</sub>-DBTs. It also indicates that transportation diesel with different composition, distribution of OSCs, and total sulfur content from marine diesel fuels, may lead to very similar low sulfur diesels (LSD) with respect to the remaining sulfur species after UAOD process. Therefore, for diesel fuels containing various levels of sulfur content and different composition and distribution of organic sulfur compounds,

through the use of catalytic oxidation and sonication, sulfur removal efficiency can reach or exceed 95 % in a short contact time at ambient temperature and pressure. This process can be a simple approach for future applications to obtain the ultra-low sulfur diesel.

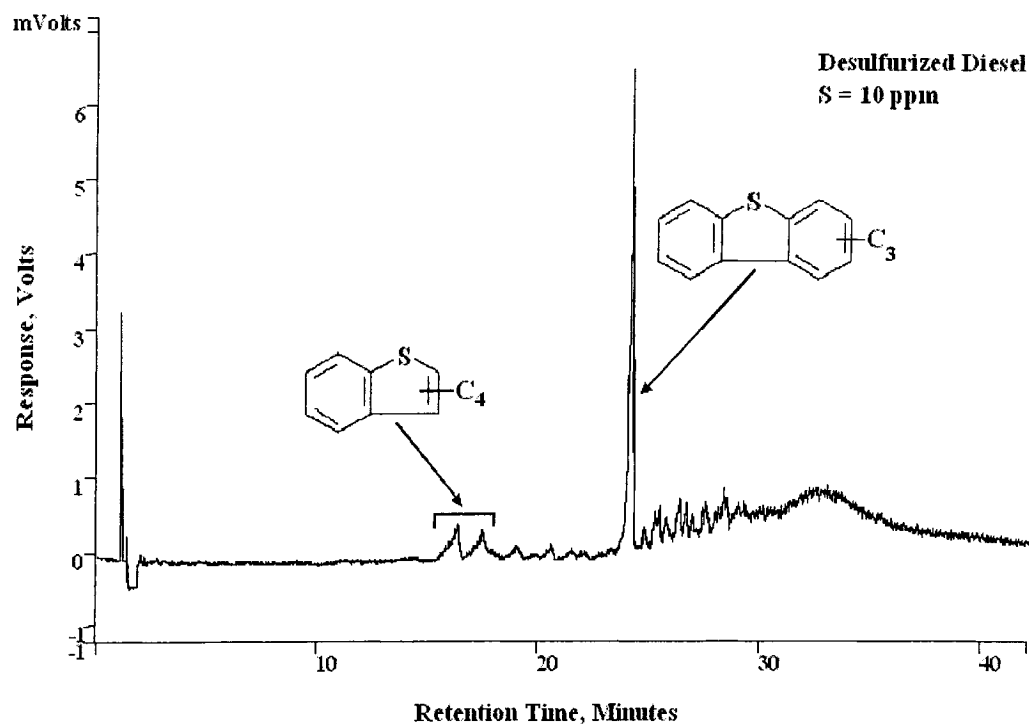


**Figure 5.12 Organic sulfur compounds remain in the desulfurized transportation diesel after UAOD process**

#### 5.4.7 Effects of UAOD on Main Hydrocarbons in Diesel Fuels

The main components of diesel fuels are saturated and aromatic hydrocarbons. Saturated hydrocarbons are dominant diesel components that include normal paraffins (*n*-paraffins), isoparaffins, and cycloparaffins (naphthenes). Aromatic compounds in diesel fuels are mainly alkylbenzenes, florenes, phenanthrens, anthracenes, and naphthenophenanthrens. Diaromatic hydrocarbons with naphthalene-type structure are more abundant aromatic components in diesel fuels. Trace amounts of polycyclic aromatic hydrocarbons (PAH) such as chrysens, pyrenes, benzanthracenes, and perylenes may also be present (Song, 2000).

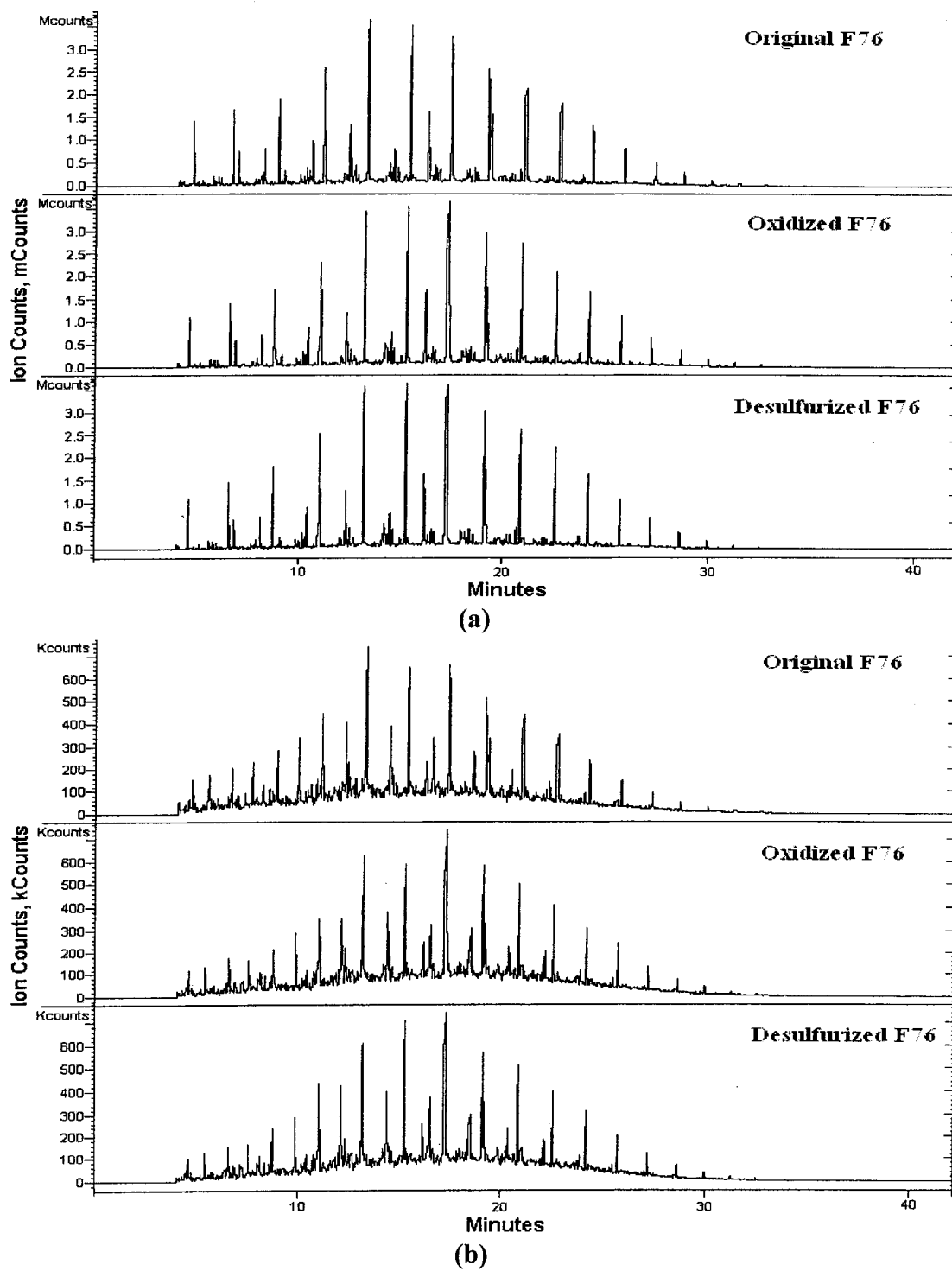
Before fully investigating the desulfurization process, a study of the selectivity of this oxidative process is very significant. It is known that a single mass chromatogram of a common characteristic fragment can present the distribution of a whole class of diesel components. For example, all of the *n*-paraffins yield  $m/z$  57 fragment ions, *n*-alkyl cyclohexanes yield  $m/z$  83 fragment ions, and *n*-alkyl benzenes yield  $m/z$  92 fragment ions. Therefore,  $m/z$  57, 83, and 92 mass chromatograms can exhibit the whole class of *n*-paraffins, *n*-alkyl cyclohexanes, and *n*-alkyl benzenes, respectively. For alkylnaphthalenes, the combination mass chromatogram of molecular ions,  $m/z$  128, 142, 156, 170, and 184 presents the distribution of alkylnaphthalenes with alkyl carbon atom from 0 to 4.

Figure 5.13 shows that there were no significant changes in both distribution and intensity of *n*-paraffins peaks (Figure 5.13a) in the original F76, oxidized F76, and desulfurized F76. The selected ion chromatograms (SICs) of 83 Da ion (Figure

5.13b) and 92 Da ion (Figure 5.14a), extracted from GC-MS analysis of F76 at different stages of UAOD, also follow the same pattern. It indicates that *n*-paraffins, *n*-alkyl cyclohexanes, and *n*-alkyl benzenes did not subject to any negative effects in both oxidation and solvent extraction steps in UAOD process.

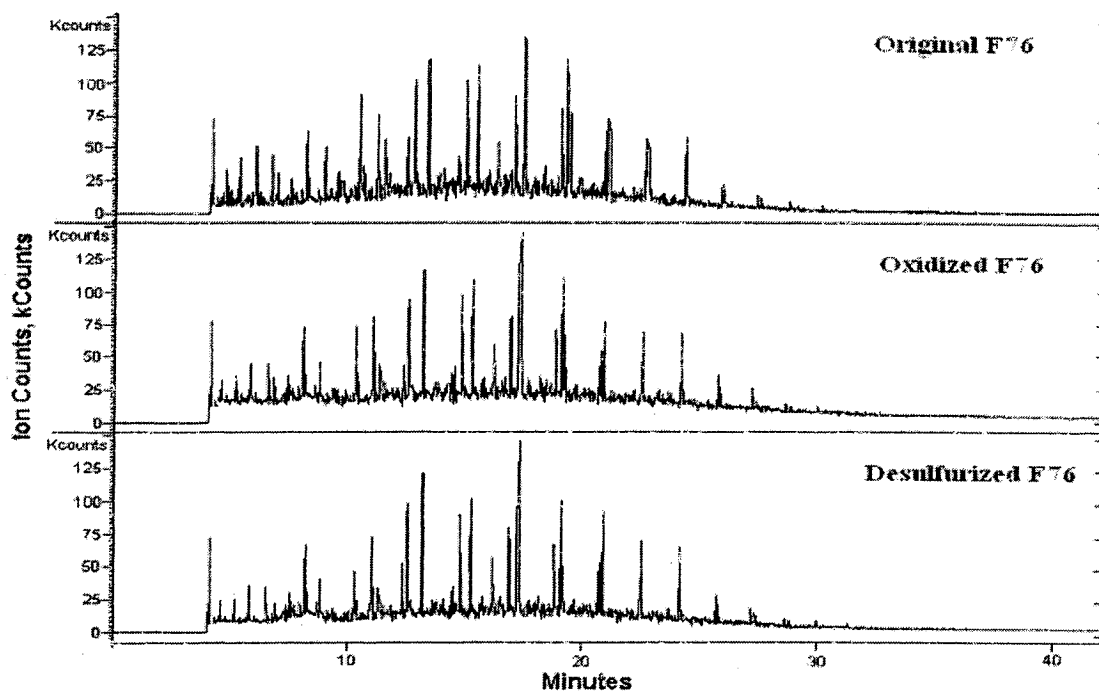
However, Figure 5.14b indicated that even though alkylnaphthalenes did not undertake significant changes in the oxidation steps, the intensity of alkylnaphthalenes peaks in the desulfurized F76 decreased obviously due to solvent extraction. It reveals that alkylnaphthalenes have relative higher polarity than saturated hydrocarbons and benzenes, and intend to partition into polar solvents. However, this portion of aromatics can be easily recovered by distillation of solvent extract. An alternative way is to change the solubility parameter of acetonitrile by blending with another solvent. These experimental findings should be optimized against the solubility of alkyl aromatics. Moreover, for MGO, JP5, and transportation diesel, this SIM analysis indicated the similar distribution and intensity of four selective compounds as F76.

Selective ion monitoring (SIM) technique in GC/MS analysis provides a unique illustration of UAOD process on diesels at a molecular level. It was employed in this study to trace the changes of OSCs as well as major hydrocarbons in diesels throughout UAOD process. It firmly demonstrated that UAOD process has high efficiency and high selectivity on oxidizing the OSCs to its corresponding sulfones.

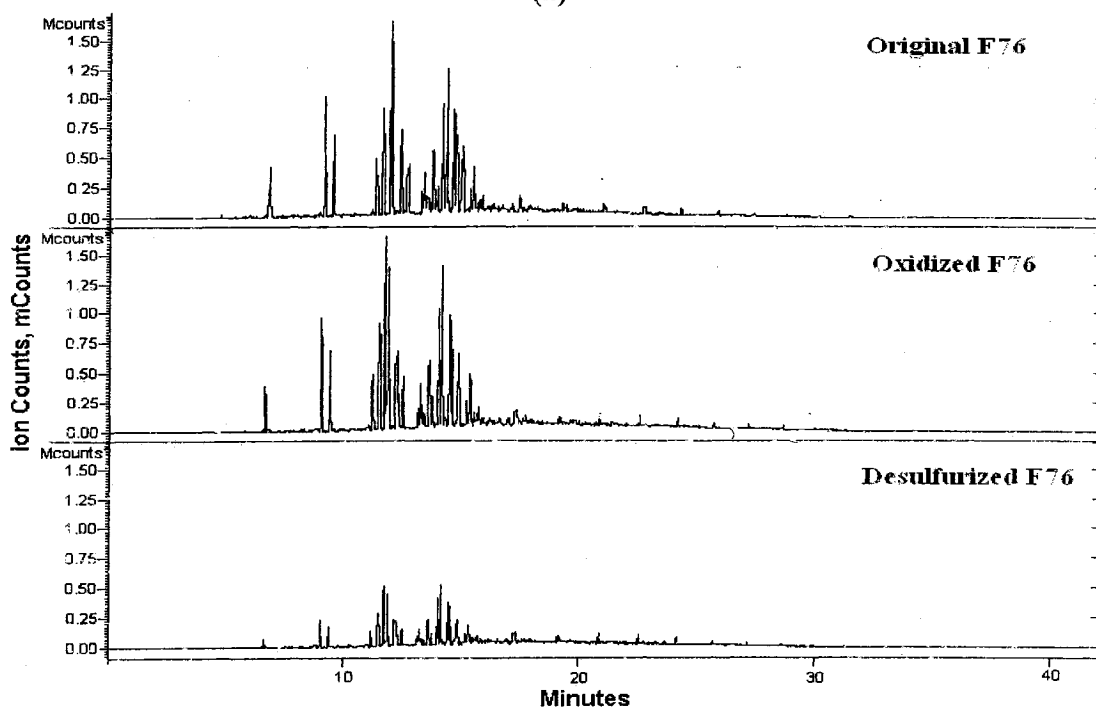


**Figure 5.13 Effects of UAOD on saturated hydrocarbons in marine logistic fuel. (a) *n*-paraffins, (b) *n*-alkyl cyclohexanes**





(a)



(b)

**Figure 5.14 Effects of UAOD on saturated hydrocarbons in marine logistic fuel.  
(a) *n*-alkyl benzenes, (b) alkylnaphthalenes**

#### 5.4.8 Catalyst Recovery

In ultrasound-assisted oxidative desulfurization (UAOD) process, oxidation of organic sulfur compounds was carried out in the presence of ultrasonication and excess  $\text{H}_2\text{O}_2$  using phosphotungstic acid as transition metal catalyst and tetraoctylammonium fluoride or as phase transfer agent. In the presence of excess  $\text{H}_2\text{O}_2$ , phosphotungstic acid, the metal precursor simply represented as POM, is a large and fast growing class of metal oxygen clusters that exhibit unique molecular structures, charge densities, acidic, and frequently reversible redox properties. However, these catalysts are usually quite expensive. The commercial viability of UAOD processes that using transition metal catalysts depends on the efficiency of catalyst recovery.

The concept of catalytical cycle consists of four steps: (a) In the presence of excess  $\text{H}_2\text{O}_2$ , phosphotungstic acid or  $\text{H}_3\text{PW}_{12}\text{O}_{40}$  is peroxidized and disaggregated to form anionic peroxometal complex, namely as  $\{\text{PO}_4[\text{WO}(\text{O}_2)_2]_4\}^{3-}$ ; (b) Quaternary ammonium salts such as  $\text{Oct}_4\text{N}^+\text{F}^-$  with large lipophilic cation can function as phase transfer agent and transfer the peroxometal anion into organic phase; (c) In organic phase, organic sulfur compounds such as benzothiophene and dibenzothiophene are oxidized by the peroxometal complex with high efficiency and high selectivity; (d) The reduced subsequent peroxy species, which dissociate with phase transfer agent, returns into aqueous phase, and thus restore the catalytic cycle.

This study was conducted by using ICP to analyze the changed tungsten concentrations before and after UAOD process. Table 5.1 shows that 99.49% of tungsten remained at aqueous phase. It indicated that the tungsten could be fully recovered after the oxidation reaction. However, the efficiency of this oxidized metal has to be examined.

**Table 5.1 Tungsten recovery after UAOD process**

<b>Original W Concentration (ppm)</b>	<b>W Concentration after UAOD Process (ppm)</b>	<b>Tungsten Recovery Percentage</b>
6128.0	6096.7	99.49 %

Base on this point, several experiments were conducted by using the spent aqueous phase mixed with original diesel to run the UAOD process. Two conditions, with and without PTA, were considered as the control parameters. Table 5.2 shows that two control units with sulfur removal percentage was 98.15% (with PTA) and 96.01% (without PTA), respectively. Comparing to the first run of UAOD process with 98.78% sulfur removal percentage on MGO, It is obvious that this anionic peroxometal complex, named as  $\{PO_4[WO(O_2)_2]_4\}^{3-}$ , still had high efficiency to permit the oxidation reaction.

In UAOD process, the transition metal catalyst plays an important role to accelerate the reaction and enhance the oxidation efficiency. However, the wasted catalyst may cause to increase the capital cost and issue the environment pollutions.

The complete catalyst recovery is essential to enhance the commercial viability of UAOD processes.

**Table 5.2 Spent catalyst reused in UAOD process**

<b>Experiment</b>	<b>Original Sulfur Conc. (ppm)</b>	<b>Final Sulfur Conc. (ppm)</b>	<b>PTA</b>	<b>Total Sulfur Removal Percentage</b>
New Catalyst	1710	20.9	TOAF	98.78 %
Spent Catalyst	1710	31.7	TOAF	98.15 %
Spent Catalyst	1710	68.3	None	96.01 %

This study indicated that the tungsten could be fully recovered after the oxidation reaction by using ICP analysis. Moreover, the spent catalyst had almost the same oxidation efficiency as the original catalyst. This information is essential to prevent the consuming cost of TMC and PTA to perform the optimization of desulfurization process.

#### **5.4.9 Different Concentrations of Hydrogen Peroxide in UAOD**

Hydrogen peroxide is a colorless and syrupy liquid, and considered an ideal “green” oxidant due to its high oxidizing ability and lack of toxic by-products. It is miscible with cold water and is soluble in alcohol and ether. Although pure hydrogen peroxide is fairly stable, it decomposes into water and oxygen when heated above about 80°C. It also decomposes in the presence of numerous catalysts, including

most metals, acids, or oxidizable organic materials. Moreover, hydrogen peroxide can be used for diverse applications to utilize its high selectivity. By simply adjusting the conditions of the reaction, hydrogen peroxide can often be made to oxidize one pollutant over another, or even favor different oxidation products from the same pollutant.

Hydrogen peroxide is available in various strengths and grades. (a) *3% Pharmaceutical Grade*: This is the grade sold at local drugstore or supermarket. This product is used as a mild bleaching agent and medicinally as an antiseptic. (b) *6% Beautician Grade*: This is used in beauty shops to color hair. (c) *30% Reagent Grade*: This is used for various scientific experimentations and also contains stabilizers. (d) *30% to 32% Electronic Grade*: This is used to clean electronic parts. (e) *35% Technical Grade*: This is a more concentrated product than the Reagent Grade and differs slightly in that phosphorus is added to help neutralize any chlorine from the water used to dilute it. (f) *35% Food Grade*: This is used in the production of foods like cheese, eggs, and whey-containing products. It is also sprayed on the foil lining of aseptic packages containing fruit juices and milk products. (g) *90% Grade*: used as an oxygen source for rocket fuel.

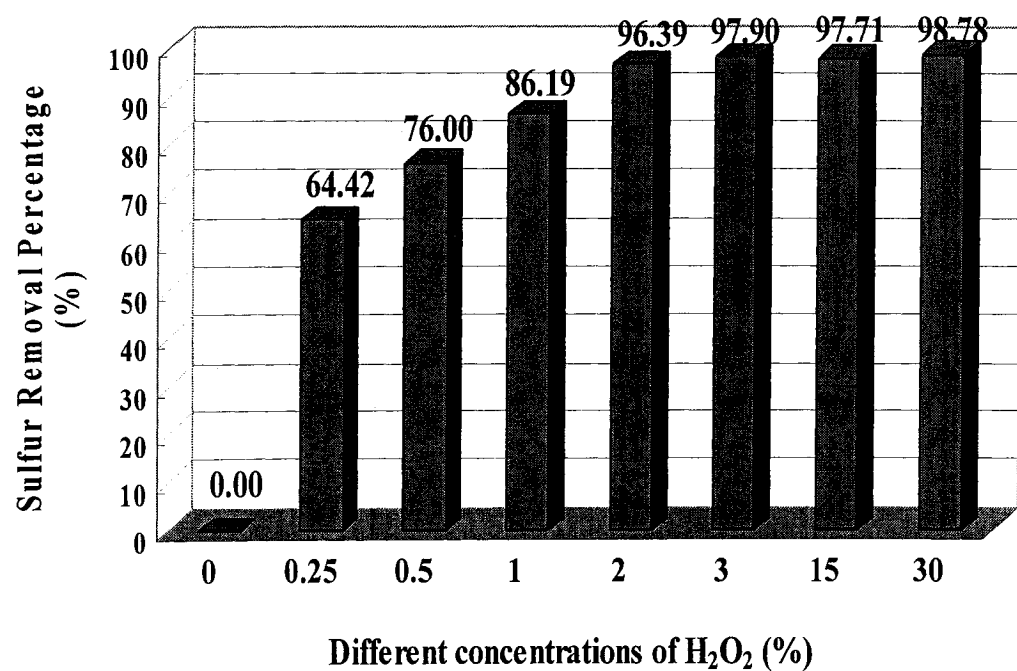
Despite its potential value as an oxidant, hydrogen peroxide has some serious drawbacks. It is inherently corrosive and, especially in high concentrations, is prone to catalytic decomposition. Using dilute aqueous solutions can minimize these problems. However, the excess water often produces a biphasic mixture with the organic substrate and the oxidant residing in different phases (Remias, et al. 2003).

Figure 5.15 shows the desulfurization efficiencies of different hydrogen peroxide concentrations on MGO in batch scale. If there was no hydrogen peroxide applied to UAOD process, there was no sulfur removal can be achieved. 0.25 % hydrogen peroxide could start the oxidation reaction, and sulfur removal was about 64.42 %. Slightly increasing the concentrations of hydrogen peroxide allowed increasing efficiency of sulfur reduction. The concentration at 3 % could dramatically increase the sulfur removal to 98.78 % under the same operation conditions that used 30 % hydrogen peroxide as oxidant. Moreover, 3% hydrogen peroxide could perform the same desulfurization efficiency in different diesel fuels, as shown in Table 5.3.

Hydrogen peroxide played an important role in Ishii-Venturello Expoxidation. If there was no hydrogen peroxide applied to UAOD process, there was no sulfur removal. However, using dilute aqueous solutions could execute the same desulfurization efficiency. Thus, UAOD process could be operated under much safer environment with diluted hydrogen peroxide condition.

**Table 5.3 Different H<sub>2</sub>O<sub>2</sub> concentrations applied to different diesels in UAOD process**

Hydrogen Peroxide Concentration (%)	Sulfur Removal Percentage (%)	
	MGO	F76
3	97.90	94.8
30	98.78	95.0



**Figure 5.15 Desulfurization efficiency of different hydrogen peroxide concentrations on MGO under UAOD conditions**

## 5.5 SUMMARY

In this chapter, three marine diesel fuels and transportation diesel fuels containing various levels of sulfur content were used with catalytic oxidation and sonication followed by solvent extraction, high removals of sulfur-bearing compounds were achieved in a short contact time under low temperature and atmospheric pressure. The results of the oxidative desulfurization of diesel fuels by UAOD process are summarized in Table 5.4.

**Table 5.4 Desulfurization efficiency of UAOD process on diesel fuels**

Diesel Fuels	Sonication time (min)	Sulfur Content (ppm)			Sulfur Removal (%)
		Original	After Oxidation	After Extraction	
F76	10	4,222	4,105	211.4	95.0
MGO	10	1,710	1,652	20.9	98.8
JP5	10	113.7	104.8	14.2	87.5
JP8	10	863	846	1.0	99.9
Transportation	10	259	216	10.0	96.1

There were four major sulfur organic compounds left either in desulfurized F76, MGO and JP5 or desulfurized transportation diesel. Those four sulfur compounds, which were categorized as the group of C<sub>3</sub>-BTs, C<sub>4</sub>-BTs, C<sub>5</sub>-BTs and C<sub>3</sub>-DBTs, were among the most refractory compounds in marine logistic diesels under UAOD conditions. This information is essential to understand the reactivities



of various organic sulfur compounds under oxidative conditions, and to carry out the model sulfur compound study. It also provides a direction for the design and optimization of desulfurization process.

Selective ion monitoring (SIM) technique in GC/MS analysis provided a unique illustration of UAOD process on diesels at a molecular level. It was employed in this study to trace the changes of OSCs as well as major hydrocarbons in diesels throughout UAOD process. It firmly demonstrated that UAOD process has high efficiency and high selectivity on oxidizing the OSCs to sulfones.

In UAOD process, the transition metal catalyst played an important role to accelerate the reaction rate and enhance the oxidation efficiency. However, the wasted catalyst may cause to increase the capital cost and issue the environment pollutions. The complete catalyst recovery was essential to enhance the commercial viability of UAOD processes. This study indicated that the tungsten could be fully recovered after the oxidation reaction by using ICP analysis. Furthermore, the recycled catalyst solution had almost the same oxidation efficiency as the original catalyst. This information is essential to prevent the consuming cost of TMC and PTA to perform the optimization of desulfurization process.

Hydrogen peroxide is a colorless and syrupy liquid, and considered an ideal “green” oxidant due to its high oxidizing ability and lack of toxic by-products. Despite its potential value as an oxidant, hydrogen peroxide has some serious drawbacks. It is inherently corrosive and, especially in high concentrations, is prone to catalytic decomposition. Using dilute aqueous solutions can minimize these

problems. This study indicated that 0.25 %hydrogen peroxide initiated the oxidation reaction and sulfur removal was about 64.42 %. 3 % hydrogen peroxide achieved the same sulfur removal under the same operation conditions with 30 % hydrogen peroxide as oxidant. This information is essential to understand the reactivity of various hydrogen peroxide concentrations under oxidative conditions, and to optimize the reaction parameter under UAOD process.

## CHAPTER 6

### A PORTABLE, MODULAR DESIGN UNIT – SONOREACTOR APPLIED TO SULFUR REMOVER ON DIESEL FUEL

#### 6.1 INTRODUCTION

Sulfur content of diesel is a source for  $\text{SO}_x$  and sulfate particulate matter (PM). Removal of sulfur compounds from diesel fuels avoids air pollution in consistence with public health. Sulfur in diesel also poisons catalytic converters and corrodes internal combustion engine parts. EPA has issued stringent rules requiring an ultra-low sulfur content in diesel fuels, making it necessary to develop alternative methods of desulfurization of fossil fuel derived oil. However, current technologies are not sufficient to solve this problem. Ultrasound-assisted oxidative desulfurization (UAOD) process operating at ambient temperature and atmospheric pressure provides the selective removal of sulfur compounds from hydrocarbons by a combination process of selective oxidation, solvent extraction, and/or solid adsorption (Mei, 2003)

In the batch process, all the reaction components were combined and performed under controlled conditions until the desired process endpoint has been reached. Reactions are typically slow, taking hours, and the product was isolated at the end of the process cycle (Anderson, 2001). In contrast, the continuous flow system can be operated at steady state with reactants continuously coming into the reaction vessel and product continuously leaving. The nature of continuous flow

system can permit itself to large productivities and great economic of scale than the cyclic operation of batch reaction (Nauman, 2001).

Developing the new chemical reactor involves major technical and financial considerations to meet a definite and practical need of the industries. The nature of continuous flow reactor permits a long production runs of high volume fuel streams in petroleum refining industries. Therefore, this study has spent one and a half years designing and developing a continuous flow system in a portable, modular design application. The concept of module design requires that each individual element exhibits the best quality or quantity purpose and performance. This process consists of several different components, and each component by itself can be an independent module.

Among all manufactories, only Branson Inc. could provide us with a commercial unit that met our requirements. However, because of the inappropriate frequency and large capacity, this unit couldn't achieve the best results. After consulted with many ultrasound experts and transducer specialists, a tailor-made module reactor, named as sonoreactor, was successfully assembled by Blatek Tech., which was the unique unit constructed specifically for oil industries among the world.

In this chapter, this continuous desulfurization system, which consisted of a sonoreactor, an RF amplifier, a function generator, and a pipeline system, was operated at ambient temperature and pressure for given time. The effect of this sonoreactor on commercial diesels (MGO) was evaluated.

## **6.2 MATERIALS AND EXPERIMENT METHOD**

### **6.2.1 Materials**

The marine logistic fuel (MGO) with sulfur content of 1,710 ppm was used as the feedstock in this study. Phosphotungstic acid (TMC) and tetraoctylammonium fluoride (PTA) were obtained from Aldrich Chemical. Acetonitrile, the polar solvent for extraction, and hydrogen peroxide (30 vol% solution) were obtained from VWR Inc.

### **6.2.2 Probe Type Ultrasound Reactor in Recirculation Loop Continuous Flow**

The probe type ultrasound reactor in recirculation loop continuous flow application was consisted of a chamber for sonication with close loop and pump. As shown in Figure 6.1, the steel chamber, manufactured by Sonic & Material Inc. (Newtown, CT), was used as the flow reactor in this experiment. This reaction vessel can screw onto the threaded end 1/2" (13 mm) probe at the nodal point (point of no activity) or slide onto the 1" (25 mm) outside diameter portion of the 5" (127 mm) tubular adapter and is secured in place by the action of a threaded nylon bushing compressing an O-ring. Moving the adapter in or out of the vessel allows the probe to be immersed at different depths, ensuring optimum transfer of energy into the sample. Moreover, the maximum capacity of the reactor was 50 ml with working volume of 42 ml. In this experiment, a single probe type ultrasound reactor was used for Continuous-Flow Stirred Tank Reactor (CSTR) in recirculation loop application.

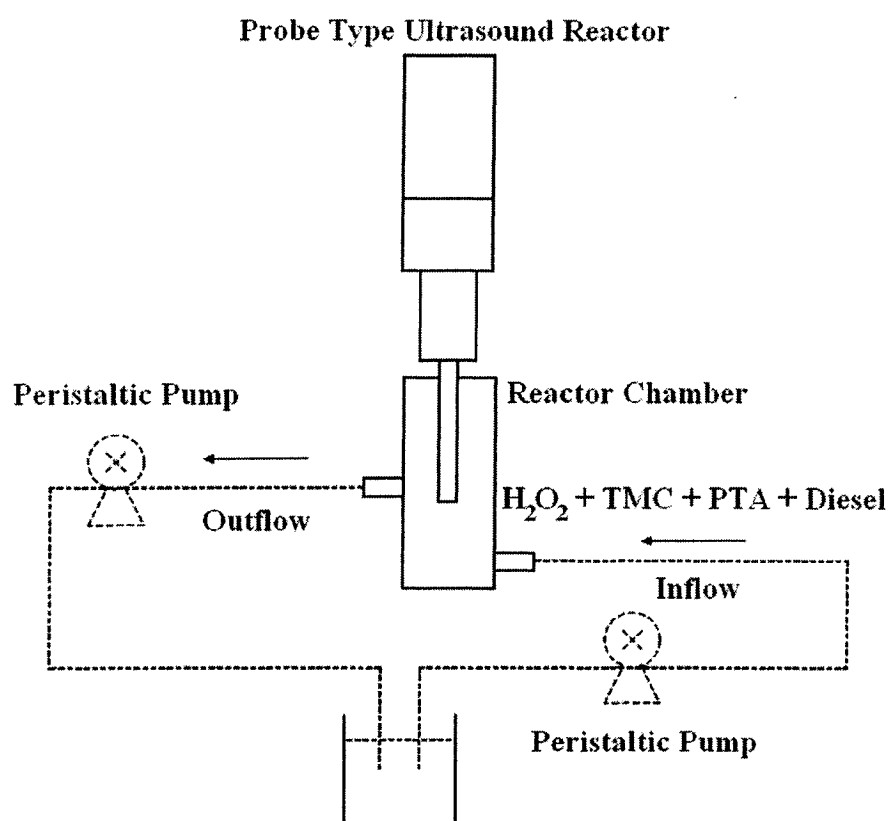


**Figure 6.1 Schematic diagram of a probe type ultrasound reactor in recirculation loop continuous flow application**

### 6.2.3 Tubular Reactors

Configurations of the tubular sonochemical reactor provide either direct or indirect sonication to the process stream. Several designs may be used to provide sonication to an external flow loop in a mixed reactor. There were two types of tubular reactor applied to this study, including Branson 8500 serious and tailor-made sonoreactor. The detail design will be discussed in this chapter.

#### 6.2.3.1 Branson 8500 Serious – Pentagonal Processor

The Pentagonal processor assembly utilizes highly efficient 40 kHz piezoelectric transducers to assure maximum energy (1500 watts) in the process tube. The tube is constructed of type 316 stainless steel for compatibility with a broad range of liquids. The maximum chamber capacity for this processor is 4 gallons. Multiple processors can be used in series to increase ultrasonic exposure and throughput. Stainless steel flanges and gasket systems are available to facilitate multi-head use.

Figure 6.2 illustrates the schematic diagram of Branson Pentagonal processor. The processor which consists of an ultrasonic tank with 35 transducers is driven by the S-8540 ultrasonic generator. These generators are equipped with a number of features which bring flexibility to liquid processing applications, including line/load power control, amplitude control and several frequency options to optimize processing (Branson, CT). Moreover, the Pentagonal processor was employed as the indirect sonication to these experiments because of the safety consideration.

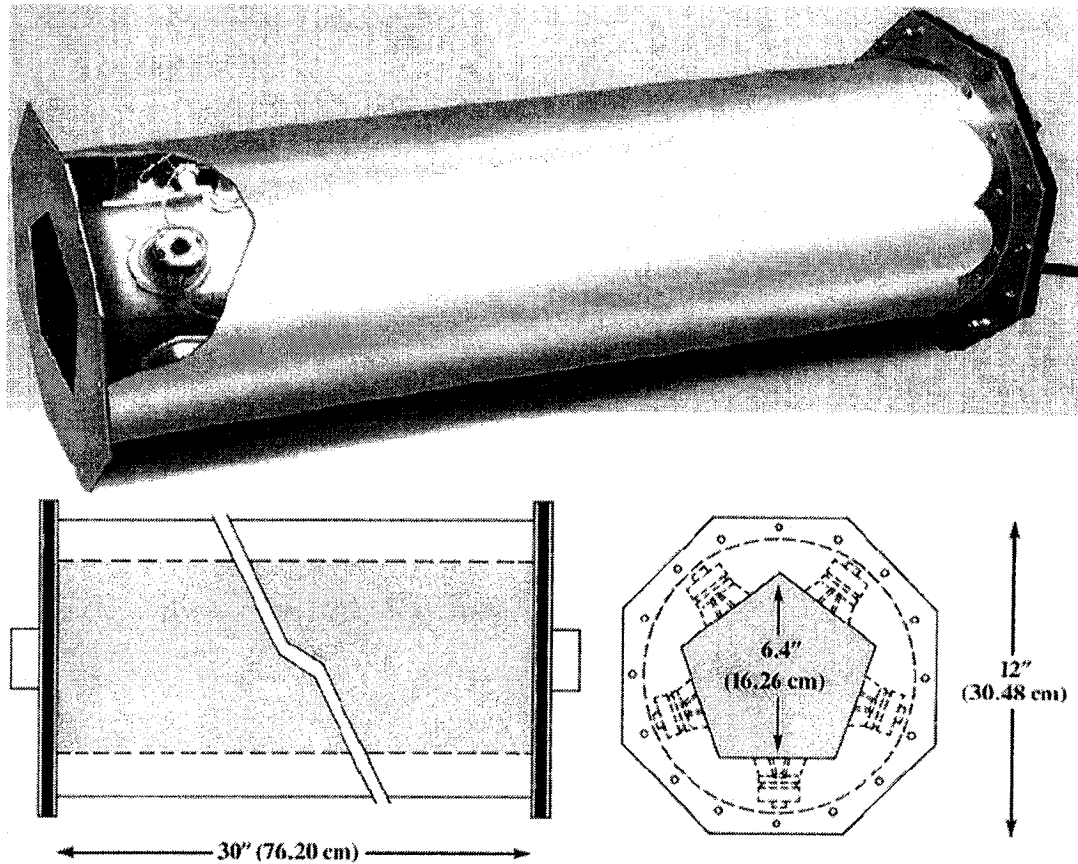


**Figure 6.2 Schematic diagram of Pentagonal processor (after Branson, CT)**



#### 6.2.3.2 Sonoreactor

As discussed in Section 3.4.2.1, the sonoreactor, tailor-made by Blatek Tech., is basically a tubular reactor mounted with highly efficient 20 kHz piezoelectric transducers with various power intensity from 100 watts to 400 watts. Figure 6.3 shows the block diagram of a portable continuous desulfurization unit. The sonoreactor can be a chamber mounted with transducers, which provided the direct sonication to the process stream and connected with recirculation loop and pump. The pretreatment micellar tank is of importance in order to change the orientation of the sulfur-bearing molecules. The sonoreactor can be a module-type representing multiple reactors in series or in parallel mode.

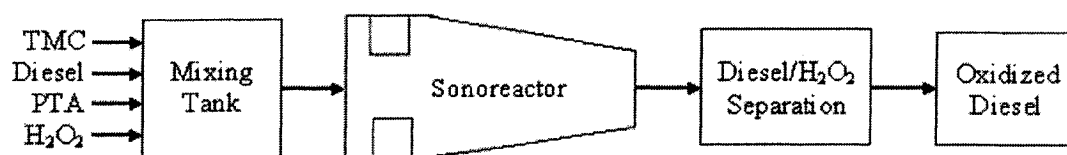


**Figure 6.3 Schematic diagram of a continuous flow sonoreactor**

#### 6.2.4 Experiment Method

Reactants were stored in two solutions: (a) An appropriate volume of the MGO with of tetraoctylammonium fluoride (250:1, w/w) and (b) An appropriate volume of 30 vol. % hydrogen peroxide containing proportional ratio of phosphotungstic acid (100:1, w/w) were fed in to the reactor by pumps. The flow

rates of both solutions were measured and adjusted equally according to the chosen residence time and to maintain a constant oil/water ratio of 1:1 (v/v) in the reactor. The mixture in the reactor was irradiated by different type of continuous flow reactor. Different sonication times were calculated under ambient temperature and pressure to obtain the optimum timing for equilibrium.

Acetonitrile was chosen because it has a relatively low boiling point at 355 K and can be easily separated by distillation from the sulfones with boiling point ranging from 550 K to 950 K. Each time the solvent-to-oil (S/O) ratio was kept at 1:1 by weight (i.e., 5 g diesel per 5 g acetonitrile) and the mixture was shaken vigorously for 1.5 min at room temperature before the oil and solvent layers were separated. Moreover, the total sulfur content was analyzed by a Sulfur-in-Oil Analyzer (SLF A-20) manufactured by Horiba Inc. The selectivity of the oxidation of organic sulfur compounds to sulfones was characterized by GC-PFPD and GC/MS analysis.

## **6.3 RESULT AND DISCUSSION**

### **6.3.1 Sulfur Removal at Different Ultrasonic Frequency**

As discussed in Chapter 2, the frequency of the ultrasonic energy is one of the crucial elements within an ultrasonic system. An increase in the frequency of the applied sound wave requires an increase in its intensity in order to remain above the threshold value needed for cavitation. Ultrasonic intensity is an integral function of the frequency and amplitude of a radiating wave. Therefore, a 20 kHz radiating wave

will be approximately twice the intensity of a 40 kHz wave for any given average power output, and consequently the cavitation intensity resulting from a 20 kHz wave will be proportionately greater than that resulting from a 40 kHz wave.

This study ompared two different types of ultrasonic devices which include a probe type reactor (Sonic & Material Inc., 20 kHz) and a tubular reactor (Branson Inc., 40 kHz). Table 6.1 illustrates the desulfurization efficiency of MGO by two different types of ultrasonic devices under different UAOD conditions. At batch scale, the probe type reactor (20 kHz) reached 98.8% sulfur removal at 71 °C in 10 minutes of sonication time. However, the tubular reactor (40 kHz) only reached 95.3% sulfur removal under similar conditions. Increasing the sonicatoin time to 25 minutes increased the sulfur removal to nearly 97.1%. This result indicated that the ultrasonic frequency operated at 20 kHz had better performance than 40 kHz for UAOD process. Moreover, Table 6.1 also exhibits that desulfurization efficiencies of diesel increased with increasing temperature. This result confirms that the cavitation process was temperature-dependent, because several of the important characteristics of a liquid that affect cavitation intensity were themselves temperature-dependent. These characteristics included vapor pressure, surface tension, the diffusion rates of gases that are dissolved in the liquid, and the solubility of air and other gases in the liquid.

**Table 6.1 Desulfurization efficiency of MGO at deferent ultrasonic frequency**

Operating Frequency	Operating Temperature (°C)	Sonication time (min)	Sulfur Content (ppm)		Sulfur Removal (%)
			Original	After Extraction	
20 kHz	71	10	1710	20.9	98.8
40 kHz	30	10	1710	527.7	69.1
	30	25	1710	166.2	90.3
	70	10	1710	80.1	95.3
	70	25	1710	48.9	97.1

For industrial and commercial applications, 40 kHz is often used for ultrasonic atomization, because the droplet size at that frequency is half that generated at 20 kHz. On the other hand, the frequency of choice for most ultrasonic liquid processing applications is 20 kHz, because the amplitude at the probe tip and the resulting cavitation is twice that generated at 40 kHz.

### **6.3.2 Sulfur Removal on Continuous UAOD Process**

For continuous flow application, there are two primary types, continuously stirred tank reactors (CSTR) and plug flow reactors (PFR). In CSTR processing, process streams are continuously mixed in reactors and continuously harvested. After a vessel is filled, the output streams overflow into another reactor at the same rate as the input streams are added, thus maintaining a constant volume under steady state conditions. The continuous, controlled movement of the process streams through

equipment increases the product throughput on a space-time basis, and allowing higher reaction efficiency to be permitted from a smaller plant with smaller capital investment would be possible under batch conditions (Anderson, 2001).

**Table 6.2 Operating conditions in the study of continuous UAOD on MGO**

Parameters	Operating Conditions	
	Probe type reactor	Sonoreactor
MGO	20 g	500 g (1.1 lb)
Total Sulfur Concentration	1710 ppm	1710 ppm
Hydrogen Peroxide (30 vol%)	25 g	625 g
Tetraoctylammonium fluoride	0.1 g	2.5 g
Phosphotungstic acid	0.2 g	5 g
Temperature	70°C ± 2°C	25°C ± 2°C
Power output	600 watts	100 watts, 200 watts
Working volume of reactor	42 mL	1.1 L
Overall feed rate	4 mL/min	1.83 L/min
Reaction time	20 min	30 min, 60 min

Financial considerations have led to the development of large-scale continuous processing. Table 6.2 shows the operating conditions of two different types of ultrasonic reactors in the study of continuous UAOD process on MGO. The treatment capacity of sonoreactor has been scaled up to 25 times larger than the probe type reactor. In this experiment, CSTR processing has been applied to control the static mixing of hydrogen Peroxide (Oxidant) along with phosphotungstic acid

(TMC) and diesel fuels (feedstock) along with tetraoctylammonium fluoride (PTA). Furthermore, this study has compared the desulfurization efficiency of MGO by the probe type unit and the sonoreactor, shown as Table 6.3. Using probe type reactor, sulfur removal reached 92.7% in 20 minutes reaction time under 600 watts as power intensity. However, the sonoreactor reached a similar sulfur removal (92.4%) at 60 minutes reaction time with much lower power intensity of 100 watts, and the capacity was 25 times larger than that of the probe type unit.

Based on Table 6.3, assuming a single sonoracter is used and operated with MGO on the weight of 1.1 pounds (lb). The sulfur reduction reached 90% in 30 minutes. For twenty four hours operations, the capacity reached 52.8 pounds (lb) per day. As we understand, diesel has density of 0.827 g/ml. Therefore, the treatment rate as high as 7.6 gallons per day was achieved at current installation.

$$Q = 52.8 \text{ lb/day} = 23.97 \text{ kg/day}, 23.97 \text{ kg/day} / 0.827 \text{ kg/l} = 28.99 \text{ l/day} = 7.7 \text{ gal/day}$$

**Table 6.3 Desulfurization efficiency of MGO by deferent continuous flow reactors**

Reactor Type	Power Output (watts)	Sonication time (min)	Sulfur Content (ppm)		Sulfur Removal (%)
			Original	After Extraction	
Probe type reactor	600	10	1710	186.1	89.12
	600	20	1710	124.2	92.74
Sono-reactor	100	30	1710	179.1	89.53
	100	60	1710	130.7	92.36
	200	30	1710	174.8	89.78

### 6.3.3 Large Scale Applications on Continuous UAOD Process

As discuss in pervious section, the treatment rate at 1.1 lb /hour of continuous UAOD process, known as 14 gallon per day, reached 92.7 % sulfur removal in one hour. However, this result is still insufficiency for practical application. In this study, the treatment capacity of sonoreactor has been scaled up to 5 lb per hour. The operation conditions were shown as Table 6.4. Moreover, Table 6.5 indicated that the desulfurization efficiency was reached at 81.57 % in very short time (less then 1 min), which indicated that this sonoreactor is extremely powerful in accelerating the oxidation reaction. The final sulfur reduction of 5 lb/hour treatment rate was reached at 94.46% in one hour. However, increasing one more hour for sonication, the sulfur reduction only increases approximately 2 % to reach 96.35%.

**Table 6.4 Operating conditions of continuous UAOD on MGO at 5 lb/hour**

Parameters	Operating Conditions
MGO	2.27 kg (5 lb)
Total Sulfur Concentration	1710 ppm
Hydrogen Peroxide (30 vol%)	2.8375 kg
Tetraoctylammonium fluoride	22.7 g
Phosphotungstic acid	11.35 g
Temperature	25°C ± 2°C
Power output	100 watts
Working volume of reactor	1.1 L
Overall feed rate	1.83 L/min
Reaction time	Variable

**Table 6.5 Desulfurization efficiency of continuous UAOD on MGO by deferent sonication time at 5 lb/hour**

<b>Sample Number</b>	<b>Number of Pass</b>	<b>Sonication Time</b>	<b>Sulfur Concentration (ppm)</b>	<b>Sulfur Removal (%)</b>
1	1	0.6	315.22	81.57
2	5	3	300.60	82.42
3	10	6	265.04	84.50
4	20	12	215.92	87.37
5	30	18	178.41	89.57
6	40	24	150.50	91.20
7	50	30	139.03	91.87
8	60	36	128.57	92.48
9	70	42	113.47	93.36
10	80	48	109.56	93.59
11	90	54	99.89	94.16
12	100	60	94.71	94.46
13	110	66	83.70	95.11
14	120	72	77.20	95.49
15	150	90	62.46	96.35
16	200	120	54.59	96.81



Several studies indicated that in presence of an excess of  $\text{H}_2\text{O}_2$ , the oxidation of organic sulfur compounds follows pseudo first order kinetics in carboxylic acid/ $\text{H}_2\text{O}_2$  and polyoxometalate/ $\text{H}_2\text{O}_2$  systems (Te, et al. 2001; Otsuki, et al. 2000; Collins, et al. 1997). Since  $\text{H}_2\text{O}_2$  was present in excess under UAOD condition, the reaction data should be fitted to a first-order rate equation. A plot of  $\ln(C_t/C_0)$  versus reaction time shows as Figure 6.4. The fitting curve displayed a linear relationship that confirmed the pseudo-first-order reaction kinetics.

The apparent rate constant for oxidation of MGO was determined to be  $0.0154 \text{ min}^{-1}$ . Compare to the oxidation reaction rate of BT ( $0.1795 \text{ min}^{-1}$ ), 2MBT ( $0.2090 \text{ min}^{-1}$ ), DBT ( $0.3073 \text{ min}^{-1}$ ), 4MDBT ( $0.3353 \text{ min}^{-1}$ ) and 46DMDBT ( $0.3410 \text{ min}^{-1}$ ), it is relatively much lower than these OSCs in batch scale. It is because a complex system as diesel fuels, there exists competitive oxidation among organic sulfur compounds and other unsaturated constituents such as olefinic compounds. Furthermore, the continuous desulfurization unit can not reach as perfect operation conditions as batch scale. This result is very important and can be applied to evaluate the performance of UAOD process on diesel fuels as well as to enhance the capacity of continuous desulfurization unit.

Our goal is to mature this technology, which is still in its infancy. For the preparation of high desulfurization efficiency, it is essential that this sonoreactor can be conducted with little variation from optimal conditions. Such steady state conditions should be reached quickly upon start-up of the processing for optimal yields. Moreover, this study is working toward investigating and developing its

potential so that others can adopt and transform this technology for viable large-scale operation.

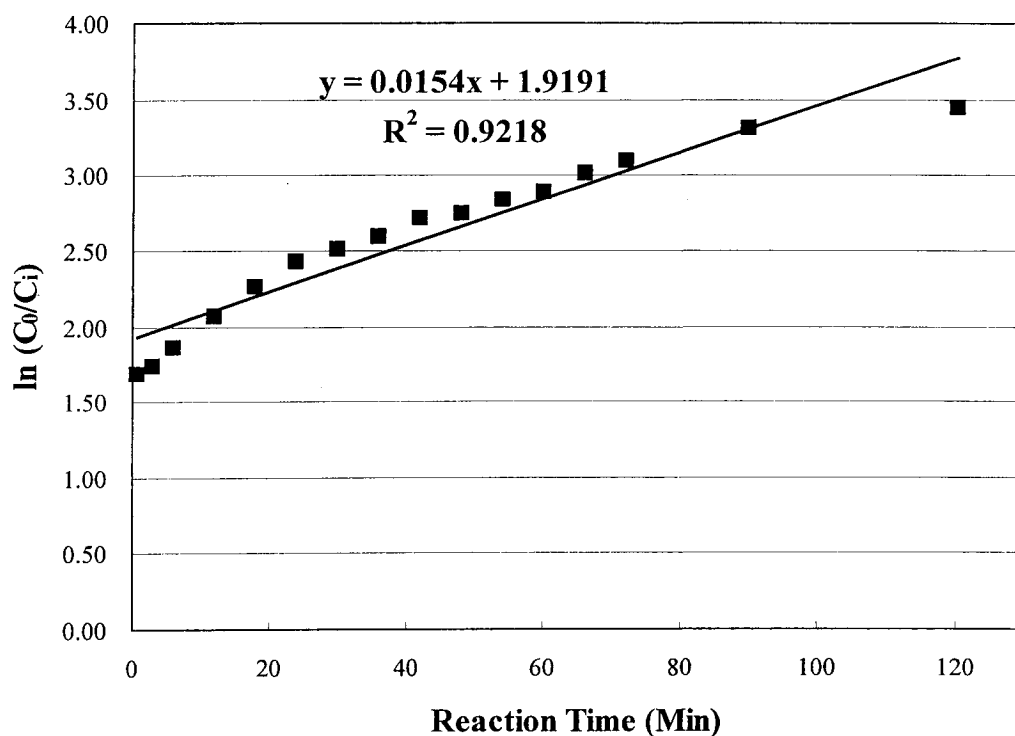


**Figure 6.4 Plot of  $\ln (C_0/C_i)$  versus time for MGO desulfurization under pseudo first order condition**

To reach the basic requirements of commercialized product and determine the largest capacity of this continuous desulfurization unit, the treatment capacity of sonoreactor has been scaled up to 12.5 lb per hour. Table 6.6 shows the operating conditions of the sonoreactor in continuous UAOD process on MGO. As shown in Table 6.7, the desulfurization efficiency was reached at 89.15 % in 30 mins, which

indicates that this sonoreactor is very powerful in accelerating the oxidation reaction. The final sulfur reduction of 12.5 lb/hour treatment rate was reached at 92.42 %.

**Table 6.6 Operating conditions of continuous UAOD on MGO at 12.5 lb/hour**

Parameters	Operating Conditions
MGO	5.68 kg (12.5 lb)
Total Sulfur Concentration	1710 ppm
Hydrogen Peroxide (30 vol%)	7.09 kg
Tetraoctylammonium fluoride	56.75 g
Phosphotungstic acid	28.13 g
Temperature	25°C ± 2°C
Power output	100 watts
Working volume of reactor	1.1 L
Overall feed rate	1.83 L/min
Reaction time	30 mins and 60 mins

**Table 6.7 Sulfur reduction of MGO by different sonication times at 12.5 lb/hour**

Sonication Time (mins)	Sulfur Content (ppm)		Sulfur Removal Percentage (%)
	Original	After Extraction	
30	1710	185.5	89.15
60	1710	129.6	92.42

This continuous desulfurization unit was designed and developed as a continuous flow system in a portable, modular design application. The concept of module design requires that each individual element exhibits the best quality or

quantity purpose and performance. If the fuel contains extremely high in certain types of sulfur compounds, more than one module of the sonoreactor are required and can be used in a series. On the other hand, if the quantity of fuel is high, sonoreactors can be used in parallel.

For the best quality or quantity purpose and performance, multiple sonoreactors can be scaled up to connect in series or in parallel, respectively. In this study, the high sulfur reduction of MGO (92%) was successfully demonstrated by a single sonoreactor at treatment rate of 12.5 lb/hour. Therefore, for quantity purpose and performance, two sonoreactors can be connected in parallel to reach high sulfur reduction (92%) under treatment rate of 25 lb/hour which reaches the basic requirement of commercial scale in naval system. Moreover, diesel has a density of 0.827 g/ml, as compared to water with a density of 0.998 g/ml. The treatment rate at 25 lb/hour is approximately 2 barrels per day (bpd). This sonoreactor has demonstrated the feasibility of large-scale operation even in a relatively small installation with low capital investment and maintenance cost.

$$Q = 25 \text{ lb/hr} = 11.35 \text{ kg/hr}, 11.35 \text{ kg/hr} / 0.827 \text{ kg/l} = 13.72 \text{ l/hr} = 87 \text{ gal/day} = 2 \text{ bpd}$$

#### 6.3.4 Different Concentrations of Hydrogen Peroxide Applied to Continuous Unit

Based on successful experiences on batch scale, the 3% hydrogen peroxide has applied to portable continuous desulfurization unit for MGO, shown as Table 6.8 and Figure 6.5. The sulfur reduction reached 81.57 % in only 0.6 minutes with 30 % hydrogen peroxide; however, only 50.51 % sulfur reduction was reached by using 3 % hydrogen peroxide. The result indicated that this sonoreactor had high and powerful efficiency and executed faster oxidation reaction in short time with sufficient hydrogen peroxide supplied.

**Table 6.8 Sulfur reduction of portable desulfurization unit by using different hydrogen peroxide concentrations on MGO**

Reaction Time (mins)	30% H <sub>2</sub> O <sub>2</sub>	3 % H <sub>2</sub> O <sub>2</sub>
	Removal Percentage (%)	Removal Percentage (%)
0.6	81.57	50.51
3	82.42	56.48
12	87.37	73.31
24	91.20	77.73
36	92.48	81.10
48	93.59	84.12
60	94.46	86.51
72	95.49	88.21
90	96.35	88.81
120	96.81	90.94

Because the continuous flow system generates inhomogeneous sonication compared to probe type ultrasound in batch scale, using 3 % hydrogen peroxide needs relatively longer time to reach the equivalent (high sulfur reduction). However, it still reached 91 % sulfur reduction in two hours. This is indicated that using dilute aqueous solutions can fulfill the requirements of practical applications and permit much safer operating conditions. This information is essential to understand the reactivities of various hydrogen peroxide concentrations under oxidative conditions, and to optimize the reaction parameter under continuous UAOD process.

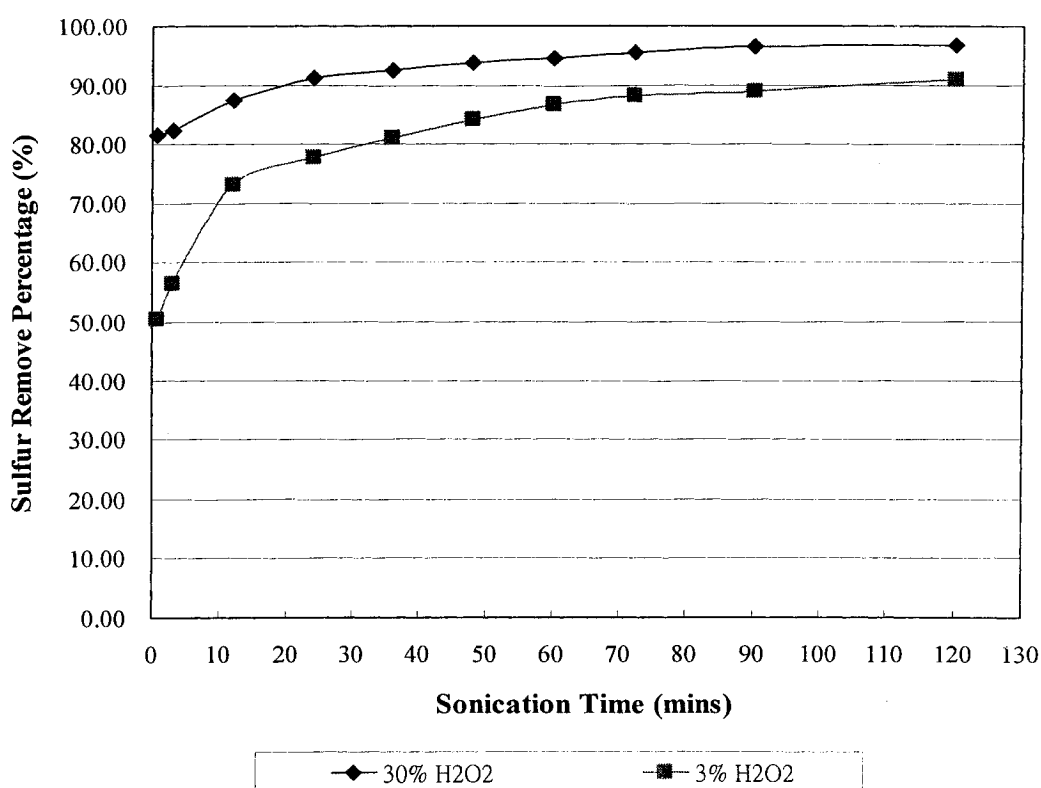


**Figure 6.5 Sulfur reduction of continuous UAOD in different H<sub>2</sub>O<sub>2</sub> Concentration**

### 6.3.5 Idea Reactor Model Applied to Continuous UAOD Process

Operating a stirred-tank reactor with continuous-flow of reactants and products (a CSTR) has some advantages over batch operation. The reactor can make products 24 hours a day for weeks at a time, whereas for a typical cycle, the batch reactor is producing only about half the time. The CSTR is an easily constructed, versatile and cheap reactor, which allows simple catalyst charging and replacement. Its well-mixed nature permits straightforward control over the temperature and pH of the reaction and the supply or removal of gases (Harriott, 2003).

Figure 6.6 shows the schematic diagram of continuous-flow stirred tank reactor (CSTR). Reactants were pumped in at an inlet port, usually at a constant rate. The reactor was vigorously stirred to ensure good mixing. The reactant solution pumped in pushes out an equal volume of the solution.

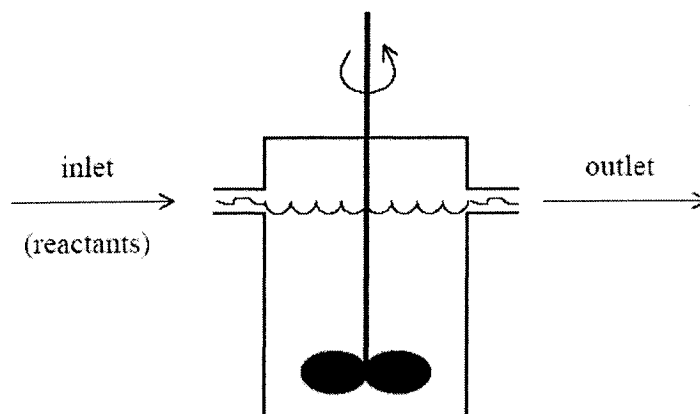


**Figure 6.6 Continuous-flow stirred tank reactor (CSTR) (Harriott, 2003)**

The average residence time in the CSTR is the volume  $V$  divided by the volumetric flow rate  $Q$ , or  $t = V / Q$ . The ratio of CSTR residence time to batch residence time is readily derived for simple kinetic models. For a first order reaction in a CSTR, the steady-state material balance is that the concentration difference between inflow and outflow is equal to the amount of reaction, shown as Eq. 6.1 (Harriott, 2003).

$$\begin{aligned} QC_{A0} - QC_A &= rV = kC_A V \\ C_{A0} - C_A &= k C_A (V/Q) = k C_A t \\ C_A (1 + kt) &= C_{A0} \\ \frac{C_A}{C_{A0}} &= \frac{1}{1 + kt} \end{aligned} \quad (\text{Eq. 6.1})$$

where the first order reaction rate constant is  $r$ , and the CSTR reaction rate constant is  $k$  (Harriott, 2003).

For a first order reaction rate constant in series of tank, the conversion is obtained using above equation. Since the equation of the concentration ratio is the same for each reactor, the calculations of two or more reactors connected in series are shown as following equations:

$$\frac{C_A}{C_{A0}} = \frac{1}{1 + k_1 t_1} \quad (\text{Eq. 6.2})$$

$$\frac{C_{A2}}{C_{A1}} = \frac{1}{1 + k_2 t_2} \quad (\text{Eq. 6.3})$$

$$\frac{C_{An}}{C_{A0}} = \frac{1}{1 + k_1 t_1} \times \frac{1}{1 + k_2 t_2} \times \dots \times \frac{1}{1 + k_n t_n} \quad (\text{Eq. 6.4})$$



where the reactors are equal in size and operate at the same temperature, the equation of n reactors connected in series is shown as Eq. 6.5 (Harriott, 2003):

$$\frac{C_{An}}{C_{A0}} = \left( \frac{1}{1 + k_1 t_1} \right)^n \quad (\text{Eq. 6.5})$$

Section 6.3.3 has proved that the continuous UAOD process is a first order reaction. Moreover, the 92% sulfur reduction of MGO has successfully demonstrated by a single sonoreactor at treatment rate of 12.5 lb/hour in one hour. The reaction rate constant can be obtained by following calculations (Eq. 6.6).

$$\ln \left( \frac{1}{1 - x} \right) = kt \quad (\text{Eq. 6.6})$$

where k is the CSTR reaction rate constant, t is the reaction time and x is the fraction conversion.

$$kt = \ln \frac{1}{0.08} = 2.53$$

$$k = \frac{2.53}{1} = 2.53 \text{ hr}^{-1}$$

For four sonoreactors connected in series, the sulfur reduction in one hour can be calculated as following:

$$\frac{C_{A3}}{C_{A0}} = \left( \frac{1}{1 + k_1 t_1} \right)^4$$

$$\left( \frac{1}{1 + 2.53 \times 1} \right)^4 = 0.006$$

Based on the calculation, the sulfur reduction of MGO with four sonoreactors connected in series reached 99.4 % under one hour operation time. Therefore, for quality purpose and performance, more sonoreactor can be connected in series to reach high sulfur reduction and permit the deep desulfurization.

#### **6.3.6 Economic Analysis of Continuous Desulfurization Unit**

Based on the experimental results obtained from the batch-scale probe type ultrasound unit and continuous desulfurization system on MGO, an economic analysis is conducted to provide information on cost and maintenance estimate for large scale continuous UAOS system.

This continuous desulfurization system has successfully demonstrated at the treatment rate of 25 lb/hr with two sonoreactors connected in series, which was approximately 2 barrels per day. Moreover, this study also indicated that the treated TMC, PTA and hydrogen peroxide can be recycled and reused. Theoretically, the operating costs include mainly electricity consumption, and usage of chemicals such as hydrogen peroxide, metal catalyst, and phase transfer agent. Assuming four times recycle rate has applied to this analysis. With rate of 5 cents/kWh, the power cost is estimated as 0.01 cent/gallon of desulfurized MGO. Assuming 92% utilization of hydrogen peroxide, the operating cost of hydrogen peroxide used in the form of 30 wt% aqueous solutions can be estimated as 2.58 cent/gallon of desulfurized MGO. Furthermore, based on the price provide by comical company, the metal catalyst is approximately estimated as 1.12 cent/gallon, and phase transfer agent is 1.85

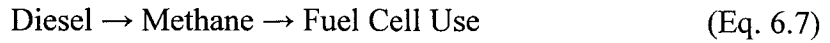
cent/gallon of desulfurized MGO. Excluding the cost for solvent extraction, the total processing cost is  $(0.01 + 1.12 + 2.58 + 1.86 = 5.49)$  cent/gallon of desulfurized MGO, which is in line with 4 or 5 cents/gallon estimated by U.S. EPA.

This continuous desulfurization system is still in its infancy. This study is working toward investigating and developing its potential so that others can adopt and transform this technology for viable large-scale operation. For example, solid adsorption of sulfone can replace the solvent extraction with relative lower expense for maintenance. Larger scale operation can reduce the cost of  $\text{H}_2\text{O}_2$ , PTA, and TMC with the concept of spent catalysts recycle and reuse. Moreover, the most important progress and beauty of this technology is that this continuous desulfurization unit is portable, compact, convenience, and needs relatively much smaller area for installation and construction compared to conventional hydrodesulfurization facilities, or the other desulfurization technologies, thus, provides a feasible solution to economically produce ultra-low sulfur diesel that meets new environmental regulations.

#### **6.3.7 Capacity for Power Generation of Continuous UAOD Process**

Fuel cell is an end use for the power generated by diesel. There are various amounts of large-size hydrocarbon molecule compounds in diesel fuels. After the desulfurization process, the reformation process converts and cracks down these hydrocarbon molecules to carbon monoxide, thus avoids the damages to catalyst.

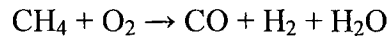
Water shift reaction converts the produced carbon monoxide to hydrocarbon forms such as methane. Therefore the simple chain of reactions is shown as Eq. 6.7:



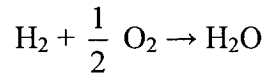
In each step, there was a loss in efficiencies of power generation. The combustion of methane is highly exothermic, as shown in Eq. 6.8:



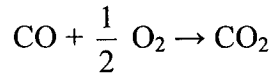
In oxidative pyrolysis, methane reacts to a methyl radical, which reacts to formaldehyde (HCHO or H<sub>2</sub>CO). The formaldehyde reacts to a formal radical (HCO), which then forms carbon monoxide (CO):



After oxidative pyrolysis, H<sub>2</sub> oxidizes and forms H<sub>2</sub>O and releases heat:



The CO oxidizes, forming CO<sub>2</sub> and releasing more heat:



In this continuous desulfurization process, the treatment rate of 25 lb/hr with two sonreactors connected in series was successfully demonstrated. The 25 lb/hr was approximately equal to 2 barrels per day. Therefore, the capacity for power generation at this treatment rate was calculated. Theoretically, the Combustion of one mole of methane produces energy of 891 kJ or 0.247 kW.hr, and 50% of diesel fuel was assumed to be the methane:

$$Q = 2 \text{ bpd} = 25 \text{ lb/hr} = 11.35 \text{ kg/hr}$$

$$\text{Methane in diesel fuel: } 11.35 \text{ kg/hr} \times 0.5 = 5.68 \text{ kg/hr} = 5680 \text{ g/hr}$$

$$(5.68 \times 10^3 \text{ g/hr}) / (16 \text{ g/mole CH}_4) = 354.69 \text{ mol/hr}$$

$$354.69 \text{ mol/hr} \times 0.247 \text{ kW.hr} = \mathbf{87.61 \text{ kW}}$$

Finally, 2 bpd of diesel approximately generated energy for **87.61 kW**. The real energy generation of this continuous desulfurization unit will be less than that, due to the amount of methane in diesels and the efficiencies of reformation process. Moreover, for applications in military system, 500 w to 60 kw power generation systems were operated on the current DoD logistical diesel fuels. This continuous UAOD system can achieve the basic treatment capacity in one day and exhibit the enormous potential to be the new technology for commercial applications.

## 6.4 SUMMARY

This study has compared two different types of ultrasonic devices which include a probe type reactor (Sonic & Material Inc., 20 kHz) and a tubular reactor (Branson Inc., 40 kHz) in batch scale. The result has indicated that the ultrasonic frequency operated at 20 kHz has better performance than 40 kHz under UAOD process. Because ultrasonic intensity is an integral function of the frequency and amplitude of a radiating wave, a 20 kHz radiating wave is approximately twice the intensity of a 40 kHz wave for any given average power output, and consequently the cavitation intensity resulting from a 20 kHz wave will be proportionately greater than that resulting from a 40 kHz wave.

To address the needs of large-scale commercial production, this study has spent one and half year designing and developing a portable, modular continuous flow system – the sonoreactor which consists of a sonicator, an RF amplifier, a function generator, a pretreatment tank, and a pipeline system housed only in a 2' x 4' x 1' space. The result for this sonoreactor indicated a remarkable 92.4% removal efficiency for the sulfur in marine logistic diesel, even at a treatment rate as high as 14 gallons per day.

For large scale operation of this continuous UAOD process, this study has successfully demonstrated the high sulfur reduction of MGO (94%) at treatment rate of 5 lb/hour. Moreover, the desulfurization efficiency can be reached at 81.57 % in very short time (less than 1 min), which indicated that this sonoreactor was extremely powerful in accelerating the oxidation reaction. Moreover, this study

indicated that in presence of an excess of  $\text{H}_2\text{O}_2$ , this continues UAOD process followed the pseudo first order kinetics.

To reach the basic requirements of commercialized product and to determine the largest capacity of this continuous desulfurization unit, the high sulfur reduction of MGO (92%) has successfully demonstrated by a single sonoreactor at treatment rate of 12.5 lb/hour. For quantity purpose and performance, two sonoreactors were connected in parallel to reach high sulfur reduction under treatment rate of 25 lb/hour which is approximately 2 barrels per day. Moreover, based on the concept of idea continuous flow reactor (CSTR), the sulfur reduction of MGO with four sonoreactors connected in series reached 99.4 % under one hour operation time. Therefore, for quality purpose and performance, more sonoreactor can be connected in series to reach high sulfur reduction and permit the deep desulfurization.

Hydrogen peroxide plays an important role in Ishii-Venturello Expoxidation. If there was no hydrogen peroxide applied to UAOD process, there was no sulfur removal. In continuous flow system, similar sulfur reduction was archived by using 3 % or 30 % hydrogen peroxide concentrations in longer reaction time. Therefore, this study indicated that hydrogen peroxide diluted to 3 % performed the similar sulfur removal under the same operation conditions that used 30 % hydrogen peroxide as oxidant. Thus, it permitted much safer operating conditions and a feasibility study of diluted hydrogen peroxide generation in continues flow desulfurization system as well as the process evaluation of UAOD on diesel fuels.

The economical analysis and the capacity simulation of power generation indicated that with appropriate process design and use of chemicals, this sonoreactor demonstrated the feasibility of large-scale operation even in a relatively small installation with low capital investment and maintenance cost. It also ensured the safety considerations by operating with diluted hydrogen peroxide under ambient temperature and pressure. Moreover, because of its portable property and modular design, this unit was easy to setup and permit a multistage process for the best quality or quantity purpose and performance.



## **CHAPTER 7**

### **CONCEPTUAL MODEL OF UAOD PROCESS**

#### **7.1 INTRODUCTION**

In UAOD process, it is believe that OSCs were oxidized by polyperoxometalate in a bimolecular reaction, which involved electrophonic oxygen transfer, the occurrence of a radical mechanism, ionic transfer between aqueous and organic phase, and possibly triggered by an electron transfer from OSCs to the peroxy complex. This study has developed the possible mechanism of UAOD process, and examined it by real experimental results.

#### **7.2 MECHANISM OF UAOD PROCESS**

UAOD process is designed to combine three complementary techniques: ultrasonication, phase transfer catalysis (PTC), and transition metal catalyzed oxidation, which is a biphasic system and consists of two immiscible phases including liquid phase catalyst phase and a product/reactant phases with intense mass transfer between them. The advantage of biphasic systems is that they combine a catalytic reaction and product separation in one unit, allowing difficult separation problem to be avoided. Therefore, in light of previous mechanistic studies on Ishii-Venturello expoxidation and the concept of phase transfer catalysis, a conceptual model of oxidation step in UAOD process is simplified and depicted as a catalytic

cycle, shown as Figure 7.1 which consists of six basic steps.

Step (1): In the presence of excess  $\text{H}_2\text{O}_2$ , phosphotungstic acid or  $\text{H}_3[\text{PW}_{12}\text{O}_{40}]$ , the metal precursor simply represented as  $[\text{PW}_{12}\text{O}_{40}]^{3-}$ , is peroxidized and disaggregated to form anionic peroxometal complex which is the polyperoxometalate  $\{\text{PO}_4[\text{WO}(\text{O}_2)_2]_4\}^{3-}$ , the effective species for expoxidation.

Step (2): With the solid salts (MX) applied to aqueous phase, Quaternary ammonium salts can form the reaction of solid-liquid anion exchange, because a thin aqueous film is formed on the surface of solid crystals and permits the anion transport. The nature of the metal cation, M, has a profound effect in the exchange process. The exchange rate and the maximum conversion obtained were found to depend on the aqueous solubility ration MX/MZ. Thus, the order of reactivity is exhibited as  $\text{Ca}^{2+} < \text{Li}^+ < \text{Na}^+ < \text{K}^+$ . In addition, if there is no solid salts added to the system, step 2 could be omitted.

Step (3): Quaternary ammonium salts such as  $\text{Oc}_4\text{N}^+\text{F}^-$  with larger lipophilic cation and smaller hydrophilic anion can function as PTA to transfer the polyperoxometal anion into organic phase. Theoretically, the reactivity of QAS is based on the lipophilicity of the quaternary ammonium cation, the degree of hydration of its anion and its stability under the reaction conditions. It is obvious that increasing the length of carbon chain will increase its lipophilicity, thus improving the extraction or transfer rate of the active ion pair to the organic phase. Moreover, a general list of anions with decreasing order extractability for a given quaternary cation (anion lipophilicity) in liquid-liquid systems is represented as picrate >>

$\text{MnO}_4^- > \text{SCN}^- > \text{I}^- \approx \text{ClO}_3^- \approx \text{ArSO}_3^- > \text{NO}_3^- > \text{Br}^- \approx \text{CN}^- \approx \text{BrO}_3^- \approx \text{ArCOO}^- > \text{NO}_2^- \approx \text{Cl}^- > \text{HSO}_4^- > \text{HCO}_3^- \approx \text{CH}_3\text{COO}^- > \text{HCOO}^- > \text{F}^- \approx \text{OH}^- > \text{SO}_4^{2-} > \text{CO}_3^{2-} > \text{PO}_4^{2-}$ . It indicates that the anion with lower lipophilicity has higher ability for hydration, thus permits the faster transfer rate of the active ion pair into the organic phase

Step (4): In organic phase, OSCs such as BTs and DBTs are oxidized to BTOs and DBTOs by the peroxometal complex with high efficiency and high selectivity. The electron density at model sulfur atom has positive relationship with the rate constants of the oxidation of these model sulfur compounds to corresponding sulfones.

Step (5): The reduced peroxometal complex, which dissociate with PTA, returns to aqueous phase. With the excess of hydrogen peroxide, these spent catalysts can be reactive and restore the catalytic cycle.

Step (6): Very fine ultrasonic emulsions, which are much smaller in size and more stable than those obtained conventionally, greatly improve the interfacial area available for reaction, increase the effective local concentration of reactive species, and enhance the mass transfer in the interfacial region. Therefore it leads to a remarkable increase in PTA reaction rate. Moreover, cavitation during sonication may also create active intermediates that permit the reaction to proceed in a short time and under mild conditions.

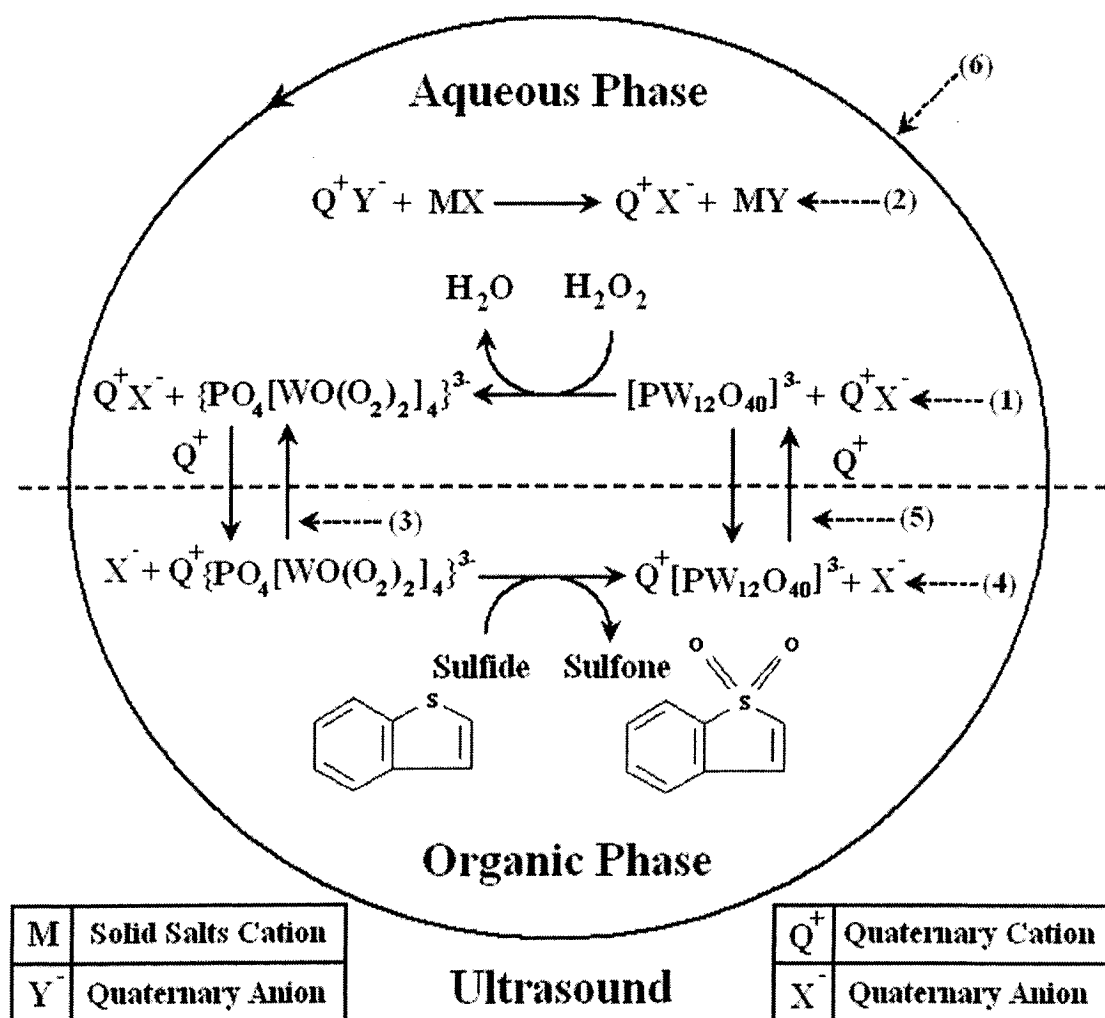


**Figure 7.1** Conceptual model of catalytic oxidation in UAOD process

### 7.3 CONCEPTUAL MODEL APPLIED TO EXPERIMENTAL RESULTS

In the following discussions, the mechanism of UAOD process has applied to experimental studies on model sulfur compounds and real diesel fuels. Real experimental results were applied to exhibit the reaction and performance of each step.

Step (1): Figure 4.14 shows the comparison of yields of BTO and DBTO by using different TMCs. It is clear that phosphotungstic compounds were much better catalyst precursors compared to molybdenum counterparts. The acid form of phosphotungstic anion performed slightly higher in oxidation activity compared to its sodium salt, suggesting that the acidic function of the catalyst was playing a significant role in oxidation process. In this reaction, phosphotungstic compounds with hydrogen peroxide exhibited the highest activity. It is because the formation of the polyoxoperoxo species in this system, such as,  $\{\text{PO}_4[\text{WO}(\text{O}_2)_2]_4\}^{3-}$ .

The  $\{\text{PO}_4[\text{WO}(\text{O}_2)_2]_4\}^{3-}$  peroxotungstate was isolated and characterized crystallographically by Venturello et al. 1983 and Ishii et al. 1985. Figure 7.2 shows the infrared spectra of the catalyst obtained on a Nicolet model 750 FT-IR spectrophotometer. The FTIR data agreed well with the values from literatures for polyperoxometalate  $\{\text{PO}_4[\text{WO}(\text{O}_2)_2]_4\}^{3-}$  with functional groups of P-O (1090 and 1057  $\text{cm}^{-1}$ ), W=O (956  $\text{cm}^{-1}$ ), O-O (818  $\text{cm}^{-1}$ ),  $(\text{W}(\text{O}_2)_2)_{s,as}$  (577, 566 and 523  $\text{cm}^{-1}$ ) (Venturello et al. 1983; Ishii et al. 1988; Duncan, et al. 1995; May, et al. 2003).

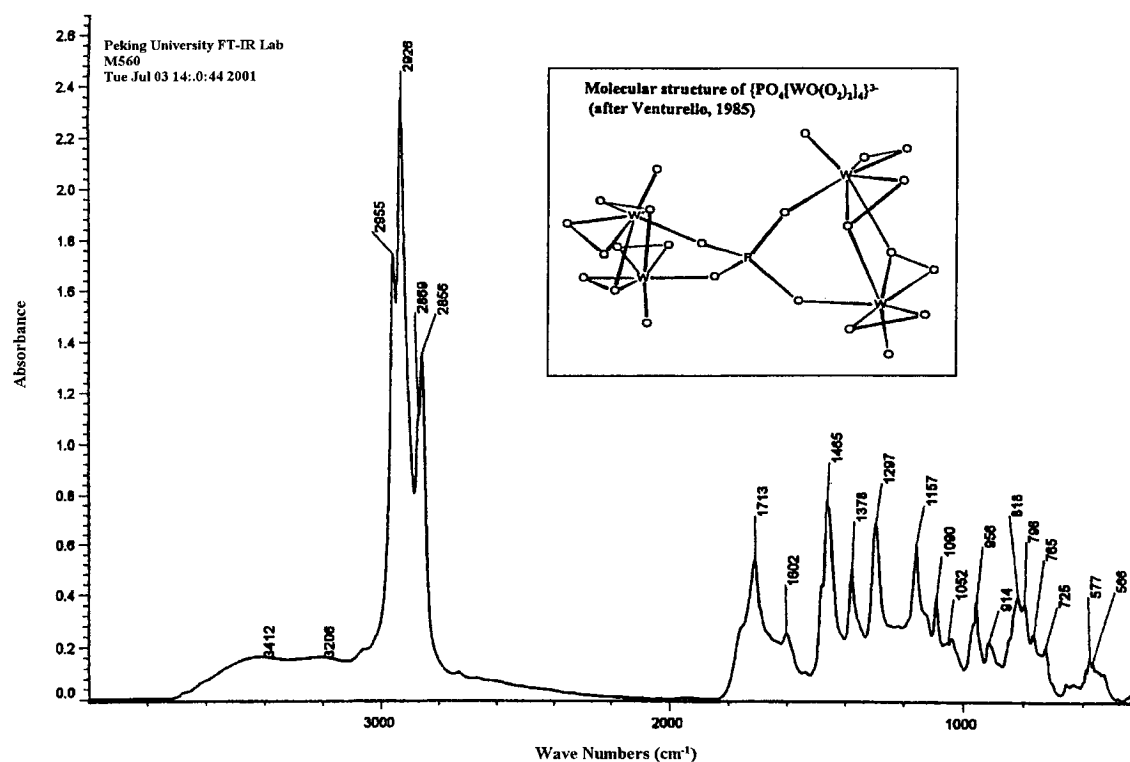


**Figure 7.2 IR spectra of catalyst isolated from UAOD system (Mai, 2003)**

Step (2): Figure 4.6 shows the oxidation of BT to BTO, which proceeded at various reaction rates in presence of sodium chloride. The oxidation efficiency of BT to BTO generally increased with increasing the amount of NaCl because of the formation of solid-liquid anion exchange,  $Oc_4tNBr + NaCl \rightarrow Oc_4tNCl + NaBr$ . Due to the better phase transfer ability of TOAC than that of TOAB, the oxidation efficiency reached 61.13% with the weight of NaCl at 0.5 g. Moreover, an important observation is that when the weight of NaCl was smaller than 0.5g, the aqueous phase was a clear homogeneous solution under the reaction conditions. If larger

amount of NaCl added, the NaCl-H<sub>2</sub>O<sub>2</sub> phase existed initially as slurry. As the reaction proceeded, the precipitated solid sodium bromide could not be extracted and thus the reaction was shifted to the right, which inhibited the produce of TOAC and reduces the efficiency of phase transfer reaction.

Step (3): Figure 4.9 illustrates the comparison of different quaternary ammonium salts that were used to convert the BT to BTO. The catalytic activities follow the order: (C<sub>8</sub>H<sub>17</sub>)<sub>4</sub>N<sup>+</sup>F<sup>-</sup> (TOAF) > (C<sub>8</sub>H<sub>17</sub>)<sub>4</sub>N<sup>+</sup>Br<sup>-</sup> (TOAB) > (C<sub>4</sub>H<sub>9</sub>)<sub>4</sub>N<sup>+</sup>Br<sup>-</sup> (TBAB) > (C<sub>4</sub>H<sub>9</sub>)<sub>3</sub>MeN<sup>+</sup>Cl<sup>-</sup> (MBAC) > (C<sub>4</sub>H<sub>9</sub>)<sub>3</sub>MeN<sup>+</sup>OH<sup>-</sup> (MBAH) > (CH<sub>3</sub>)<sub>4</sub>N<sup>+</sup>F<sup>-</sup> (TMAF). It indicated that QASs with larger lipophilic cation can easily transfer the metal anion into organic phase and thus permit faster reaction. Moreover, Figure 4.13 shows the comparison of different model sulfur compounds by using TOAB and TOAF as PTA. TOAF showed better oxidation efficiency in all kinds of model sulfur compounds than TOAB. It indicates that the anion with lower lipophilicity had higher ability for hydration, thus permits the faster transfer rate of the active ion pair into the organic phase (ability for hydration, F<sup>-</sup>>Cl<sup>-</sup>>Br<sup>-</sup>>I<sup>-</sup>).

Based on the qualitative analysis, there were four major sulfur organic compounds left either in desulfurized F76, MGO, JP5, and transportation diesel after UAOD process. Those four sulfur compounds, categorized as the group of C<sub>3</sub>-BTs, C<sub>4</sub>-BTs, C<sub>5</sub>-BTs and C<sub>3</sub>-DBTs, were among the most refractory compounds in marine logistic diesels under UAOD conditions. This information is essential to understand the reactivity of various organic sulfur compounds under oxidative conditions, and provide a direction for optimization of desulfurization process.

Step (4): In most of our experiments, oxidation of model sulfur compounds and diesel fuels were carried out in presence of ultrasonication and excess  $\text{H}_2\text{O}_2$  using phosphotungstic acid as transition metal catalyst and tetraoctylammonium fluoride as phase transfer agent. The relationship between the sulfone conversions of model compounds and reaction time is showed as figure 4.15. In addition, the results of the oxidative desulfurization of diesels fuels by UAOD process are summarized in Table 5.4. Obviously, the UAOD process reached high sulfur removal by the peroxometal complex with high efficiency and high selectivity in a short contact time at low temperature and atmospheric pressure.

Step (5): Using ICP to analyze the changed tungsten concentration before and after UAOD process, Table 5.1 shows that 99.49% of tungsten remained at aqueous phase. It indicated that the tungsten could be fully recovered after the oxidation reaction. Moreover, Table 5.2 shows that the spent catalyst applied to UAOD proves on MGO. The sulfur removal percentage of 98.15% (with PTA) and 96.01% (without PTA) were examined. Compare to the first run of UAOD process with 98.78% sulfur removal percentage on MGO, this anionic peroxometal complex, namely as  $\{\text{PO}_4[\text{WO}(\text{O}_2)_2]_4\}^{3-}$ , still performed high efficiency to permit the oxidation reaction. Therefore, it can be concluded that the reduced peroxometal complex, which dissociates with PTA, returns to aqueous phase. Those recovered peroxometal complexes still exhibit high efficiency and high selectivity, and thus restore the catalytic cycle.



Step (6): Figure 7.3 shows the conversion of DBT to DBTO with and without the use of ultrasound. It was seen that the oxidation of DBT to DBTO reached over 85% and 95% within 1 and 3 min of ultrasonication, respectively. In 7 min, DBT was completely oxidized to DBTO. In comparison, the conversion of DBT to DBTO in the absence of ultrasound was only 21% in 1 min and reached barely above 80% in 7 min, which was still less than the conversion with 1 min sonication. This result demonstrated that the efficiencies of the oxidation reactions can be significantly improved by using ultrasound (May et al. 2003).

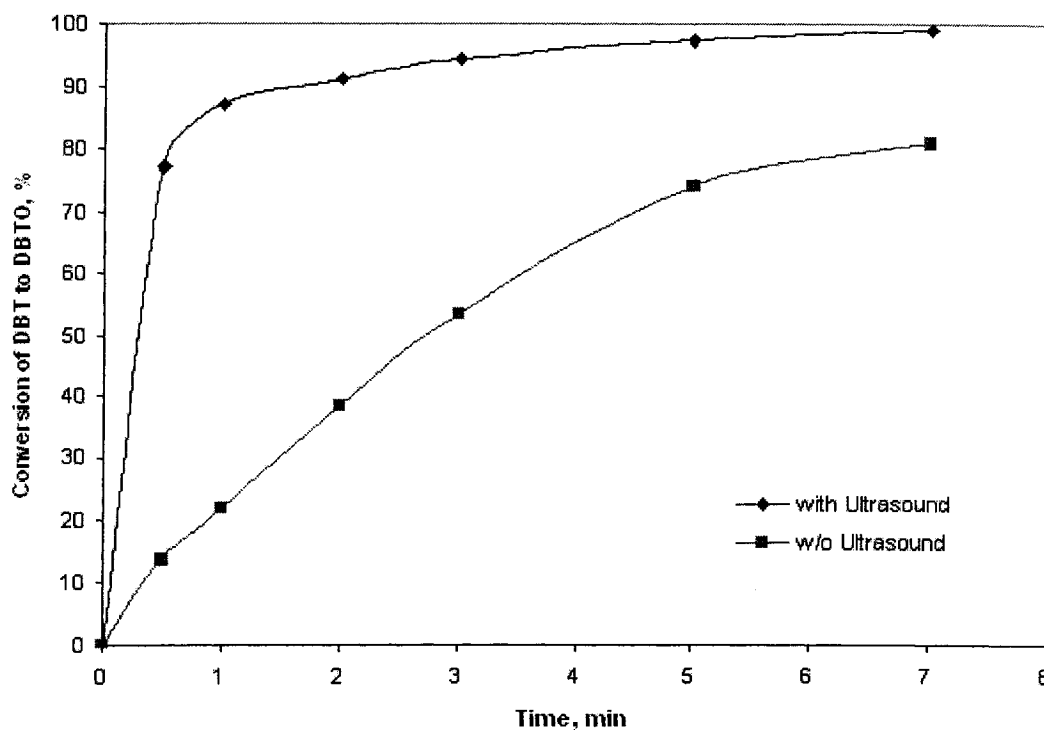


**Figure 7.3 Conversion of DBT to DBTO with and without the use of ultrasound (May et al. 2003)**

## 7.4 SUMMARY

In light of previous mechanistic studies on Ishii-Venturello epoxidation and phase transfer catalysis, a conceptual model of oxidation step in UAOD process was simplified and depicted as a catalytic cycle, which consists of six basic steps: Step (1): In the presence of excess  $\text{H}_2\text{O}_2$ , polyoxometalates is peroxidized and disaggregated to form the polyperoxometalate  $\{\text{PO}_4[\text{WO}(\text{O}_2)_2]_4\}^{3-}$ , the effective species for epoxidation. Step (2): Solid-liquid anion exchange in aqueous phase. Step (3): Quaternary ammonium salts reacts as phase transfer agent. Step (4): Organic sulfur compounds are oxidized their corresponding sulfones by the peroxometal complex with high efficiency and high selectivity. Step (5): The reduced peroxometal complex dissociates with PTA and returns to aqueous phase. Step (6): Ultrasound enhances the efficiencies of oxidation reaction.

This chapter has applied the experimental results to examine this conceptual model. The results indicated that each step of these mechanistic studies was confirmed literally and perfectly matched with real experimental data. This information is essential to understand the basic concept of UAPD process and also provide a direction to the process evaluation of UAOD process on all kinds of diesel fuels.

## CHAPTER 8

### SUMMARY AND RECOMMENDATION

#### 8.1 SUMMARY

This dissertation represents an attempt to optimize the current ultrasound assisted desulfurization (UAOD) process and develop a portable, continuous desulfurization unit. In a batch scale UAOD, it has been demonstrated that using alkyl substituted quaternary ammonium salts with small anion as phase transfer agent and transition metal catalyst with assistant of ultrasound, model sulfur compounds such as benzothiophene and dibenzothiophene can be quantitatively oxidized in minutes under ambient temperature and atmospheric pressure. For various marine logistic diesel or transportation diesel containing different levels of sulfur concentration, the UAOD process followed by solvent extraction can reach or exceed 95% sulfur reduction in short contact time under mild conditions.

In continuous UAOD process, this study has spent one and a half years designing and developing a continuous flow system in a portable, module design application. After overcame a lot of difficulties, this portable unit, which contains an RF amplifier, a function generator, a pretreatment tank, and a pipeline system, was finally developed and operated in ambient environment. The performance of continuous UAOD process on MGO with different operation conditions was investigated. Finally, an economical analysis of a pilot scale continuous UAOD system was conducted.

### 8.1.1 The Optimization of UAOD Process

#### 1. The Fundamental of UAOD Process:

UAOD process is designed to combine three complementary techniques: ultrasonication, phase transfer catalysis (PTC), and transition metal catalyzed oxidation.

#### 2. Quaternary Ammonium Salts as Phase Transfer Agent:

The reactivity of Quaternary Ammonium Salts (QASs) is based on the lipophilicity of the quaternary ammonium cation, the degree of hydration of its anion and its stability under the reaction conditions. It is obvious that increasing the length of carbon chain will increase its lipophilicity, thus improving the extraction or transfer rate of the active ion pair to the organic phase. The order is represented as picrate  $\gg$   $\text{MnO}_4^-$   $>$   $\text{SCN}^-$   $>$   $\text{I}^- \approx \text{ClO}_3^- \approx \text{ArSO}_3^-$   $>$   $\text{NO}_3^-$   $>$   $\text{Br}^- \approx \text{CN}^- \approx \text{BrO}_3^- \approx \text{ArCOO}^-$   $>$   $\text{NO}_2^- \approx \text{Cl}^-$   $>$   $\text{HSO}_4^-$   $>$   $\text{HCO}_3^- \approx \text{CH}_3\text{COO}^-$   $>$   $\text{HCOO}^-$   $>$   $\text{F}^- \approx \text{OH}^-$   $>$   $\text{SO}_4^{2-}$   $>$   $\text{CO}_3^{2-}$   $>$   $\text{PO}_4^{2-}$ .

#### 3. Enhance Efficiency of Fluoride Containing QAS as PTA:

In ultrasound-assisted oxidative desulfurization (UAOD) process, bromo by-products were formed by using tetraoctylammonium bromide (TOAB) as phase transfer agent (PTA). 2-bromo and 3-bromo compounds were formed and their sulfones as well. This is caused by the bromide used as PTA, which is the anion of the quaternary salt.

This study used a longer carbon chain and smaller anion of QASs as surfactant in order to prevent a few side effects under ultrasound, including foaming and excessive decomposition of hydrogen peroxide in the reaction. A group of typical sulfur compounds in diesel were studied to evaluate the effectiveness of UAOD process and to determine their relative reactivity by using TAOF as PTA. The oxidation reactivity of these OSCs was found in very high yield and free of any by-products.

#### 4. Phosphotungstic Compounds as Transition Metal Catalyst:

In the presence of excess  $\text{H}_2\text{O}_2$ , the transition metal catalysts are peroxidized and disaggregated to form anionic peroxometal complex which is the polyperoxo-metalate  $\{\text{PO}_4[\text{WO}(\text{O}_2)_2]_4\}^{3-}$ , the effective species for expoxidation. The experimental results indicated that phosphotungstic compounds were much better catalyst precursors compared to molybdenum counterparts.

#### 5. Kinetic Study of UAOD Process:

This study was conducted by using series of model molecules representative of the different class of sulfur compounds presented in diesel fuels. These compounds, either reactive or resistant to hydrodesulfurization, are all susceptible with different reaction rate for oxidation. Figure 4.16 displayed a linear relationship between oxidation rate and reaction time that confirmed the pseudo-first-order

reaction kinetics. The oxidation reactivity of these sulfur compounds was found in a decreasing order of 46DMDBT > 4MDBT > DBT > 2MBT > BT.

The electron density on the sulfur atom of sulfur compounds and their reaction rate, including benzothiophen, dibenzothiophen and their methyl-substituted derivatives, are shown as Table 4.6. Figure 4.17 shows that the reactivity of sulfur compounds for oxidation is increased with the increase of electron density on sulfur atom. The reactivity of BT and DBT derivatives are influenced by the electron donation of substituted methyl groups.

#### 6. Effects on Main Hydrocarbons of Diesel Fuels after UAOD Process:

GC-PFPD, GC-MS, and GC- Selective Ion Monitoring (SIM) methods have been successfully employed to evaluate the efficiency and the selectivity of the UAOD process on diesels. Figure 5.11 shows that UAOD process has no deleterious effects on main hydrocarbons in the original, oxidized and desulfurized diesels.

#### 7. Diluted Hydrogen Peroxide Applied to UAOD Process:

Hydrogen peroxide is a colorless, syrupy liquid and considered an ideal “green” oxidant due to its high oxidizing ability and lack of toxic by-products. Despite its potential value as an oxidant, hydrogen peroxide has some serious drawbacks. It is inherently corrosive and, especially in high concentrations, is prone to catalytic decomposition. Using dilute aqueous solutions can minimize these problems. Figure 5.13 shows the desulfurization efficiency of different hydrogen

peroxide concentrations on MGO in batch scale. If there is no hydrogen peroxide applied to UAOD process, there is no sulfur removal can be achieved. Hydrogen peroxide diluted to 0.25 % can start the oxidation reaction and reach sulfur removal at 64.42 %. Slightly increasing the concentrations of hydrogen peroxide allowed increasing efficiency of sulfur reduction. Hydrogen peroxide diluted to 3 % can perform the same sulfur removal under the same operation conditions that used 30 % hydrogen peroxide as oxidant. Moreover, 3% hydrogen peroxide can perform the same desulfurization efficiency in different diesel fuels, as shown in Table 5.3. Thus, UAOD process could be operated under much safer environment.

#### 8. Conceptual Model of UAOD Process:

The conceptual model of oxidation step in UAOD process is simplified and depicted as a catalytic cycle, shown as Figure 7.1 which consists of six basic steps: Step (1): In the presence of excess  $\text{H}_2\text{O}_2$ , polyoxometalates is peroxidized and disaggregated to form the polyperoxometalate  $\{\text{PO}_4[\text{WO}(\text{O}_2)_2]_4\}^{3-}$ , the effective species for expoxidation. Step (2): Solid-liquid anion exchange in aqueous phase. Step (3): Quaternary ammonium salts reacts as phase transfer agent. Step (4): Organic sulfur compounds are oxidized their corresponding sulfones by the peroxometal complex with high efficiency and high selectivity. Step (5): The reduced peroxometal complex dissociates with PTA and returns to aqueous phase. Step (6): Ultrasound enhances the efficiencies of oxidation reaction.

### **8.1.2 Development of a Portable, Continuous Desulfurization Unit**

#### **1. The Design of Sonoreactor:**

Transducers used in modern power ultrasonic systems are almost without exception based upon the pre-stressed piezoelectric design. Figure 3.10 shows the schematic diagram of the sonoreactors which is designed by 9.1 inch length with 1 inch inlet diameter, and operated at fixed frequency of 20 kHz with various power intensity from 100 watts to 400 watts. In this construction, four piezoelectric ceramics are bolted between a pair of metal end masses, which couples with a coupling cone (horn type taper) made by titanium alloys. The piezo elements would be a pre-polarized lead titanate composition, which exhibit high activity coupled with both low loss and ageing characteristics.

#### **2. Sulfur Removal at Different Ultrasonic Frequency:**

This study has compared two different types of ultrasonic devices which include a probe type reactor (Sonic & Material Inc., 20 kHz) and a tubular reactor (Branson Inc., 40 kHz) in batch scale. Table 6.1s exhibited that the ultrasonic frequency operated at 20 kHz has better performance then 40 kHz under UAOD process. Because ultrasonic intensity is an integral function of the frequency and amplitude of a radiating wave, a 20 kHz radiating wave will be approximately twice the intensity of a 40 kHz wave for any given average power output, and consequently the cavitation intensity resulting from a 20 kHz wave will be proportionately greater than that resulting from a 40 kHz wave.



### 3. Sulfur Removal on Continuous Flow Reactors:

To address the needs of large-scale commercial production, this study has spent one and half year designing and developing a portable, modular continuous flow system – which consists of a sonoreactor, an RF amplifier, a function generator, a pretreatment tank, and a pipeline system, was operated at room conditions for a given time. The size for a single unit is 2' x 4' x 1', as shown in Figure 3.12. Moreover, Table 7.5 has exhibited that the probe type reactor can reach 92.7% sulfur removal in 20 minutes reaction time under 600 watts as power intensity. However, the sonoreactor can reach a similar sulfur removal (92.4%) at 60 minutes reaction time with much lower power intensity of 100 watts, and the capacity is 25 times larger than that of the probe type unit. Moreover, for single sonoreactor operation, a treatment rate as high as 14 gallons per day can be achieved.

To reach the basic requirements of commercialized product and determine the largest capacity of this continuous desulfurization unit, the treatment capacity of sonoreactor has been scaled up to 12.5 lb per hour. As shown in Table 6.7, the desulfurization efficiency was reached at 89.15 % in 30 mins, which indicates that this sonoreactor is very powerful in accelerating the oxidation reaction. The final sulfur reduction of 12.5 lb/hour treatment rate was reached at 92.42 %. Moreover, for quantity purpose and performance, two sonoreactor can be connected in parallel to reach high sulfur reduction under treatment rate of 25 lb/hour which is approximately 2 barrels per day.

The 3% hydrogen peroxide has applied to portable continuous desulfurization unit for MGO. The results indicated that using dilute hydrogen peroxide can fulfill the requirements of practical applications and permit much safer operating conditions. Moreover, the economic analysis indicated that UAOD process would provide commercially solution to produce ultra-low sulfur diesel that meets future environmental standards.

The economical analysis and the capacity simulation of power generation indicated that with appropriate process design and use of chemicals, this sono reactor demonstrated the feasibility of large-scale operation even in a relatively small installation with low capital investment and maintenance cost. It also ensures the safety considerations by operating under ambient temperature and pressure. Moreover, because of its portable property and modular design, this unit is easy to setup and permit a multistage process for the best quality or quantity purpose and performance.

The most important progress and beauty of this technology is that this continuous desulfurization unit is portable, compact, convenience, and needs relatively much smaller area for installation and construction, compared to conventional hydrodesulfurization facilities, or the other desulfurization technologies, thus, provides a feasible solution to economically produce ultra-low sulfur diesel that meets new environmental regulations.

## 8.2 RECOMMENDATION

A block diagram of a continuous UAOD system on diesel fuels is illustrated in Figure 8.1. This continuous UAOD system consists of two stages operation: ultrasound-assisted catalytic oxidation and sulfone elimination. In this study, the sonoreactor has significantly demonstrated that large amounts of diesel fuels can be treated in a short sonication time to reach high desulfurization efficiency under ambient temperature and pressure. In order to achieve high efficiency and optimal condition, two or more sonoreactors can be connected in series for quality purpose and performance, or in parallel for quantity purpose and performance.

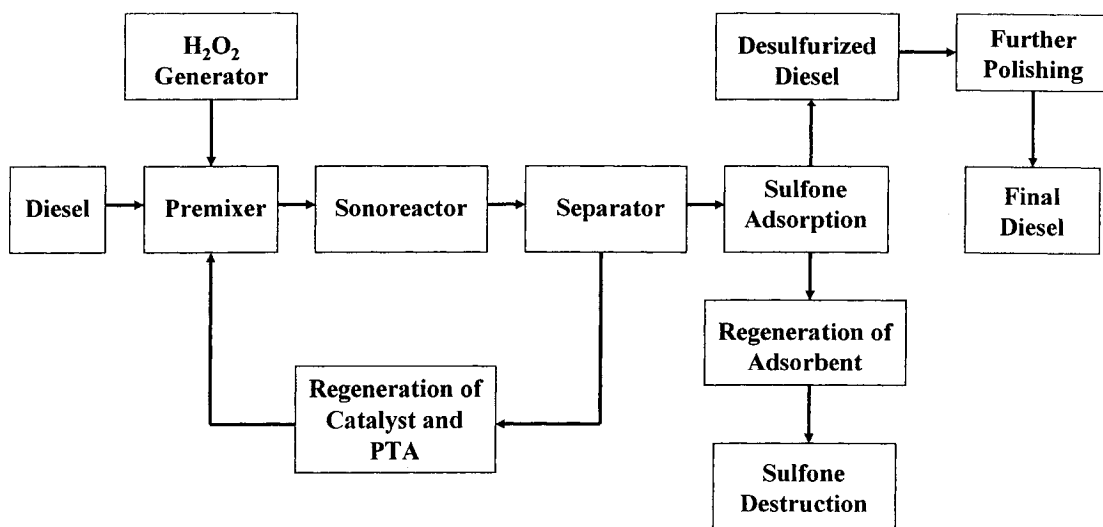


**Figure 8.1 Block diagram of continuous UAOD process**

After sonication, the oxidized diesels are delivered to a separator which is used for the de-emulsification or separation of the oxidized oil from aqueous phase.

The used PTA and TMC in aqueous phase can be regenerated and delivered back to the premixed tank. The sulfone can be removed from the oxidized diesels using adsorption tower. Activated alumina is used as a solid adsorbent in ambient temperature and atmospheric pressure. The alumina can be regenerated by heating, while the sulfones can be thermally destructed. Finally, the desulfurized diesels are sent to further polishing and become the final products.

It is suggested that the future work should emphasis on the development of a commercial scale continuous UAOD system. The optimization of current system can provide the insight to its technical and economical feasibility for potential industrial application. Several important issues are described as below:

1. Scale up the sonoreactor:

In Chapter 3 and Chapter 6, this sonoreactor has demonstrated the feasibility of large-scale operation even in a relatively small installation with low capital investment and maintenance cost. However, it is still in the laboratory scale. To reach the commercial applications, this sonoreactor can be scaled up to six times larger than original design (information provided by Dr. Geng at Blatek Tech.). Moreover, a multistage process that consists of two or more sonoreactors in parallel or series can be considered.

## 2. Optimization study of this sonoreactor:

As described in section 6.3.3, the high sulfur reduction of MGO (92%) has successfully demonstrated by a single sonoreactor at treatment rate of 12.5 lb/hour. It is suggested that this sonoreactor can be conducted with little variation from optimal conditions. Several operation conditions should be examined to process for optimal yields, including different power intensity and wave fictions (square waves) applied to sonication, slower pumping speeds applied to delivery system, and longer reaction chamber connected to sonoreactor.

## 3. Solid-phase adsorption:

Alumina is a solid adsorbent that has the potential to be used commercially for separating the organic sulfur compounds (OSC) in diesel. Three grades of activated alumina can be clarified to select the highest adsorption capacity among them: (1) Acidic alumina that favors neutral and anionic species, (2) Basic alumina that favors cation exchange, and (3) Neutral alumina that has affinity for adsorbing electronegative compounds. The nature of the adsorption sites in these different grades of alumina is a function of pretreatment and the activation conditions. Acidic alumina shows the highest adsorption capacity after UAOD process (Etemadi, 2004).

Activated alumina is capable of adsorbing organic sulfur compounds, which can be considered as a substitute for liquid/liquid extraction after UAOD process. Activated alumina is used as a solid adsorbent in room temperature and atmospheric pressure. Etemadi, 2004 has approved that alumina-packed column has the same

efficiency of sulfone remove as liquid/liquid extraction. The recovery of alumina from sulfone adsorbent had been proved in high rates (94%) recovery by a polar compound (N,N-Dimethyl Formamide) (Etemad, 2004).

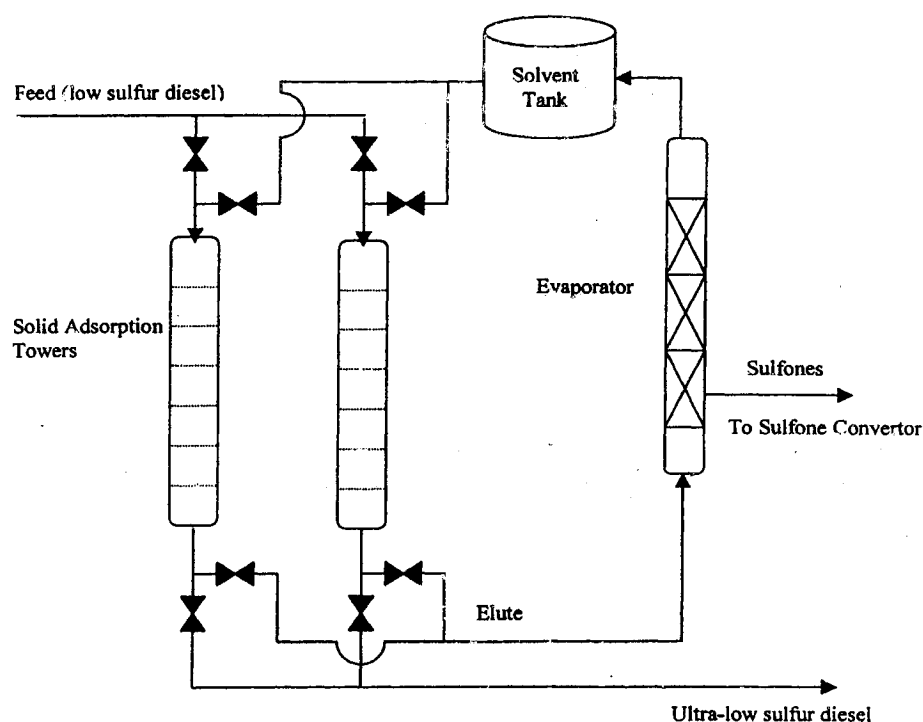


**Figure 8.2 Schematic flow diagram of the solid adsorption tower after continuous UAOD process (Yen, 2003)**

Although, alumina-packed column appears to be a capable substitute for liquid/liquid extraction after UAOD process, this technology is still in its infancy. Multiple columns for the solid adsorption tower are needed for the low sulfur diesel obtained after sonoreactor. Figure 8.2 is a schematic drawing of dual solid adsorption towers. In this case a solvent will be used to extract the sulfone, which is retained in

the solid matrix of the packed tower. Screening for the best adsorbent will be made at this stage with the proper adsorption isotherm test and column breakthrough test. It is anticipated that an ultra low sulfur-containing diesel can be obtained after the remaining sulfur is removed.

#### 4. In-situ hydrogen peroxide supply:

Hydrogen peroxide is an environmental friendly oxidizing agent that leaves only water and oxygen after reaction. However, it is dangerous to store high concentration  $\text{H}_2\text{O}_2$  on site. In-situ hydrogen peroxide generation is needed for commercialized UAOD process.

The Commercial production of large amounts of  $\text{H}_2\text{O}_2$  is based on the auto oxidation process of an organic compound. The  $\text{H}_2\text{O}_2$  is released when anthraquinol is oxidized with air through a catalyst. The resulting anthraquinone can be recycled by hydrogenation with another catalyst. Most recently, electrolytic cell process has been developed for  $\text{H}_2\text{O}_2$  production by using hydrogen and oxygen (Wakita et al., 2001). Moreover, ultrasound can generate a small amount of hydrogen peroxide and hydroxyl radical from water with dissolved gas. Although hydrogen peroxide may be produced when water is exposed to ultrasonic waves of frequencies as low as 20 kHz, it is shown that irradiation at higher frequencies leads to greater enhancements in reaction rates. Hua et al., 1997 reported the highest production rate of hydrogen

peroxide by ultrasonic irradiation as  $3\mu\text{M}/\text{min}$  ( $\sim 1 \times 10^{-4} \text{g/L-min}$ ) for 600 ml of Kr-saturated solution at 513 kHz, as shown in Figure 8.3 (Hua et al., 1997).

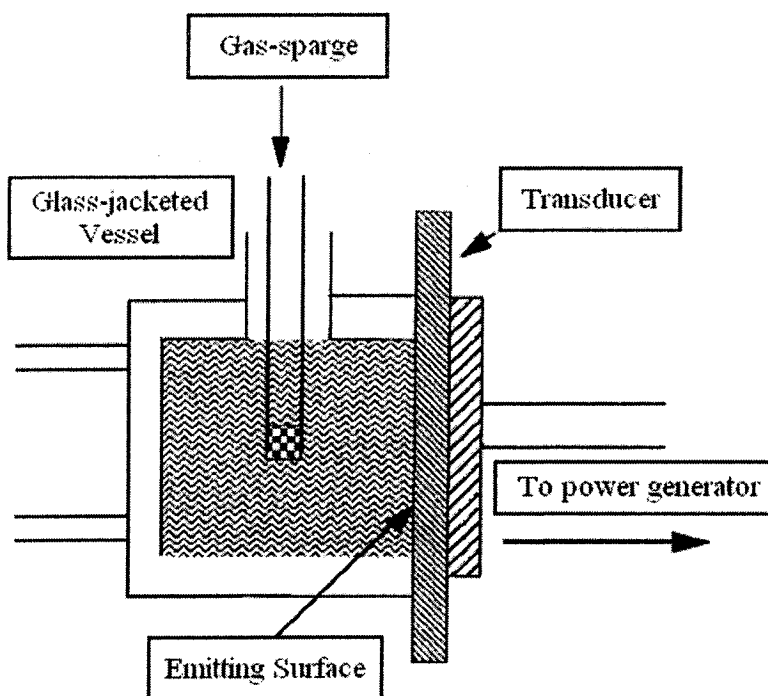


**Figure 8.3 Ultrasonic reactor configurations for sonications at 513 kHz (Hua, 1997)**

##### 5. Solid catalyst applied to oxidative desulfurization:

Zeolites are a crystalline aluminosilicate with a cage structure, which are aluminosilicate framework structures made from corner sharing  $\text{SiO}_4$  and  $\text{AlO}_4$  tetrahedra. Figure 8.4 shows that the zeolites are form by cage structures. The success of zeolites in numerous industrial catalytic processes simulated the search for



catalyst that containing elements different from  $\text{Al}^{3+}$  in a silica lattice. The reason of introducing foreign atoms into solids to change their catalytic properties is the heart of heterogenous catalysis (Cheng, 2005).

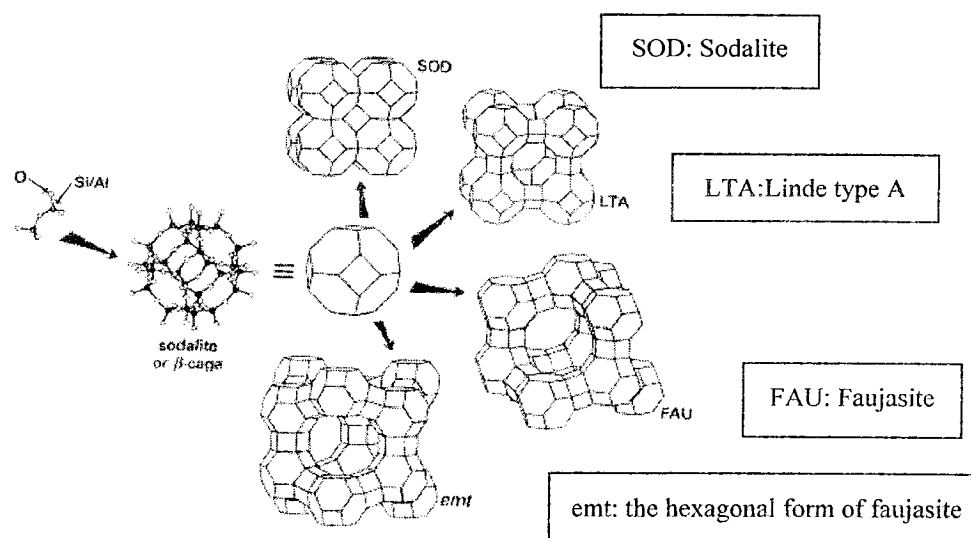


**Figure 8.4 Formation of different zeolites by cage structure (Cheng, 2005)**

In 1980, first titanium silicates (TS-1) has been synthesis by Taramasso et al, 1983, which has the crystalline structure of silicate-1 with  $\text{Ti}^{\text{IV}}$  in framework position (tetrahedral coordination in substituting for  $\text{Si}^{\text{IV}}$  in framework positions of crystalline silica). Through the years, TS-1 has been applied as a powerful catalyst in oxidation reactions with hydrogen peroxide as oxidant. The results indicated that many organic compounds could be oxidized in high selectivity and efficiency. Cheng, 2005 has reported that using TS-1 as catalyst could easily oxidize the benzothiphenes and its families with  $\text{H}_2\text{O}_2$  as oxidant under mild condition (99 %). However, the oxidation

rates slow down when OSCs have more than ten carbon rings, such as dibenzothiophene and its families.

Many research activities were devoted to the study of catalytic materials having: (1) Titanium ions in the framework positions of different zeolites structures with larger pore size (Ti-beta) or mesoporous materials (MCM-41). (2) Different transition metal ions, in pentasyl-type zeolites (structure similar to TS-1) or different types of zeolite structures, or mesoporous materials. Therefore, some new types of titanium containing large pore zeolites with Ti were synthesis, such as Ti-beta, Ti-HMS (Hexagonal Mesoporous silica) (Cheng, 2005).

As described in Chapter 5, there are four major sulfur organic compounds left in desulfurized diesel. Those four sulfur compounds, which were categorized as the group of C<sub>3</sub>-BTs, C<sub>4</sub>-BTs, C<sub>5</sub>-BTs and C<sub>3</sub>-DBTs, will be among the most refractory compounds after UAOD process. Solid catalyst has high oxidation efficiency in oxidation of benzothiophene and its families. Thus, the model compound studies of different OSCs reacting with different pore sizes of solid catalysts will be the supplementary methods after UAOD process to reach zero sulfur containing diesel.

## 6. Sulfur density

Quantum mechanics provides a recipe for calculating the probability of finding an electron at a particular point in space, and this quantity is called the “probability density” or “electron density”. Therefore, a map that shows how the probability density varies from point to point in a molecule is a model of the

molecule's electronic structure (Shusterman, et al. 1997). Moreover, Otsuki, et al., 2000 has reported that the Computer Aided Chemistry (CACHe) worksystem provided by CACHe Scientific Inc. could be used to calculate the electron density of the sulfur atom in the sulfur compounds by using the Sony Tektronixs CACHe system (CACHe, 1995) and the Molecular Orbital Package (MOPAC, Version 6.00). The PM3 (Modified Neglect of Diatomic Overlap, Parametric Method 3) semiempirical Hamiltonian developed by Stewart (1989) was employed to solve the Schro"dingler equation to calculate the optimum geometry and electronic properties of the sulfur compounds using the standard parameters (Otsuki, et al. 2000). Therefore, examining the relationship between sulfur density of various BT and DBT families and their oxidation reaction rates can propose a hypothesis to indicate and explain the most refractory compounds under UAOD conditions.

## REFERENCES

- Anderson, N. G. 2001. Practical Use of Continuous Processing in Developing and Scaling Up Laboratory Processes. *Org. Process Res. Dev.*, 5(6): 613-621.
- Baker, L. C. W. and Glick, D. C. 1998. Present General Status of Understanding of Heteropoly Electrolytes and a Tracing of Some Major Highlights in the History of Their Elucidation, *Chemical Reviews*, 98 (1): 3-50
- Ballistreri, F. P., Tomaselli, G. A., Toscano, R. M., Conte, V. and Furia, F. D. 1994. Spectroscopic and Structural Properties of some Molybdenum and Tungsten Polyoxoperoxo Complexes. A Comparison with Mononuclear Complexes. *J. Mol. Cat. A*, 89: 295-301.
- Ballistreri, F. P., Bazzo, A., Tomaselli, G. A. and Toscano, R. M. 1992. Reactivity of Peroxopolyoxo Complexes. Oxidation of Thioethers, Alkenes, and Sulfoxides by Tetrahexylammonium Tetrakis(diperoxomolybdo)phosphate. *J. Org. Chem.*, 57: 7074-7077.
- Biltz, J. 1967. *Fundamentals of Ultrasonic*. New York Plenum Press, London.
- Bortolini, O., Furia, F.D., Modena, G. and Seraglia, R. 1985. Metal Catalysis in Oxidation by Peroxides. Sulfide Oxidation and Olefine Epoxidation by Dilute Hydrogen Peroxide Catalyzed by Molybdeum and Tungsten Derivatives under Phase Transfer Conditions. *J. Org. Chem.*, 50: 2688-2690.
- Branson Inc., Pentagonal, Ultrasonic Inline Liquid Processing, [http://www.bransoncleaning.com/index\\_oem.html](http://www.bransoncleaning.com/index_oem.html)
- Campestrini, S., V., Furia, F.D. Modena, G. and Bortolini, O. 1988. Metal Catalysis in Oxidation by Peroxides. Electrophilic Oxygen Transfer from Anionic, Coordinatively Saturated Molybdeum Peroxo Complexes. *J. Org. Chem.*, 53:5721-5724.
- Carlin, B. 1960. *Ultrasonic*. McGraw-Hill Book Company, Inc., New York.
- Cheng S. S. 2005. *Army Research Laboratory Monthly Report*.
- Collins, F. M., Sharp, C., Lucy, A. R. 1997. Oxidative Desulphurisation of Oil via Hydrogen Peroxide and Heteropolyanion Catalysis. *J Mol. Cat. A: Chem.*, 17: 397-402.

ConocoPhillips, <http://www.fuelstechnology.com/szorbldiesel.htm>, 2005.

Contamine, F., Faid, F., Wilhelm, A. M., Berlan, J., Delmas, H. 1994. Chemical Reactions Under Ultrasound: Discrimination of Chemical and Physical Effects. *Chem. Eng. Sci.*, 49 (24B): 5865-5873.

Contant, R.; Herve, G. 2002. The Heteropolytungstates: Relationships Between Routes of Formation and Structures *Reviews in Inorganic Chemistry*. 22(2): 63-111.

Dehmlow, E. V. and Dehmlow, S. S. 1993. *Phase Transfer Catalysis*. VCH, New York.

Dermeik, S., Sasson Y. 1985. Effect of water on the extraction and reactions of fluoride anion by quaternary ammonium phase-transfer catalysts, *J. Org. Chem.*, 50(6): 879-882.

Duncan, D. C., Chambers, R. C., Hecht, E. and Hill, C. L. 1995. Mechanism and Dynamics in the  $H_3[PW_{12}O_{40}]$ -Catalyzed Selective Epoxidation of Terminal Olefins by  $H_2O_2$ . Formation, Reactivity, and Stability of  $\{PO_4[MO(O_2)_2]_4\}^{3-}$ , *J. Am. Chem. Soc.*, 117: 681-691.

Etemadi, O. 2004. *Army Research Laboratory Monthly Report*.

Fitzgerald, M. E., Griffing, V., Sullivan, J. 1956. Chemical Effects of Ultrasonics "Hot Spot" Chemistry. *J. Chem. Phys.*, 25 (5): 926-933.

Folsom B. R., Schieche D. R., DiGrazia P. M., Werner J., Palmer S. 1999. Microbial desulfurization of alkylated dibenzothiophenes from a hydrodesulfurized middle distillate by *Rhodococcus erythropolis* I-19. *Appl Environ Microbiol*. 65: 4967-4972.

Frye, C.G., Mosby, J.F. 1967. Kinetics of hydrodesulfurization, *Chem. Eng. Prog.* 63: 66.

Gates, B.C., Topsoe, H. 1997. Reactivities in deep catalytic hydro-desulfurization: challenges, opportunities, and the importance of 4-methyldibenzothiophene and 4,6-dimethyl-dibenzothiophene, *Polyhedron* 16: 3213.

Goobnow G. L. 1969. *Ultrasonic – Theory and Application*. Hart Publishing Company, Inc., New York.

Girgis, M.J., Gates, B.C. 1991. Reactivities, reaction networks, and kinetics in high-pressure catalytic hydroprocessing, *Ind. Eng. Chem.* 30: 2021.

Griffing, V. 1952. The Chemical Effects of Ultrasonics. *J. Chem. Phys.*, 20 (6): 939-942.

Harriott, P. 2003. *Chemical Reactor Design*. Marcel Dekker, Inc.

Hernandez-Maldonado, A. J., Yang, R. T. 2003. Desulfurization of Commercial Liquid Fuels by Selective Adsorption via  $\pi$ -Complexation with Cu(I)-Y Zeolite, *Ind. Eng. Chem. Res.* 2003, 42: 3103-3110.

Hernandez-Maldonado, A. J., Yang, R. T. 2004. Desulfurization of Diesel Fuels by Adsorption via  $\delta$ -Complexation with Vapor-Phase Exchanged Cu(I)-Y Zeolites, *JACS Communications*, published on Web, 2004.

Hill, C. L. and McCartha, C. M. P. 1995. Homogeneous Catalysis by Transition Metal Oxygen Anion Clusters. *Coordination Chemistry Reviews*, 143: 407-455.

Hill, C. L., Strukul, G. (ed.) 1992. *Catalytic Oxidation with Hydrogen Peroxide as Oxidant*. Kluwer Academic Publishers, Dordrecht, p. 253.

Houalla, M., Broderick, D.H., Sapre, A.V., Nag, N.K., De Beer, V.H., Gates, J. B.C., Kwart, H. 1980 Hydrodesulfurization of methyl-substituted dibenzothiophene catalyzed by sulfided CoO–MoO<sub>3</sub>/Al<sub>2</sub>O<sub>3</sub>, *J. Catal.* 61: 523.

Hua, I, and Hoffmann, M. R., Optimization of Ultrasonic Irradiation as an Advanced Oxidation Technology; *Environ. Sci. Technol.* 31: 2237-2243, 1997

Hutte, R. S.; Ray, J. D. 1992 *Sulfur-Selective Detectors, in Detectors for Capillary Chromatograph*. Hill, H.H.; Mcminn, D. G. Ed.; Jone Wiley & Sons, New York; Chapter 9.

Ino et al., *U.S. Patent* 6,254,762, 2001.

Ishii, Y., Yamawaki, K., Ura, T., Yamada, H., Yoshida, T. and Ogawa, M. 1988. Hydrogen Peroxide Oxidation Catalyzed by Heteropoly Acids Combined with Cetylpyridinium Chloride: Epoxidation of Olefines and Allylic Alcohols, Ketonization of Alcohols and Diols, and Oxidative Cleavage of 1,2-Diols and Olefins. *J. Org. Chem.*, 53: 3587-3593.

Jones., R. A. 2001 *Quarternary ammonium salts : their use in phase-transfer catalysis*. Academic Press.

Kabe, T., Ishiharam, A., Tajima, H. 1992. Hydrodesulfurization of sulfur-containing polyaromatic compounds in light oil, *Ind. Eng. Chem. Res.* 31: 1577.

Katsoulis, D. E. 1998. A Survey of Applications of Polyoxometalates, *Chemical Reviews*, 98 (1): 359-388

Kilanowski, D.R., Teeuwen, H., De Beer, V.H.J., Gates, B.C., Schuit, B.C.A., Kwart, H. 1978. Hydrodesulfurization of thiophene, benzothiophene, dibenzothiophene, and related compounds catalyzed by sulfided CoO–MoO<sub>3</sub>/Al<sub>2</sub>O<sub>3</sub>: low-pressure reactivity studies, *J. Catal.* 55: 129.

Kobayashi, M., Horiuchi, K., Yoshikawa, O., Hirasawa, K., Ishii, Y., Fujino, K., Sugiyama, H., Maruhashi, K., 2001. Kinetic analysis of microbial desulfurization of model and light gas oils containing multiple alkyl dibenzothiophenes, *Biosci. Biotechnol. Biochem.* 65 (2): 298–304.

Kozhevnikov, I. V. 1998. Catalysis by Heteropoly Acids and Multicomponent Polyoxometalates in Liquid-Phase Reactions, *Chemical Reviews*, 98 (1): 171-198.

Kozhevnikov, I. V., Mulder, G. P., Steverink-de Zoete, M. C. and Oostwal, M. G. 1998. Epoxidation of oleic acid catalyzed by peroxo phosphotungstate in a two-phase system, *Journal of Molecular Catalysis A: Chemical.*, 134, Issues 1-3, 223-228

Lange, E.A., Lin, Q. 1998. Preparation of surfactants from a byproduct of fossil fuel biodesulfurization, *American Chemical Society, Division of Petroleum Chemistry*, 43(4): 550-552.

Luche, J. L. 1998 *Synthetic Organic Sonochemistry*. Plenum Press, New York

Ma, X. L., Kim J. H., Song C. S, 2004. *Nonlinear Response and Quenching Effect in GC-PFD and GC-PFPD for Quantitative Sulfur Analysis of Low-Sulfur Hydrocarbon Fuels*. American Chemical Society, California

Ma, X. L., Sakanishi, K., Mochida, I. 1994. Hydrodesulfurization reactivities of various sulfur compounds in diesel fuel, *Ind. Eng. Chem.* 33: 218.

Ma, X. L., Sakanishi, K., Isoda, T. Mochida, I. 1995. Hydrodesulfurization reactivities of narrow-cut fractions in a gas oil, *Ind. Eng. Chem. Res.* 34: 748.

Ma, X. L., Sun, L; Song, C. S. 2002. A new approach to deep desulfurization of gasoline, diesel fuel and jet fuel by selective adsorption for ultra-clean fuels and for fuel cell applications, *Catalysis Today*, 77: 107-116.

Madanshetty, S. I., Apfel, R. E. 1991. Acoustic Microcavitation: Enhancement and Applications. *J. Acoust. Soc. Am.*, 90 (3): 1508-1514.

Magnetostrictive Versus Piezoelectric Transducers for Power Ultrasonic Applications, [http://www.blackstone-ney.com/04.TP\\_mag\\_vs\\_piezo.php](http://www.blackstone-ney.com/04.TP_mag_vs_piezo.php).

Mason, T. J. 1999. *Sonochemistry*. Oxford University Press Inc., New York.

Mason, T. J. (ed.) 1990. *Sonochemistry: The Uses of Ultrasound in Chemistry*. RS. C, UK.

Mason, T. J. 1991. *Advances in Sonochemistry – A Research Annual. Volume 2*. Jai Press Ltd., London, England.

Mei, H. 2003. *The Feasibility Study of Desulfurization of Diesel Fuels by Ultrasound-Assisted Oxidative Desulfurization (UAOD)*, Dissertation. USC.

Mei, H. Mei, W. Yen, T. F. 2003. A new method for obtaining ultra-low sulfur diesel fuel via ultrasound assisted oxidative desulfurization, *Fuel*, 82 (4): 405-414.

Mochida, I., Sakanishi, K., Ma, X., Nagao, S., and Isoda, T. 1996. Deep Hydrodesulfurization of Diesel Fuel: Design of Reaction Process and Catalysis. *Catalysis Today*, 29: 185.

McFarland, B. L., Boron, D. J., Deever, W. J., Meyer, J. A., Johnson, A. R. and Atlas, R. M. 1998. Biocatalytic Sulfur Removal from Fuels: Applicability for Producing Low Sulfur Gasoline, *Critical Reviews in Microbiology*, 24(2): 99-147.

Moffat, J. B. 2001. Metal-Oxygen Clusters: *The Surface and Catalytic Properties of Heteropoly Oxometalates*, Kluwer Academic/Plenum Publisher, New York.

Moiseev, I. I., in Murahashi, S. I. And Davies, S. G (ed.) 1999. *Transition Metal Catalysed Reactions*, Blackwell Science, UK, p. 343.

Monticello, D.J., 1998 Biodesulfurization of diesel fuels, *Chemtech* 28 (7): 38–45.

Moulton, K. J., Koritala, S., Frankel, E. N. 1983. Ultrasonic Hydrogenation of Soybean Oil. *J. Am. Oil Chem. Soc.*, 60 (7): 1257-1258.

Moulton, K. J., Koritala, S., Warner, K., Frankel, E. N. 1987. Continuous Ultrasonic Hydrogenation of Soybean Oil. II. Operating Conditions and Oil Quality. *J. Am. Oil Chem. Soc.*, 64 (4): 542-547.

---

Murahashi, S. I. and Davies, S. G. (ed.) 1999. *Transition Metal-Catalyzed Reactions*, Blackwell Science, UK.





Nauman, E. B. 2001. *Chemical Reactor Design, Optimization, and Scaleup*. McGraw-Hill, Inc., New York.

Otsuki, S., Nonaka, T., Takashima, N. Qian, W. H., Ishihara, A., Imai, T. and Kabe, T. 2000. Oxidative Desulfurization of Light Gas Oil and Vacuum Gas Oil by Oxidation and Solvent Extraction. *Energy & Fuels*, 14(6): 1232-1239.

Patai, S. (ed.) 1983. *The Chemistry of Peroxides*. John Wiley & Sons, Inc., New York.

Payne, P. A. 2002. *Transducer*, Access Science, McGraw-Hill, <http://www.accessscience.com>, DOI 10.1036/1097-8542.704500

Phillipson, J.J. 1971. Kinetics of hydrodesulfurization of light and middle distillates, *Paper Presented at the American Institute of Chemical Engineers Meeting*, Houston, TX.

Pope, M. T. 1983. *Heteropoly and Isopoly Oxometalates*. Springer-Verlag, Dordrecht, Netherlands.

Pope, M. T. and Muller, A. (ed.) 2001. *Polyoxometalate Chemistry From Topology via Self-Assembly, to Applications*. Kluwer Academic Publishers, Berlin, Germany.

Ratoarinoro, N., Contamine, F., Wilhelm, A. M., Berlan, J., Delmas, H. 1995. Power Measurement in Sonochemistry. *Ultrason. Sonochem.* 2 (1): 543-547.

Remias, J. E., Pavlosky, T. A. and Sen, A. 2003. Catalytic hydroxylation of benzene and cyclohexane using in situ generated hydrogen peroxide: new mechanistic insights and comparison with hydrogen peroxide added directly. *Journal of Molecular Catalysis A: Chemical*, 203 (1-2): 179-192.

Salles, L., Aubry, Thouvenot, C. R., Robert, F., Doremieux-Morin, C., Chottard, G., Ledon, H., Jeannin, Y., and Bregeault, J. M. 1994. 31P and 183W NMR Spectroscopic Evidence for Novel Peroxo Species in the " $\text{H}_3[\text{PW}_{12}\text{O}_{40}] \cdot n\text{H}_2\text{O} / \text{H}_2\text{O}_2$ " System. Synthesis and X-ray Structure of Tetrabutylammonium ( $\mu$ -Hydrogen phosphato)bis( $\mu$ -peroxo)bis(oxoperoxotungstate) (2-): A Catalyst of Olefin Epoxidation in a Biphasic Medium. *J. Inorg. Chem.* 33: 871-878.

Sasson, Y. and Neumann, R. (ed.) 1997. *Handbook of Phase Transfer Catalysis*. Blackie Academic & Professional, London, UK.

- Schramm, L. L. (ed.) 1992. *Emulsions: Fundamentals and Applications in the Petroleum Industry*. American Chemical Society, Washington, DC.
- Shah, Y. T., Pandit, A. B., and Moholkar, V. S. 1999. *Cavitation Reaction Engineering*. Kluwer Academic/Plenum Publishers, New York.
- Sheldon, R. A. and Kochi, J. K. 1981. *Metal-Catalyzed Oxidation of Organic Compounds*. Academic Press, Inc., London.
- Shiraishi, Y., Naito, T., and Hirai, T. 2003. Vanadosilicate Molecular Sieve as a Catalyst for Oxidative Desulfurization of Light Oil, *Ind. Eng. Chem. Res.* 42 (24): 6034-6039.
- Shusterman, G. P. and Shusterman A. J. 1997. *Journal of Chemical Education*. 74 (7) 771-776.
- Song, C. S. 2003. An overview of new approaches to deep desulfurization for ultra-clean gasoline, diesel fuel and jet fuel, *Catalysis Today*, 86, Issues 1-4: 211-263
- Song, C. S., Hsu, C. S., and Mochida, I. 2000. *Chemistry of Diesel Fuels*. Taylor & Francis, New York.
- Starks, C., Liotta, C. and Halpern, M. 1994. *Phase-Transfer Catalysis: Fundamentals, Applications & Industrial Perspectives*. Chapman & Hall, Inc., New York.
- Strukul, G., in Strukul, G. (ed.) 1992. *Catalytic Oxidation with Hydrogen Peroxide as Oxidant*. Kluwer Academic Publishers, Dordrecht
- Suslick, K. S. 1988. *Ultrasound: Its Chemical, Physical and Biological Effects*. VCH, New York.
- Takahashi, A., Yang, F. H., Yang, R. T. 2003. New Sorbents for Desulfurization by  $\pi$ -Complexation: Thiophene/Benzene Adsorption, *Ind. Eng. Chem. Res.* 41: 2487-2496.
- Te, M., Fairbridge, C. and Ring, Z. 2001. Oxidation Reactivities of Dibenzothiophenes in Polyoxometalate/H<sub>2</sub>O<sub>2</sub> and formic acid/ H<sub>2</sub>O<sub>2</sub> systems. *Appl. Cat. A: General*, 219: 267-280.
- Thompson, L.H. and Doraiswamy, L.K. 1999. Sonochemistry: Science and Engineering. *Ind. Eng. Chem. Res.*, 38: 1250-1249.

U.S. EPA. 2000. Regulatory Announcement: Heavy-Duty Engine and Vehicle Standards and Highway Diesel Fuel Sulfur Control Requirements, EPA 420-F-00-057.

Taramasso, M., Perego, G., and Notari B., *U.S. Patent*. 4,410,501, 1983.

Vasudevan, P.T., and Fierro, J.L.G. 1996. A review of deep hydrode-sulfurization catalysis, *Catal. Rev.-Sci. Eng.* 38: 161.

Venturello, C., Alneri, E. and Ricci, M. 1983. A New, Effective Catalytic System for Epoxidation of Olefins by Hydrogen Peroxide under Phase- Transfer Conditions. *J. Org. Chem.*, 48: 3831-3833.

Venturello, C., Aloisio, R. D., Bart, J. J. and Ricci, M. 1985. A New Peroxotungsten Heteropoly Anion with Special Oxidizing Properties: Synthesis and Structure of Tetrahexylammonium Tetra (diperoxotungstio) phosphate (3-). *Tetra. Letter.*, 107-110.

Wakita et al., *U.S. Patent* 6,159,349, 2000.

Yadav, G. D. and Pujari, A. A. 2000. Epoxidation of Styrene to Styrene Oxide: Synergism of Heteropoly Acid and Phase- Transfer Catalyst under Ishii- Venturello Mechanism. *Organic Process Research & Development*, 4: 88-93.

Yen T. F. 1999, *Environmental Chemistry: Esseventials of Chemistry for Engineering Practice, Volume 4A*, Prentice Hall.

Yen, T. F. 2003. *A Portable, Modular Process for Sulfur Removal and Disposal in Naval Fuel Cell Systems*, Proposol.

Yen, T. F., Mei, H., and Lu, S. H., 2002 "Oxidative Desulfurization of Fossil Fuels with Ultrasound", *U.S. Patent* 6,402,939.

Yang, R. T., Takahashi, A., Yang, F. H. 2002. Hernandez-Maldonado; A. Selective Sorbents for Desulfurization of Liquid Fuels, *United States and non-U.S. Patent applications filed*.

Yang, R. T., Herna'ndez-Maldonado, A. J., Yang, F. H. 2003 Desulfurization of Transportation Fuels with Zeolites Under Ambient Conditions, *Science*, 301: 79-81.